

**P.O.L.**

**SURGE PREDICTION AT BARROW-IN-FURNESS**

**BY  
M. AMIN, R.A. FLATHER, K.P. HUBBERT  
AND J.B. RAE**

**REPORT NO. 4  
1988**

**NATURAL ENVIRONMENT  
PROUDMAN OCEANOGRAPHIC  
LABORATORY  
RESEARCH COUNCIL**

**PROUDMAN OCEANOGRAPHIC LABORATORY**

**Bidston Observatory  
Birkenhead, Merseyside, L43 7RA, U.K.  
Tel: 051 653 8633  
Telex: 628591OCEANSB  
Fax: 051 653 6269**

Director: Dr. B.S. McCartney

*Natural Environment Research Council*

PROUDMAN OCEANOGRAPHIC LABORATORY  
REPORT No. 4

Surge prediction at Barrow-in-Furness

M. Amin, R.A. Flather, K.P. Hubbert  
and J.B. Rae

1988

## DOCUMENT DATA SHEET

<b>AUTHOR</b> AMIN, M., FLATHER, R.A., HUBBERT, K.P. AND RAE, J.B.		<b>PUBLICATION DATE</b> 1988
<b>TITLE</b> Surge prediction at Barrow-in-Furness		
<b>REFERENCE</b> Proudman Oceanographic Laboratory Report, No. 4, 112pp		
<b>ABSTRACT</b> Over a period of 18 months starting September 1985, simultaneous sea-level measurements have been taken at Barrow-in-Furness, at two locations to the north and south of Walney Island, at Roa Island, and at an offshore position to the south of Walney Island. Subsequently, statistical formulae have been evolved relating the surge at each observational point to the surge at Heysham and to local meteorological variables. Using the forecast surge at Heysham, obtained from the Continental Shelf Model running in real time, a regression model has been developed to predict surges in the vicinity of Barrow-in-Furness. Emphasis has been placed on the correct reproduction of negative surges. Experimental runs have been carried out with a regional model of Morecambe Bay to assess the influence of local winds on sea level differences within the Bay.		
This work has been carried out under contract to the Ministry of Defence. The results may be used in the formulation of Government policy, but at this stage they do not necessarily represent Government policy.		
<b>ISSUING ORGANISATION</b> Proudman Oceanographic Laboratory Bidston Observatory Birkenhead, Merseyside L43 7RA UK  Director: Dr B S McCartney		<b>TELEPHONE</b> 051 653 8633  <b>TELEX</b> 628591 OCEAN BG  <b>TELEFAX</b> 051 653 6269
<b>KEYWORDS</b> BARROW-IN-FURNESS TIDE MEASUREMENT STORM SURGE PREDICTION SEA LEVEL MEASUREMENT		<b>MODELLING</b> MORECAMBE BAY REGRESSION ANALYSIS NEGATIVE STORM SURGES  <b>CONTRACT</b> NSN 21A/88977  <b>PROJECT</b> 3310 M1K-57-1  <b>PRICE</b> £27

Copies of this report are available from:  
The Library, Proudman Oceanographic Laboratory.

<u>Contents</u>	<u>Page No</u>
1. OBJECTIVE	7
2. SYNOPSIS	7
3. SUMMARY OF THE WORK	7
4. SEA LEVEL MEASUREMENTS	10
5. SEA LEVEL DATA PROCESSING	13
6. STATISTICAL ANALYSIS OF SURGE DATA	14
6.1 Introduction	
6.2 Analysis of observed surges and meteorological data	
6.2 Regression technique	
6.4 Relationship between negative surge and tide phases	
6.5 Numerical model	
6.6 Conclusions	
7. NUMERICAL MODEL OF MORECAMBE BAY	21
7.1 Introduction	
7.2 Outline of the model	
7.3 Results for $M_2$ and spring tides	
7.4 Response of Morecambe Bay to local winds and externally generated surges	
7.5 Simulation of a negative surge using the Morecambe Bay model	
7.6 Conclusions	
8. RECOMMENDATIONS	32
9. ACKNOWLEDGEMENTS	32
10. REFERENCES	33
TABLES	
FIGURES	

## 1. OBJECTIVE

The main objective of this work has been to develop a scheme for the prediction of negative storm surge heights during spring tides at Barrow-in-Furness and on a southerly sea route from that port as far as the 10 metre depth contour.

## 2. SYNOPSIS

Over a period of eighteen months beginning September 1985, simultaneous sea-level measurements have been taken at Barrow-in-Furness, at two locations to the north and south of Walney Island respectively, at Roa Island, and at an offshore position to the south of Walney Island near to the Halfway Shoals Buoy.

Subsequently, statistical formulae have been evolved relating the surge at each observational point to the surge at Heysham and to local meteorological variables. Using the forecast surge at Heysham, obtained from the Continental Shelf Model running in real time, a regression model has been developed to predict surges in the vicinity of Barrow within two hours of a HW at HW Springs ( $\pm 4$  days). Emphasis has been placed on the correct reproduction of negative surges.

To assist in the development of the prediction scheme a number of experimental runs have been carried out with a regional model of Morecambe Bay, to assess the influence of local winds on sea-level differences within the Bay. Earlier model simulations of negative surges within the Bay have also been examined.

## 3. SUMMARY OF THE WORK

a. Hourly surge values for Heysham, Holyhead and Port Patrick, derived from the Continental Shelf Model running in real time, have been collected continuously between September 1984 and December 1987. Special arrangements were made with the Meteorological Office to run the model during the summer months involved, thereby avoiding a break in the series of surge values. A sub-set of this data from October 1985 to December 1986 was used for the statistical analysis of negative surges.

b. EHM hourly tidal predictions for Heysham, Holyhead and Port Patrick have been prepared for the period January 1986 to May 1987. These were subtracted from observed hourly values to provide hourly residuals for each port.

c. Model and observed surge values for Heysham have been compared statistically to assess the accuracy of the model forecasts near to High Water Springs. This statistical analysis of residual surges is necessary so that Heysham can be used as a reference port. Regression of the observed surge against the model forecast provides some improvement in the surge forecast. Frequency bands of high residual energy were isolated to explain those components of the surge which were not predicted properly by the model.

d. In June 1985 an Aanderaa recorder was attached to the existing bubbler tide gauge at Ramsden Dock. In September 1985 bubbler tide gauges with Aanderaa recorders were installed at Lowsy Point and Roa Island, and an Aanderaa recorder was attached to a bubbler gauge at Hawes Point. Simultaneous records were collected from all of these recorders for nineteen months until April 1987. The gauges at Ramsden Dock and Roa Island covered the full tidal range, but there was some ponding at the Lowsy Point gauge and the gauge at Hawes Point dried out at low spring tides. These gauges were levelled in and maintained every four months when the data tapes and batteries were changed.

Also in September 1985 offshore tide gauges were deployed near the Halfway Shoals and Lightning Knoll buoys. These gauges were deployed in fixed frames with surface moorings so that the pressure recorders could be recovered from the frames and redeployed by divers every four months. The Lightning Knoll gauge was dragged from its position by a ship, its mooring lost, and a number of recovery attempts proved to be unsuccessful. The Halfway Shoals gauge was successful and was finally recovered on 30 October 1987.

Precision laboratory calibrations of all the pressure recorders were carried out before installation and after recovery.

e. Tidal analyses were carried out on the data obtained from each installed recorder and hourly residuals have been extracted for the eighteen month period from September 1985 to February 1987.

f. Curves have been derived giving the probability of occurrence of surges at Heysham on a seasonal and state-of-tide basis. Twenty-two years of data were used for this purpose.

g. All of the available data has been collated and negative surges observed in the vicinity of Barrow-in-Furness during October 1985 to December 1986 have been statistically analysed. The response of the sea to meteorological forces is frequency dependent, reaching a peak level in the 0.25-0.50 cycles per day band. Compilation of amplitude and phase responses in the tidal bands were not reliable because noise levels were high due to cusps and humps in the spectrum resulting from interaction between low frequency noise and tides. Although some variations were observed, an average 80 per cent of the surge energy was in the low frequency region below 0.5 cycles per day.

A regression formula for forecasting negative surges has been derived. The coefficient of air pressure is slightly less than the inverted barometric effect, and linear winds from 10°T are the most effective in generating negative surges. Numerical models underestimate surges at Roa Island and at Ramsden Dock by about 4 per cent, and by 1 per cent at Halfway Shoals. The performance is quite good at low frequencies where it accounted for more than 75 per cent of the energy. In the diurnal band efficiency decreased to 33 per cent and in the semi-diurnal and high frequency regions of the spectrum it reduced to zero. If only meteorological variables were used as input to the regression model the efficiency was marginally less than that of numerical models, the difference being mainly in the diurnal band.

h. Experiments were carried out with a regional model of Morecambe Bay to investigate the variations within the Bay arising from combinations of local wind, externally generated surge, and tide. An understanding of these variations and their causes could provide a basis for deriving improved surge estimates at points along the approach channel to Ramsden Dock from surge forecasts for Heysham produced by the operational shelf model running at the Meteorological Office. The Morecambe Bay model was used to obtain results for the  $M_2$  constituent of the tide and the model solution was verified against observations. Results were examined for spring tide conditions, with uniform winds from the north and east acting over the Bay, and for an externally generated negative surge introduced at the open boundary of the model. Simulation of a negative



surge in the period 29 January to 7 February 1986 was also carried out.

#### 4. SEA LEVEL MEASUREMENTS

The sea level measurements used in this work were from the three permanent tide gauges at Heysham, Holyhead and Port Patrick, from specially installed coastal gauges at Lowsy Point, Ramsden Dock, Roa Island and Hawes Point, and from an offshore gauge deployed at Halfway Shoals (Figure 1).

The gauges at Heysham, Holyhead and Port Patrick are part of the UK permanent tide gauge network. Heysham and Port Patrick are both stilling well and float gauges with Lea chart recorders. The installation at Holyhead has been upgraded to the modernised standard for the permanent network and integrated fifteen minute digital data is obtained by telephone link from a potentiometer unit connected to a float in a stilling well and from a differential pressure sensor connected to a bubbler system (PALIN & RAE 1987).

The coastal tide gauges installed at Lowsy Point, Ramsden Dock, Roa Island and Hawes Point all used air bubbling systems to transfer pressure from a pressure point, fixed at a known datum below low water level, to a pressure recording instrument on land. Aanderaa differential pressure recording instruments were used to record the pressure differences between the air bubbling tube and atmosphere every fifteen minutes. Measurements of sea water density allow mean values to be estimated for each site and these were used in conjunction with accurate laboratory calibrations of the pressure transducers to compute sea levels above the pressure points from the recorded data.

At Ramsden Dock permission was obtained to attach a differential pressure recorder to an existing air bubbler gauge operated by Associated British Ports. The pressure point was installed by Associated British Ports at Admiralty Chart Datum. This recorder and a POL air control unit were installed on 7 January 1985, and the instrument was maintained and data tapes retrieved on 29 April and 15 September in 1985, on 17 February, 13 May and 23 September in 1986, and on 11 February in 1987. The recorder was removed on 29 April 1987. During the first year some loss of data was caused by the compressed air supply running out, and on 21 October 1985 the air cylinders used by Associated British Ports were replaced by a POL compressor which overcame the problem.

At Lowsy Point a bubbling system with compressed air cylinders, air control unit and differential pressure recorder were installed on 14 September 1985. The datum of the pressure point was at 8.54 metres below a POL bench mark and ponding occurred at low spring tides. This installation was maintained and the data tape replaced on 18 February, 13 May and 23 September in 1986, and on 11 February in 1987. An air supply leak was responsible for loss of data after 31 July 1986 until the maintenance visit on 23 September 1986. The installation was removed on 29 April 1987.

With permission from the Royal National Lifeboat Institution the gauge at Roa Island was installed at the Barrow Lifeboat Station with the pressure point at the end of the slipway, 4.37 metres below Ordnance Datum Newlyn. The pressure point, tubing, compressed air bottles, air control unit and differential pressure recorder were installed on 16 September 1985. Due to engineering work on the slipway the air line to the pressure point had to be repositioned on 12 December 1985 but there was no evidence of significant data loss at this time. The installation was maintained and the data tape replaced on 18 February, 14 May and 23 September in 1986, and on 12 February in 1987. There was some loss of data between 14 May 1986 until the maintenance visit on 23 September 1986 due to tape problems and an air leak in the bubbling system. The installation was removed on 30 April 1987.

On 17 September 1985 a differential pressure recorder and an air control unit were attached to the bubbling system operated by Vickers at Hawes Point. The pressure point and air line of this gauge were moved by Vickers to another structure on 24 September 1985, and difficulties were reported in purging water from the air line until about 20 October 1985. The datum of the pressure point was reported as being 2.81 metres below Ordnance Datum Newlyn and there was drying out at low spring tides. This installation was maintained and the data tape replaced on 19 February, 14 May and 23 September in 1986, and on 11 February in 1987. There were some problems with data tapes between 19 February and 14 May 1986 and between 24 September and 11 February 1987. The Aanderaa recorder and air control unit were removed on 30 April 1987. Water samples were taken at each of these sites and a value of water density derived so that the pressure measurements could be converted to sea levels.

Offshore tide gauges were deployed at Halfway Shoals and at Lightning Knoll,

consisting of Aanderaa absolute pressure recording instruments mounted in heavy steel bottom frames. The frames were anchored and marked by surface buoys and pellet lines (Figure 2). Both gauges were deployed on 24 September 1985 using the Associated British Ports Hydrographic Survey Launch the Dova Haw, POL boats and a POL diving team. The Halfway Shoals gauge was deployed at position 54°01.5N, 3°11.5W, about 2.6 metres below Chart Datum, and the Lightning Knoll gauge at 53°59.7N, 3°16.0W, about 11.5 metres below Chart Datum. These sites were agreed with Associated British Ports and Trinity House, and Notices to Mariners were published and distributed to appropriate authorities and organisations (Figures 3 and 4).

On 4 December 1985 the Halfway Shoals surface buoy was reported missing, and was later recovered from Kirkcudbright. The gauge remained in position and was relocated on 21 February 1986 when POL divers retrieved the pressure recording instrument, which was maintained and replaced in the bottom frame. The surface buoy and pellet floats were replaced at the same time. The Lightning Knoll surface buoy was reported to be in position and flashing correctly on 4 December 1985, but was found floating freely and recovered by a local fisherman off Roa Island on 24 December 1985. Efforts to relocate this gauge and to replace the surface buoy were delayed by non-coincidence of good weather, tidal conditions, ship and diver availability.

The Halfway Shoals pressure recorder was again recovered and redeployed in its frame on 2 June 1986 using the Dova Haw and POL divers. The divers also carried out an unsuccessful bottom search for the Lightning Knoll frame.

On 25 September 1986 POL divers again used the Dova Haw to recover and redeploy the Halfway Shoals pressure recorder. At the same time the acoustic telemetry signal from the Lightning Knoll gauge was picked up on a hydrophone, and a marker pellet was deployed at the expected position. Attempts at dragging for the ground line were unsuccessful and acoustic contact only gave a location within about 50 metres. The Dova Haw was not available on 26 September and a 50 foot boat was hired from the Bay Towage and Salvage Company. Further acoustic contact was made with the Lightning Knoll gauge, but an extensive diver survey and further dragging revealed nothing. To have a reasonable chance of recovery by diver search the gauge would have to be located within a radius of about 5 metres by use of a double hydrophone system. Some tests were subsequently

carried out indicating that this could be feasible.

The surface marker from the Halfway Shoals gauge was reported to be on a beach at Hawes Point in April 1987 and was subsequently recovered. On 6 May 1987 attempts were made to recover the pressure recorder at Halfway Shoals and to re-locate the gauge at Lightning Knoll, using the Dova Haw fitted with a Hi-fix positioning system. At the Halfway Shoals position the divers were unable to locate any part of the gauge or its mooring within a 40 metre radius, although acoustic transmissions were received by a hydrophone system on the ship. Due to high noise levels the hydrophone system was unable to provide directional information and further diver survey was not possible. Acoustic transmissions were also received at the Lightning Knoll position but again it did not prove possible to obtain directional information without which it was considered that a further diver search would be unproductive.

On 30 October 1987 a further attempt was made to recover the two offshore tide gauges using the Dova Haw. The Halfway Shoals gauge was located on its original position and the pressure recorder was successfully recovered by POL divers. At this time it was not possible to locate the Lightning Knoll gauge and it is now considered that further recovery attempts would be unproductive since the recorder battery will be exhausted, resulting in the loss of acoustic transmissions.

A summary of the data recovered from these installed and deployed tide gauges is given in Table 1.

## 5. SEA LEVEL DATA PROCESSING

Charts from the Lea tide gauge at Heysham have been digitised and processed to hourly levels above Admiralty Chart Datum for the period 1 January 1986 to 25 May 1987. The data was analysed using the Tidal Elevation Reduction Package (GRAFF & KARUNARATNE 1980) to provide daily, monthly, and annual mean sea levels (Table 2), monthly and annual maxima and minima elevations (Table 3), and hourly residuals (Figure 5). The residuals were obtained by comparing the hourly values derived from measurements with predicted values based on an analysis of 8 years of data starting 1 January 1964, giving 112 harmonic constants (Table 4). Also, sea levels at Heysham between 1964 and 1986 were analysed to show the probability

of surges occurring at high waters (Figure 6), at low waters (Figure 7), and on a monthly basis (Figure 8).

Similarly, charts from the Lea tide gauge at Port Patrick were digitised and processed to hourly values above 3 metres below ACD for the period 1 January 1986 to 27 April 1987. Daily, monthly, and annual mean sea levels (Table 5), monthly and annual maxima and minima elevations (Table 6), and hourly residuals (Figure 9) were calculated. The predicted hourly values were based on an analysis of 9 years of data starting 2 January 1968, giving 111 harmonic constants (Table 7).

For Holyhead, hourly heights above ACD for the period 1 January 1986 to 12 May 1987 were filtered from 15 minutes levels obtained from the differential pressure sensor and bubbler system mounted outside of the stilling well. Daily, monthly, and annual mean sea levels (Table 8), monthly and annual maxima and minima (Table 9), and hourly residuals (Figure 10) were calculated. The predicted hourly values were based on an analysis of 8 years of data starting 1 January 1964, giving 115 harmonic constants (Table 10).

At Ramsden Dock, Lowsy Point, Roa Island, Hawes Point and Halfway Shoals the output from pressure sensors, integrated over 40 seconds, was recorded on magnetic tape every 15 minutes. After translation from the data tapes the 15 minute values were converted to pressure values by application of the appropriate pressure sensor calibration data. The pressure values were then converted to sea levels using the density values derived from sea water samples taken from each of the sites. The 15 minute values were then filtered to hourly values and the resulting series tidally analysed to provide the harmonic constants listed in Tables 11 to 15. These harmonic constants were then used to calculate predicted hourly values for the period of the observations. The predicted hourly values were then subtracted from the observed hourly values to provide the residuals, examples of which are shown in Figures 11 to 15.

## **6. STATISTICAL ANALYSIS OF SURGE DATA**

### **6.1 Introduction**

Sea level responds to meteorological forces, affecting the local conditions almost instantaneously whereas the response to distant change is delayed. The

positive surge, that is the increase in sea level above the predicted tidal level due to meteorological conditions, brings floods, and negative surges, or the decrease in sea level below the predicted level, is a navigational hazard. To determine the true sea level a good surge forecast is as essential as accurate tidal predictions. DOODSON (1924) made an extensive correlation between daily mean sea level, air pressure and wind, and applied the regression technique to compute the contribution of pressure gradient to daily and monthly mean sea level. DARBYSHIRE & DARBYSHIRE (1956) applied the regression technique to investigate storm surges in the North Sea and detected external surges which travel from outside. HUNT (1972) and TOWNSEND (1975) applied similar regression techniques to surges on the east coast of Great Britain with additional terms to account for the effects of external surges. The response of the deep ocean to air pressure is static, but in shallow and coastal areas, wind stress and boundary conditions have significant influence on the sea level. Opinions differ on whether a linear or quadratic form of wind stress gives the best results. WELANDER (1961) used the quadratic wind stress for compilation of surges in the North Sea but suggested a very low value for the frictional constant. DAVIES ET AL (1985) have argued for a higher frictional constant in certain regions. DARBYSHIRE & DARBYSHIRE (1956) have shown that a linear wind stress gives as good results as a quadratic form. Locally, meteorological conditions may be normal, but changes which take place far away from the area under consideration can influence the sea level. To account for these external surges the areas where meteorological conditions influence surges at a port should be investigated. A simple approach is to compute the effect of external surges and to correlate surges at different ports. Surges at a port where the surge leads can then be used to update the surge at ports where it lags by estimating time lags and amplification factors. This technique can be applied if surges are consistent in progression. The approach worked well for positive surges on the east coast of Britain (DARBYSHIRE & DARBYSHIRE, 1956). However, progression of negative surges differ from those of positive surges in that the amplification factor and rate of progression is found to vary from surge to surge (TOWNSEND, 1975).

Statistical methods are unable to deal with the decaying process of a surge when meteorological forces are removed, with surge-tide interaction or with the dynamics of the system. HEAPS (1969) introduced a numerical method and used a numerical model based on a finite difference scheme to study the dynamics of surges and tides. The Celtic Sea and the Irish Sea are now extensively explored

by these numerical techniques (PROCTOR, 1987). At present, numerical models have been developed to the stage where an operational model (FLATHER, 1981) is regularly used for computing surges in the Irish Sea.

The main objectives of the present work are: (a) to develop a regression model for forecasting surges, negative surges in particular, in the vicinity of Barrow-in-Furness; (b) to examine the efficiency of numerical and regression models and to locate the areas where differences arise.

## **6.2 Analysis of observed surges and meteorological data**

Time series of surge elevations, air pressures, east-west (u) and north-south (v) components of winds have been statistically examined for changes both in the time and frequency domains. Surges from all stations are strongly correlated (Table 16) and surges at Holyhead lead others by about one hour. Typical cross-correlation functions between observed surges at Heysham, Port Patrick, Ramsden Dock and Halfway Shoals are shown in Figure 16a. Cross-correlations between surges and air pressure, and surges and the v-component of winds are very strong (Figure 16b). However, correlations between surges and the u-component of winds are weak but are still above the level of significance. These cross-correlations further suggest that surges lead air pressure. Depressions, which are responsible for time-variation of air pressure, often travel eastward and the response of the sea is faster than the rate of travel of these depressions. This tendency for sea level to lead air pressure changes was first identified in Newlyn observations by DOODSON (1924). The time lead of surge elevations is considered to be due to winds which are correlated with, and anticipate, pressure changes. The sub-tidal energy is continuous across the spectrum and accounts for over 80% of the energy (Figure 17). The spectrum of air pressure energy is much steeper than those of the wind components. This suggests that the contribution of air pressure to surges is relatively large at low frequencies.

## **6.3 Regression technique**

Under normal meteorological conditions, variations in the sea level are due to the influence of well-defined tide-generating forces and the interaction of waves due to these forces. These changes in the sea level can be predicted on

any time scale. The changing pressure fields and associated winds over the sea surface introduce new forces into the system and sea level adjusts itself to accommodate these forces. Under the combined influence of tidal and meteorological forces, sea level at time  $t$ , measured from the mean sea level at a port, can be expressed as

$$\zeta_t = \zeta_t^{(T)} + S_t + Z_t \quad (1)$$

where  $\zeta_t^{(T)}$  is the tidal component,  
 $S_t$  is the surge component,  
 $Z_t$  is the noise due to forces which  
 are not accounted for here.

Since  $\zeta_t^{(T)}$  can be estimated quite accurately, the surge and changes due to meteorological forces can be separated as

$$R_t = \zeta_t - \zeta_t^{(T)} = S_t + Z_t \quad (2)$$

In the previous section, it is shown that surge elevations are correlated with air pressure as well as with winds, and it is difficult to distinguish between the contribution of one input force from that of the other. The response to these inputs is frequency dependent and the error on estimated values increases with frequency. A better approach is to use a multi-regression technique in which surge elevations are regressed with simultaneous air pressure and wind components as

$$R_t = a_1 P_{t-\tau_1} + a_2 u_{t-\tau_2} + a_3 v_{t-\tau_3} + Z_t \quad (3)$$

for a time sequence  $t_s = [s=0(1)m]$ , if  $l < m$  meteorological variables are included, equation (3) gives a system of equations which can be written as

$$\underline{R}_t = \underline{M}\underline{a} + \underline{Z} \quad (4)$$

since  $\underline{Z}$  has no direct relationship with the surge, the least squares solution of the system of equations (3) gives

$$\underline{a} = [\underline{M}'\underline{M}]^{-1} \underline{M}'\underline{R} \quad (5)$$

where  $\underline{M}'$  is the transpose of  $\underline{M}$ .



Regression coefficients computed from the observed input meteorological variables and the output surges, give the response of the sea level to individual forces. Some further refinement can be made to optimise the solution by replacing the linear wind by a quadratic wind stress and by changing the time lags so that the efficiency of the model is maximised.

The effectiveness of meteorological variables and their relative importance in the generation of surges at different ports is clearly demonstrated by the high level of correlations in Figure 16. To maximise the efficiency of the regression model, meteorological inputs and surge output are filtered to remove high frequencies ( $> 1.5$  cpd) which are not correlated. However, it is found that this filtering process does not affect the results very much as energy in the high frequency region is very small (Figure 17).

The surge at Holyhead has the greatest time lead over the surge at Ramsden Dock, being of the order of one hour, and this could not be included in the model as a spatial variable. The surge at Fishguard could not be included because of poor quality data.

For these reasons the regression model was based on meteorological inputs from Squires Gate. First, equation (4) was solved for all surges in bi-monthly sets, with wind input in the linear form, and the resulting coefficients are listed in Table 17. Coefficients were also estimated by using wind in the quadratic form and by adjusting the time lags. The results shown in Table 17 are for the optimal solution when winds are in the linear form, with air pressure leading the surge by one hour, and the v-component of wind leading the surge by 6 hours. The response of sea level to the u-component of wind is instantaneous. Time lags, computed from the simultaneous solution for air pressure, v-component and u-component of wind, are significantly different from those given by the correlation functions in Figure 16, thus suggesting that the contribution of one variable has considerable influence on the function of the other.

Air pressure has an almost inverted barometric effect on the sea level. The v-component of the wind is four times more effective than the u-component in the generation of surges around Barrow. The most effective directions of winds for negative and positive surges are  $10^{\circ}$ T and  $190^{\circ}$ T respectively.

Averaged coefficients were used to compute Oct-Dec 1985 surges, which were not used in the evaluation of regression coefficients. Statistics in Table 18 show that the regression model gives almost as good results as a numerical model.

When equation (4) is solved to compute the regression coefficients for only negative surges in 1986, a considerable change in the response of the sea level is observed. Coefficients in Table 19 show that the response to wind is doubled although the influence of air pressure is almost unchanged. The most effective wind direction for the generation of negative surges is  $17^{\circ}\text{T}$ . There may be a small time lag between meteorological inputs and surge output but this is not detected because the scanning interval is 3 hours and the response of the sea level appears to be instantaneous.

Surges reproduced by using the regression coefficients in Table 19 are shown in Figure 18. Visually, it is difficult to establish whether regression model surges or numerical model surges are best. Mathematically, the superiority of numerical models is quite clearly shown by the variance of unpredicted surges (Table 20).

#### **6.4 Relationship between negative surge and tide phases**

The phases of observed surges are examined for their relationship with the phase of tide. No particular relationship is observed as surge peaks are shown to occur at rising as well as falling tides (Figure 19). Some troughs of surges are also seen to occur at high tides and others at low tides. Also troughs of negative surges are underestimated in magnitude in that forecast surges are always higher than the minima of observed surges.

#### **6.5 Numerical Model**

Numerical models can take the dynamics of the system into account and can therefore deal with natural oscillations and the decaying process of the surge when meteorological forces are removed. Regression models have no mechanism to deal with these problems (PROUDMAN & DOODSON, 1924). Numerical models can also deal better with external surges and their progression as compared with regression models. An operational model of the Irish Sea (FLATHER, 1981) was used to forecast surges for the 1985-86 period. A comparison between the spectra

of the observed and model surges (Figure 20a) shows that the model underestimates the surge energy throughout the spectrum. Differences between the regression model and the numerical model occur in the diurnal band where the numerical model is more efficient. The amplitude responses of the Heysham model to observed negative surges are given in Table 21. The response of the surge to input from the model (Figure 21) confirms the result that model surges are underestimated and lag observed surges. Also, models are not efficient enough to deal with the frequency dependence of the response functions. The performance of the numerical model in different frequency bands is shown in Figure 20b. This suggests that models collapse in semi-diurnal and higher frequency regions where surge-tide interaction is more important than the direct influence of meteorological forces. On average the numerical model is about 5% more efficient than the regression model (Table 18).

## 6.6 Conclusions

(1) The efficiencies of the numerical model and of the regression model in reproducing surges vary from surge to surge. On average, the numerical model can account for 65% and the regression model for 59% of the variance of a surge.

(2) In the regression model, the response of the sea level to air pressure is about  $-0.81\text{cm mb}^{-1}$ , and winds from  $10^{\circ}\text{T}$  ( $190^{\circ}$ ) are the most effective for the generation of negative or positive surges.

(3) The regression model performs better with linear winds than with quadratic winds.

(4) Spatial gradients of air pressure were always small and could not improve the regression model.

(5) In the frequency domain, both the numerical model and the regression model are quite efficient at low frequencies where they can account for over 75% of the surge variance. In the diurnal band the efficiency drops to 33% for the numerical model and to 25% for the regression model.

(6) Both the numerical and the regression models are unable to reproduce semi-diurnal surges or surges resulting from surge-tide interaction.

(7) The numerical model surges are underestimated by 4% at Ramsden Dock and at Roa Island and by 1% at Halfway Shoals.

(8) In the case of negative surges, the efficiency of both the numerical and regression models decreases further. The influence of wind is almost twice as much as that for all surges, but the response to air pressure is unchanged. The effective wind direction for negative surges is  $17^\circ T$ . However, a change in this direction has only a small effect, possibly because of the uncertainty due to the small sample size.

## 7. NUMERICAL MODEL OF MORECAMBE BAY

### 7.1 Introduction

In this section, we describe some experiments with a regional model of Morecambe Bay. The aim of the experiments was to investigate the variations within the Bay arising from combinations of local wind, externally generated surge and tide. An understanding of these variations and their causes could provide a basis for deriving improved surge estimates at points along the approach channel to Ramsden Dock from surge forecasts for Heysham produced by the operational shelf model running at the Meteorological Office.

In the following sub-sections, we give an outline of the model; describe results obtained for the  $M_2$  constituent of the tide, with verification of the model solution against observations; and give results for spring tide conditions, uniform winds from the north and east acting over the Bay, and for an externally generated negative surge introduced at the open boundary of the model. Simulation of a negative surge in the period 29 January to 7 February 1986 is also described.

### 7.2 Outline of the model

The model used in the investigations is based on the depth-averaged equations expressed in spherical polar co-ordinates, which take the form:

Continuity

$$\frac{\partial \zeta}{\partial t} + \frac{1}{R \cos \phi} \left\{ \frac{\partial}{\partial \chi} (DU) + \frac{\partial}{\partial \phi} (DV \cos \phi) \right\} = 0 \quad (1)$$

U equation of motion

$$\begin{aligned} & \frac{\partial U}{\partial t} - 2\omega \sin\phi V + \frac{U}{R \cos\phi} \frac{\partial U}{\partial \chi} - \frac{UV}{R} \tan\phi + \frac{V}{R} \frac{\partial U}{\partial \phi} \\ = & - \frac{g}{R \cos\phi} \frac{\partial \zeta}{\partial \chi} - \frac{1}{\rho R \cos\phi} \frac{\partial p_a}{\partial \chi} + \frac{\tau_{sx}}{\rho D} - \frac{\tau_{bx}}{\rho D} \end{aligned} \quad (2)$$

V equation of motion

$$\begin{aligned} & \frac{\partial V}{\partial t} + 2\omega \sin\phi U + \frac{V}{R} \frac{\partial V}{\partial \phi} + \frac{U^2 \tan\phi}{R} + \frac{U}{R \cos\phi} \frac{\partial V}{\partial \chi} \\ = & - \frac{g}{R} \frac{\partial \zeta}{\partial \phi} - \frac{1}{\rho R} \frac{\partial p_a}{\partial \phi} + \frac{\tau_{sy}}{\rho D} - \frac{\tau_{by}}{\rho D} \end{aligned} \quad (3)$$

where the notation is:

$\chi, \phi$	east-longitude and latitude, respectively,
$t$	time
$\zeta$	elevation of sea surface above the undisturbed level,
$h$	undisturbed depth of water,
$D=h+\zeta$	total depth of water,
$R$	radius of the Earth,
$\omega$	angular speed of the Earths rotation,
$\rho$	density of sea water,
$g$	acceleration due to gravity,
$\tau_{sx}, \tau_{sy}$	components of surface wind stress to the east and north respectively,
$\tau_{bx}, \tau_{by}$	components of bottom stress to the east and north resp.,
$p_a$	atmospheric pressure at the sea surface,
$U, V$	components of depth mean current given by

$$U = \frac{1}{d} \int_{-h}^{\zeta} u(z) dz \quad , \quad V = \frac{1}{d} \int_{-h}^{\zeta} v(z) dz \quad (4)$$

$u(z), v(z)$  components of current in the directions of increasing  $\chi, \phi$  respectively, at a depth  $z$  below the undisturbed sea surface.

The surface stress,  $\tau_s$ , is assumed to be related to the surface wind velocity at 10m,  $w$ , by a quadratic law:

$$\tau_s = C_D \rho_a w |w| \quad (5)$$

where  $\rho_a$  is the density of air and  $C_D$  is a surface drag coefficient, itself related to wind speed by

$$C_D = (0.63 + 0.066|w|).10^{-3} \quad (6)$$

(SMITH & BANKE, 1975).

A quadratic law of bottom friction is used to relate the bottom stress,  $\tau_b$ , to the depth mean current:

$$\tau_b = k\rho\bar{U}|\bar{U}| \quad (7)$$

where k takes a constant value of 0.0025.

In the equations of motion, the surface and bottom stresses are divided by the total water depth, D. In order to prevent these terms from becoming infinite in the shallow water areas where drying occurs, a minimum value for D of 1.0m is used in these terms.

Boundary conditions of zero normal flow

$$q_n = 0 \quad (8)$$

are applied on coastal or land boundaries, where  $q_n$  is the normal component of depth mean current. On open-sea boundaries, either elevation is specified as a function of position and time

$$\zeta = \hat{\zeta}(\chi, \phi, t) \quad (9)$$

or a "radiation" condition

$$q_n = \hat{q}_n - \frac{c}{h}(\zeta - \hat{\zeta}) \quad (10)$$

is applied, where  $\hat{q}_n$  and  $\hat{\zeta}$  are specified and  $c = (gh)^{\frac{1}{2}}$ .

The equations are solved by means of an explicit finite-difference technique, incorporating the essential elements of the schemes described in FLATHER & HEAPS (1975) and DAVIES & FLATHER (1978). An important feature of the system is that it allows for the displacement of the coastal boundary, so permitting the exposure of drying banks with the falling tide and their subsequent submergence as the tide rises again to be represented in the model solution. The approach used was developed by FLATHER & HEAPS (1975) and

incorporates a critical elevation difference between adjacent grid boxes. This was set to be 0.1m.

The computational grid, covering Morecambe Bay and part of the neighbouring eastern Irish Sea, is shown in Figure 22 and is an adaptation and improvement of that used by STEPHENS (1983). The resolution has 54 grid elements per degree of longitude and 81 per degree of latitude, giving a grid size of 1.21 km E-W and 1.37 km N-S. This is sufficient to represent the main features of the bathymetry of the Bay but does not allow the narrow channels, such as that between Ramsden Dock and Hawes Point to be represented in detail: a grid size of no more than 100m would be required for this. The model bathymetry is plotted in Figure 23. The important features to note are the Lune Deep with a maximum depth of 47m, which forms a deep water channel to Heysham, the extensive area of shallow banks in the northern part of the Bay and the channel through to Barrow. The timestep used in the model calculations was 37.26 s.

### 7.3 Results for $M_2$ and spring tides

Calculations were carried out first to reproduce the main  $M_2$  constituent of the tide. Open boundary input data for use in the (preferred) radiation condition (10) were taken from STEPHENS (1983). Starting from an initial state of zero surface elevation and no motion, the model was run for a total of 12 cycles of  $M_2$  to establish the tidal regime. Data, comprising arrays of computed surface elevation and depth-mean current were stored at intervals of 1/4 lunar hour during the final cycle for subsequent analysis.

Figure 24 shows contours of amplitude and phase of  $M_2$  obtained from this analysis. It is closely similar to the distributions previously published, but amplitudes are slightly (~10cm) larger than those obtained by FLATHER & HEAPS (1978) and slightly (~5cm) smaller than those produced by STEPHENS (1983).

A comparison between computed and observed values of the amplitude and phase of  $M_2$  is given in Table 22, along with the source of the "observed" data. The observed values from DOODSON & CORKAN (1932) are, in fact, estimates which are less reliable than values derived from harmonic analyses. It should also be noted that some comparisons, indicated by \*, are affected by the fact that either the relevant model grid point dries out near low water or the tide gauge is

located in an area subject to "ponding" or both.

Overall, the agreement is excellent, particularly along the approach channel to Barrow (see results for Ramsden Dock, Roa Island and Halfway Shoals). The phase differences between Ramsden Dock and Halfway Shoals ( $6.0^\circ$  in the model and  $6.1^\circ$  from the observations) and the equivalent amplification of the  $M_2$  constituent (1.044 in the model and 1.038 from observations) suggest that the model reproduces the tidal propagation extremely accurately, remarkably so given the rather coarse representation of the channel mentioned earlier.

Having established the ability of the model to reproduce the  $M_2$  tide accurately, consideration was given to modelling spring tide conditions. Two alternative approaches were available: (i) introduce an additional constituent,  $S_2$ , which, combined with  $M_2$  gives a variation in the tidal range from approximately mean spring to mean neap conditions; (ii) scale the  $M_2$  tidal input by an appropriate factor so as to approximate mean spring tides.

For investigation of the response of the Bay to surges at spring tides, the first option has the disadvantage of yielding a continually varying tidal range, which presents some difficulties in synchronising spring tides and the surge effects to be investigated. The second approach, on the other hand, would give perpetual spring tide conditions, effectively removing this difficulty. Consequently the second approach was adopted for this purpose whereas the first approach was used in simulating a specific surge event as described later.

An examination of observed tidal ranges at Barrow, Heysham, Liverpool and Holyhead suggested that the appropriate scaling factor was  $4/3$  and the input values of elevation and depth-mean current for  $M_2$  were consequently multiplied by this factor to approximate mean spring conditions. The model was then re-run, in similar fashion to that described earlier for  $M_2$ , except that arrays of elevation and current at every timestep during the final tidal cycle were stored, permitting a detailed examination of the results. The maximum and minimum values of computed elevation were then extracted and the difference taken, giving an estimate of the mean spring tidal range from the model. Equivalent values from observations are not readily available, and indeed, mean high water springs (MHWS) and mean low water springs (MLWS) are parameters which cannot be derived easily from a set of harmonic constants nor from a tidal record. However,



approximate values are published in the Admiralty Tide Tables, and a fair estimate can be derived from harmonic constants by taking twice the sum of the amplitudes of  $M_2$  and  $S_2$ . Table 23 gives a comparison of the various estimates available for locations not affected by drying (in the model) or ponding. The agreement overall is very good. In particular, the model reproduces the varying range of spring tide along the approach channel to Barrow remarkably accurately.

#### 7.4 Response of Morecambe Bay to local winds and externally generated surges

Having established that the model is capable of representing the tides, and in particular, spring tides with good accuracy, the next stage in the investigation was to consider surge effects. Surges will, in general, be made up of a component generated with the Bay, mainly by the local winds acting over its surface, and a component generated outside the Bay in the eastern Irish Sea and beyond. Previous work on surge variations within Morecambe Bay (FLATHER 1981) suggested that there could be significant local variability associated with drying and other processes, and that resolution could be important in determining how a model represented these effects. The grid size of the present model is finer (by a factor of 3) than the finest model used by FLATHER (1981) and so should give a more realistic representation of these effects than obtained previously.

Three basic model runs were carried out to determine the response of the Bay to:

- (i) a uniform easterly wind stress acting over the interior;
- (ii) a uniform northerly wind stress; and
- (iii) an external surge, constant in time and uniform in magnitude, introduced at the open boundary.

In cases (i) and (ii), the wind stress magnitude was taken to be  $1 \text{ N/m}^2$ , which, adopting the drag coefficient due to SMITH & BANKE (1975) as used in the operational storm surge model (e.g. FLATHER, 1984), corresponds to a wind speed of about 20m/s, which is gale force. In case (iii), the external surge magnitude was taken to be -1m. In every case, the storm surge response was computed together with the spring tide so as to take account of interaction effects.

The procedure adopted was to start from the solution for spring tides established previously and to switch on the appropriate forcing. For case (iii), using the radiation condition (10), the external surge contribution to  $\hat{\zeta}$  was taken to be -1m at all open boundary points, and the corresponding contribution to  $\hat{q}_n$  was assumed to be zero. The model was then run for a further 3 tidal cycles to allow the solution to adjust to the additional forcing. During this period, data were stored at intervals of 1/4 lunar hour and at every timestep during the final cycle. A corresponding run without meteorological forcing or external surge input gave the solution for spring tides alone, which could be subtracted from the combined solution to give the surge residual.

The evolution of the surge residuals for a sample of grid points shown in Figure 25 is plotted in Figures 26 (east wind), 27 (north wind) and 28 (external surge) for the 3 tidal cycles during which the forcing was applied. It is clear from Figures 26-28 that the adjustment of the Bay was very rapid, taking only a few (perhaps 2-3) hours. This is an important point, since it suggests that, except for local winds or external surges that vary rapidly in time, the response of the Bay will be nearly stationary. The surge responses do nevertheless show very significant variations with time, but these variations are clearly related to the tidal cycle and repeat with the tidal period. They can, therefore, be attributed to surge-tide interactions. The most extreme manifestation of these effects can be seen in Figure 28, where, for some locations zero (or near-zero) residuals occur during part of each tidal cycle when the grid point is "dry".

The response to easterly winds tends to be small except, predictably, near the eastern side of the Bay, where residuals are typically -25cm; see, for example, point (32,23) corresponding to Heysham. Here, the residuals are slightly enhanced near low waters and decreased near high waters, consistent with the variability in the forcing term,  $\tau_s/D$ , implied by tidal changes in total water depth,  $D$ . At shallower points in the east of the Bay, the tidal variation is much stronger, with residuals reaching -70cm in the early stages of the rising tide. These effects are associated with a phase lag of the low water of tide and surge on that due to tide alone.

Detailed responses, comprising variations of tide alone, tide with easterly winds and residual plotted using values stored at every timestep during the final cycle for points located along the approach channel from Halfway Shoals to Barrow

are shown in Figure 29. These plots show a number of interesting features. First, a distortion of the tidal curve, increasing towards Ramsden Dock, and producing not only the expected lengthening of the period of falling tide and shortening of the rising tide but a marked "bumpiness" in the 2-3 hours before high water. This may be due to interaction between the flows entering the channel from the north and the south. The effect is closely similar in both tide with surge and tide only solutions. Also apparent are shorter period oscillations, again affecting both tide only and tide + surge solutions in similar fashion. These oscillations are seiching motions set up in sections of the channel by the drying out or flooding of neighbouring model elements. Their periods, typically a few minutes, depend on the water depth in the particular section of channel affected. Both of these effects could be influenced by the rather coarse model resolution and the lack of detailed bathymetric data for the channel from Ramsden Dock to Lowsy Point. However, the main conclusion is that the residuals due to easterly winds acting over the Bay are small, only about -10cm in magnitude near high water.

The response to winds from the north tends to be larger at points in the northern part of the Bay, with values reaching -100cm at some locations and certain times. The detailed plots, Figure 30, show that the largest residuals, occurring in the early stages of the rising tide, increase in magnitude towards Ramsden Dock reaching a maximum of -65cm there. However, the residuals near high water are substantially smaller, typically -20cm, although the "bumpiness" and seiching effects mentioned earlier cause some variability. The model results for winds from the east and north are, therefore, consistent with those from the analysis of observations in suggesting that the wind direction most likely to produce negative surges at Barrow is roughly NNE.

Finally, Figures 28 and 31 show equivalent results for the externally generated surge. The responses are substantially greater than those typical of local wind effects, reaching a maximum magnitude of about -180cm. There is a marked contrast between the results at locations in deeper water close to the main body of the Bay such as Heysham (32,23), Halfway Shoals (18,23) and Wyre Light (27,29), and at points in the shallower regions, for example Ramsden Dock (17,18). At deeper points, the response is fairly constant and equal to the input value, with small variations of order 10cm. At shallower locations, the variations, closely related to the tides, are dominant. Figure 31 shows very

clearly the development of the interaction between Halfway Shoals and Ramsden Dock. The greatest variation in the residual, from -45cm to -172cm at Ramsden Dock, occurs near low water but significant residual oscillations with amplitude 10-20cm persist up to the time of high water. It would appear, therefore, that tide-surge interactions which develop along the approach channel to Barrow will be very important in determining surges and total water levels at Ramsden Dock. The fact that the operational surge model, with resolution 30km, is unable to even begin to resolve this channel implies that it would not on its own be able to predict these variations.

It is of interest, then, to examine the possibility that the present model, taking account of those interaction effects, might give improved predictions for Ramsden Dock. This question is examined in the next section.

#### **7.4 Simulation of a negative surge using the Morecambe Bay model**

In order to examine further the development of surges in the approaches to Ramsden Dock and to determine whether the Morecambe Bay model might improve on the predictions produced by the operational shelf model, a simulation of the period 29 January to 7 February 1986 was carried out with the model. This period contained the largest negative surge registered at Ramsden Dock during the period of the measurements.

Two model runs were carried out: the first for tide alone, with open boundary input representing the  $M_2$  and  $S_2$  constituents. The  $S_2$  data required were inferred from the  $M_2$  data by assuming a constant amplitude ratio ( $S_2/M_2$ ) of 0.324, and a constant phase difference ( $S_2-M_2$ ) of -315.850; these values being derived from tidal analyses for Ramsden Dock. Specification of two input constituents yields a tide with a spring-neap variation (as discussed earlier) approximating the true tide during the period of interest. Figure 32 shows the model-predicted tides for representative locations. The second model run was for tide and surge together. In this, the externally generated surge, introduced with the tide on the model open boundary was assumed to be given by the surge predicted by the operational model at the nearest grid point to Morecambe Bay. Output distributions of surface wind and pressure computed by the Met. Office's 15-level weather prediction model were processed to provide forcing by components of wind stress (using (5) and (6)) and variations in surface atmospheric

pressure.

Model computed distributions of elevation and depth-mean current in components from both solutions were stored at intervals of 1 hour. Differences, giving the surge component, were then computed. Time series of computed surge for points along the channel from Halfway Shoals to Ramsden Dock and for Heysham are plotted in Figure 33, with hourly observed residuals at Halfway Shoals, Ramsden Dock and Heysham also included. As might be expected from results presented in the preceding section, there is increasing variability in the form of short period oscillations with amplitude 0(20cm) towards Ramsden Dock.

Figure 34 shows, on a larger scale, for Halfway Shoals and Ramsden Dock, the surge residuals derived from observations, from the present solution, and from the operational shelf model. The times of tidal high water are indicated by a circle on the nearest hourly observed residual. At Halfway Shoals there are differences of up to 7cm between the surge computed using the Morecambe Bay model and that from the shelf model with, perhaps, some small improvement in accuracy on the basis of comparison with the observations. However, this improvement is small compared with the largest errors, which are up to 30cm.

For Ramsden Dock, there are much greater differences - up to 20cm - between the surge computed using the present model and that from the shelf model. These differences are substantially due to the oscillations which occur in the Morecambe Bay model solution and which, on the basis of the results of the preceding section, are associated with tide-surge interaction effects in the approach Channel. However, there is also a more slowly varying component which does appear to give better agreement with observations than provided by the shelf model; in particular near the peak of the negative surge early on 2 January.

The accuracy to which the surges at Halfway Shoals and Ramsden Dock can be predicted is clearly dependent upon the accuracy of the externally generated surge open boundary input. This is illustrated in Figure 34 on the second day of the storm (30 January 1986) when both the Morecambe Bay and operational models considerably underestimate the magnitude of the negative surge.

## 7.5 Conclusions

1. The Morecambe Bay model is able to reproduce the  $M_2$  component of the tide with good accuracy. Spring tide conditions also seem to be reproduced very well.
2. The model was used to investigate the responses of the Bay to local winds and to externally generated surges. The adjustment time of the Bay to imposed forcing was found to be short, perhaps 2-3 hours.
3. The wind responses were consistent with the findings of the statistical analysis in suggesting that winds from NNE would be most effective in generating negative surges at Barrow.
4. There are significant "tidal" variations in the surge residuals taking the form of damped oscillations which increase in magnitude along the approach channel to Barrow. These effects appear to be due to tide-surge interactions.
5. The computed responses suggest that these locally generated variations will be significant in determining surge residuals at Ramsden Dock. The effect of local winds blowing over the Bay was to produce negative surges at Ramsden Dock at high water in the range 10-20 cm. The response at Ramsden Dock to an externally generated negative surge of 1m also included variations in the surge residual of this magnitude near tidal high water.
6. Simulation of surge and tide motion during the period 29 January to 7 February 1986 gave results consistent with those expected on the basis of the analysis of responses.
7. Significant local variations were predicted by the model and there was some indication that the results were marginally better than those from the operational shelf model. However, a substantial contribution to the total error arose from the surge introduced on the open boundary of the Morecambe Bay model, taken directly from the shelf model.

8. If surges along the approach channel to Barrow are to be predicted with typical accuracy better than 20cm, improved estimates of the externally generated surge component and the ability to take account of the local surge-tide interactions will be needed.
9. The limitations of the present model in resolving the approaches to Barrow must be borne in mind. It would be useful to construct and experiment with a high resolution (~100m grid) model to confirm (or otherwise) the importance of the surge-tide interactions found here.
10. A very high resolution model could also provide information on currents which could be useful for navigation and dredging purposes.

## **8. RECOMMENDATIONS**

Regarding the requirement for practical forecasts, both the regression model and the operational surge model can provide useful information. It is suggested that both approaches be implemented and the "worst case", whether this results from the regression model or the dynamical model, be used. It should be noted that both techniques tend to underestimate the magnitude of negative surges on some occasions.

The experiments with the Morecambe Bay model suggested that effects due to local winds and interaction in the approaches to Ramsden Dock must be significant. Further work might provide a better understanding of these local influences, leading eventually to a more satisfactory forecast procedure.

## **9. ACKNOWLEDGEMENTS**

This work has been carried out by the Proudman Oceanographic Laboratory under contract to the Ministry of Defence. The authors gratefully acknowledge the contributions of a number of colleagues at POL, especially those involved in the hard work of measurement and processing of the tidal data required.

## 10. REFERENCES

- AMIN, M. 1982. On analysis of forecasting of surges on the west coast of Great Britain.  
Geophysical Journal of the Royal Astronomical Society, 68, 79-94.
- DARBYSHIRE, J. & DARBYSHIRE, M. 1956. Storm surges in the North Sea during the winter 1953-54.  
Proceedings of the Royal Society of London, A, 235, 260-274.
- DAVIES, A.M. & FLATHER, R.A. 1978. Application of numerical models of the north west European continental shelf and the North Sea to the computation of the storm surges of November to December, 1973.  
Deutsche Hydrographische Zeitschrift, Ergänzungsheft, A, No.14, 72pp.
- DAVIES, A.M., SAUVEL, J. & EVANS, J. 1985. Computing near coastal tidal dynamics from observations and a numerical model.  
Continental Shelf Research, 4, 341-366.
- DOODSON, A.T. 1924. Meteorological perturbations of sea-level and tides.  
Monthly Notices of the Royal Society, Geophysical Supplement, 1, 124-147.
- DOODSON, A.T. & CORKAN, R.H. 1932. The principal constituent of the tides in the English and Irish Channels.  
Philosophical Transactions of the Royal Society of London, A, 231, 29-53.
- FLATHER, R.A. & HEAPS, N.S. 1975. Tidal computations for Morcambe Bay.  
Geophysical Journal of the Royal Astronomical Society, 42, 489-517.
- FLATHER, R.A. 1984. A numerical model investigation of the storm surge of 31 January and 1 February 1953 in the North Sea.  
Quarterly Journal of the Royal Meteorological Society, 110, 591-612.
- GRAFF, J. & KARUNARATNE, D.A. 1980. Accurate reduction of sea level records.  
International Hydrographic Review, 57(2), 151-166.
- HEAPS, N.S. 1969. A two-dimensional numerical model.  
Philosophical Transaction of the Royal Society of London, A, 265, 93-137.
- HEAPS, N.S. & JONES, J.E. 1975. Storm surge computations for the Irish Sea using a three-dimensional numerical model.  
Memoires de la Societe Royal des Sciences de Liege, Series 7, 6, 287-333.
- HUNT, R.D. 1972. North Sea storm surges.  
Marine Observer, 42, 115-124.



- PALIN, R.I.R. & RAE, J.B. 1987. Data transmission and acquisition systems for shore-based sea-level measurements.  
pp. 1-6 in, Fifth International Conference on Electronics for Ocean Technology, Heriot-Watt University, 1987. London: Institution of Electronic and Radio Engineers. 225pp. (IERE Publication No.72).
- PROCTOR, R. 1987. A three dimensional numerical model of the eastern Irish Sea.  
pp. 25-45 in, Numerical modelling: applications to marine systems, (Ed. J. Noye). Amsterdam: North-Holland. 295pp.
- PROUDMAN, J. & DOODSON, A.T. 1924. Time relations in meteorological effects on the sea.  
Proceedings of the London Mathematical Society, Series 2, 24, 140-149.
- SMITH, S.D. & BANKE, E.G. 1975. Variation of the sea surface drag coefficient with wind speed.  
Quarterly Journal of the Royal Meteorological Society, 101, 665-673.
- STEPHENS, C.V. 1983. Hydrodynamic modelling developments for the west coast of the British Isles.  
Liverpool University, Ph.D. thesis. 213pp.
- TOWNSEND, J. 1975. Forecasting 'negative' storm surges in the southern North Sea.  
Marine Observer, 45, 27-35.
- WELANDER, P. 1961. Numerical prediction of storm surges.  
pp. 315-379 in, Vol.8, Advances in geophysics, (Ed. H.E. Landsberg & J. Van Miegheem). New York: Academic. 392pp.

<u>Location</u>	<u>Visits</u>	<u>Data Recovery</u>	<u>Comments</u>
Lowsy Point	14 Sept 85		Installed (ponding)
	18 Feb 86	14 Sept - 16 Feb	Tape run out
	13 May 86	18 Feb - 13 May	
	23 Sept 86	13 May - 31 July	Air supply leak
	11 Feb 87	23 Sept - 11 Feb	
	29 Apr 87	11 Feb - 29 Apr	Data loss (tape problems)
Ramsden Dock	7 Jan 85		Aanderaa installed
	29 Apr 85	7 Jan - 29 Apr	Air supply problems
	15 Sept 85	29 Apr - 15 Sept	Compressor fitted
	17 Feb 86	15 Sept - 17 Feb	
	13 May 86	17 Feb - 13 May	
	24 Sept 86	13 May - 24 Sept	
	11 Feb 87	24 Sept - 11 Feb	
29 Apr 87	11 Feb - 29 Apr	22 extra scans	
Roa Island	16 Sept 85		Installed
	18 Feb 86	16 Sept - 12 Feb	Tape run out
	14 May 86	18 Feb - 14 May	
	23 Sept 86	14 May - 23 Sept	Air leak, errors
	12 Feb 87	23 Sept - 12 Feb	
	30 Apr 87	12 Feb - 30 Apr	Some data loss (tape)
Hawes Point	17 Sept 85		Installed (dries)
	19 Feb 86	20 Oct - 19 Feb	Air supply problems
	14 May 86	19 Feb - 14 May	
	24 Sept 86	14 May - 24 Sept	
	11 Feb 87	24 Sept - 11 Feb	
	30 Apr 87	11 Feb - 30 Apr	6 extra scans
Halfway Shoals	23 Sept 85		Deployed
	21 Feb 86	23 Sept - 15 Feb	Tape run out
	2 June 86	21 Feb - 2 June	
	25 Sept 86	2 June - 25 Sept	Set to 30 min sampling
	6 May 87		Recovery attempt
	30 Oct 87	25 Sept - 4 Aug	Recovered
Lightning Knoll	23 Sept 85		Deployed
	21 Feb 86		Recovery attempt
	2 June 86		" "
	25/26 Sept 86		" "
	6 May 87		" "
	30 Oct 87		" "

Table 1: Data recovery from POL installed tide gauges

## MEAN SEA LEVEL PRINT-OUT

PORT - HEYSHAM

YEAR - 86

UNITS - M

DATUM = DATUM OF DATA

JANUARY															
5.190	5.010	4.871	5.177	5.117	4.895	4.963	5.029	5.111	5.519	5.461	5.249	5.519	5.816	5.108	
4.975	5.111	5.316	5.513	5.524	5.453	5.678	5.607	5.030	5.042	5.160	5.140	5.234	5.115	4.721	
4.683															
MONTHLY MEAN SEA LEVEL				5.204	NO OF DAYS			31							
FEBRUARY															
4.494	4.504	4.807	4.913	4.952	4.857	4.834	4.962	4.998	5.029	5.008	4.912	4.892	4.901	5.014	
4.941	4.943	5.091	5.150	5.158	5.258	5.132	4.981	5.032	5.011	4.857	4.746	4.660			
MONTHLY MEAN SEA LEVEL				4.930	NO OF DAYS			28							
MARCH															
4.643	4.891	5.147	5.455	5.427	5.328	5.133	5.174	5.123	5.017	5.027	5.072	5.097	5.138	5.152	
5.164	5.110	5.156	5.089	5.515	5.115	5.393	5.381	5.344	5.166	5.209	5.460	5.399	5.232	5.192	
5.275															
MONTHLY MEAN SEA LEVEL				5.194	NO OF DAYS			31							
APRIL															
5.181	5.107	4.989	4.940	4.869	4.771	4.608	4.589	4.645	4.603	4.883	4.999	5.099	5.149	5.147	
5.061	4.936	5.132	5.224	5.334	5.273	5.271	5.235	5.195	5.113	5.132	5.133	5.224	5.169	5.214	
MONTHLY MEAN SEA LEVEL				5.041	NO OF DAYS			30							
MAY															
5.119	5.108	5.151	5.144	5.195	5.217	5.238	5.192	5.217	5.494	5.362	5.513	5.418	5.311	5.268	
5.154	5.350	5.390	5.081	5.200	5.483	5.379	5.300	5.285	5.360	5.274	5.470	5.130	5.017	5.076	
5.101															
MONTHLY MEAN SEA LEVEL				5.258	NO OF DAYS			31							
JUNE															
5.070	5.071	5.134	5.108	5.073	5.086	5.157	5.229	5.387	5.270	5.103	5.120	5.084	4.983	4.988	
5.074	5.107	5.037	5.020	4.935	4.985	5.053	5.073	5.183	5.092	4.999	5.003	5.006	5.006	5.069	
MONTHLY MEAN SEA LEVEL				5.083	NO OF DAYS			30							
JULY															
5.122	5.154	5.181	5.239	5.239	5.227	5.168	5.120	5.110	5.074	5.030	5.027	5.036	5.051	5.051	
5.204	5.110	5.002	5.042	5.121	5.116	5.114	5.116	5.119	5.194	5.244	5.280	5.276	5.285	5.281	
5.302															
MONTHLY MEAN SEA LEVEL				5.149	NO OF DAYS			31							
AUGUST															
5.271	5.537	5.123	5.130	5.140	5.289	5.193	5.098	5.037	5.012	5.013	5.047	5.174	5.303	5.449	
5.306	5.149	5.098	5.066	5.054	5.126	5.081	5.049	5.023	4.968	4.773	5.062	5.134	5.090	5.041	
5.139															
MONTHLY MEAN SEA LEVEL				5.128	NO OF DAYS			31							
SEPTEMBER															
5.197	5.218	5.051	5.023	5.076	5.095	5.085	5.034	5.054	5.075	5.072	5.084	5.148	5.129	5.039	
5.006	4.942	4.839	4.941	5.028	5.099	5.098	5.074	5.052	5.079	5.150	5.196	5.190	5.086	5.071	
MONTHLY MEAN SEA LEVEL				5.074	NO OF DAYS			30							
OCTOBER															
5.139	5.057	5.025	5.015	5.103	5.101	5.149	5.113	5.282	5.222	5.121	5.141	5.178	5.159	5.039	
5.003	5.078	5.357	5.482	5.489	5.498	5.592	5.392	5.699	5.810	5.232	5.357	5.391	5.447	5.601	
5.202															
MONTHLY MEAN SEA LEVEL				5.273	NO OF DAYS			31							
NOVEMBER															
4.977	5.077	5.097	5.097	5.287	5.116	5.414	5.420	5.725	5.676	5.299	5.290	5.436	5.402	5.381	
5.497	5.382	5.442	5.309	5.248	5.287	5.886	5.512	5.477	5.620	5.424	5.193	5.168	5.097	5.128	
MONTHLY MEAN SEA LEVEL				5.345	NO OF DAYS			30							
DECEMBER															
5.304	5.337	5.616	5.530	5.594	5.314	5.519	5.425	5.292	5.364	5.506	5.433	5.493	5.311	5.641	
5.441	5.510	5.581	5.448	5.193	5.015	4.884	4.958	5.151	5.168	5.266	5.268	5.435	5.446	5.570	
5.374															
MONTHLY MEAN SEA LEVEL				5.367	NO OF DAYS			31							
ANNUAL MEAN SEA LEVEL				5.171	NO OF DAYS			365							

Table 2

-----  
 EXTREME HOURLY ELEVATIONS PRINT-OUT  
 -----

PORT - HEYSHAM

YEAR - 86

UNITS - M

DATUM = DATUM OF DATA

MONTH	I	MINIMA			I	MAXIMA		
		HEIGHT	DAY	HR.		HEIGHT	DAY	HR.
JANUARY	I	0.879	30	21	I	10.319	14	14
FEBRUARY	I	0.379	27	20	I	9.793	11	13
MARCH	I	0.810	26	18	I	10.720	27	12
APRIL	I	0.597	25	18	I	10.159	26	12
MAY	I	0.916	24	18	I	10.180	25	12
JUNE	I	0.962	23	6	I	9.803	24	0
JULY	I	0.828	24	8	I	9.880	24	1
AUGUST	I	0.806	21	7	I	9.963	21	0
SEPTEMBER	I	0.675	19	6	I	9.821	20	0
OCTOBER	I	0.684	6	7	I	10.000	19	0
NOVEMBER	I	0.699	4	7	I	10.090	5	13
DECEMBER	I	0.896	2	6	I	10.439	3	12
ANNUAL	I	0.379	27	20	I	10.720	27	12

DATUM = ORDNANCE DATUM (NEWLYN)

MONTH	I	MINIMA			I	MAXIMA		
		HEIGHT	DAY	HR.		HEIGHT	DAY	HR.
JANUARY	I	-4.021	30	21	I	5.419	14	14
FEBRUARY	I	-4.521	27	20	I	4.893	11	13
MARCH	I	-4.090	26	18	I	5.820	27	12
APRIL	I	-4.303	25	18	I	5.259	26	12
MAY	I	-3.984	24	18	I	5.280	25	12
JUNE	I	-3.938	23	6	I	4.903	24	0
JULY	I	-4.072	24	8	I	4.980	24	1
AUGUST	I	-4.094	21	7	I	5.063	21	0
SEPTEMBER	I	-4.225	19	6	I	4.921	20	0
OCTOBER	I	-4.216	6	7	I	5.100	19	0
NOVEMBER	I	-4.201	4	7	I	5.190	5	13
DECEMBER	I	-4.004	2	6	I	5.539	3	12
ANNUAL	I	-4.521	27	20	I	5.820	27	12

Table 3

## PORT TITLE ENGLAND, WEST COAST - HEYSHAM

IOS PORT NO	ATT PORT NO	IHB SHEET NO	COUNTRY CODE	SEA CODE	LATITUDE	LONGITUDE
50	441		74	19	54 2' 0.3"N	2 54' 42.3" W

DATA LENGTH (DAYS)	TYP	D	M	YEAR	CONSTANTS NDC OTH SWC	UNIT	TIME ZONE	TIME STEP	SOURCE	RECORD NUMBER
7064	0	01	1	1964	91 -47	0	m	GMT	3.0	POL

TIDE GAUGE ZERO (TGZ)	OBSERVATION DATUM (OBD)	ADMIRALTY CHART DATUM (ACD)	SO (TO OBD)
ODN + 0.000 m ACD + 4.900 m TGEM - 7.190 m	TGZ + 0.000 m	ODN - 4.90 m	0.249 m

TGEM : BOLT SOUTH QUAY SD 4030 6012

## NODAL CORRECTIONS U AND F OF DOODSON CONSTANTS SET TO 0. AND 1. FOR PREDICTIONS

*** CONSTITUENTS ***					*** CONSTITUENTS ***				
H	G	SIG	NO	NAME	H	G	SIG	NO	NAME
0.095	239.77	0.04107	1	SA	0.012	263.51	58.43973	49	SN4
0.025	127.93	0.08214	2	SSA	0.115	294.20	58.98410	50	MS4
0.013	205.66	0.54437	3	MM	0.033	300.53	59.06624	51	MK4
0.020	226.79	1.01590	4	MSF	0.014	335.14	60.00000	52	S4
0.023	216.30	1.09803	5	MF	0.008	345.65	60.08214	53	SK4
0.007	291.36	12.85429	6	2Q1	0.010	350.85	86.40794	54	2MN6
0.037	345.69	13.39866	8	Q1	0.019	11.65	86.95231	55	M6
0.009	351.72	13.47151	9	RH01	0.006	41.45	87.42383	56	MSN6
0.111	42.70	13.94304	10	O1	0.020	56.13	87.96821	57	2MS6
0.011	277.77	14.02517	11	MP1	0.006	56.90	88.05035	58	2MK6
0.011	265.00	14.49205	12	M1	0.004	94.07	88.98410	59	2SM6
0.003	133.73	14.91786	14	PI1	0.004	107.93	89.06624	60	MSK6
0.044	183.33	14.95893	15	P1	0.005	203.02	26.40794	61	2MN2S2
0.012	101.80	15.00000	16	S1	0.010	224.84	26.87018	62	3M(SK)2
0.121	191.54	15.04107	17	K1	0.017	215.72	26.95231	63	3M2S2
0.005	143.50	15.08214	18	PSI1	0.004	249.23	28.35759	65	SNK2
0.003	190.17	15.12321	19	PHI1	0.005	248.96	42.38277	68	MQ3
0.003	221.83	15.51259	20	THETA1	0.003	341.85	43.00928	69	2MP3
0.004	290.16	15.58544	21	J1	0.004	172.04	44.56955	70	2MQ3
0.006	19.33	16.05696	22	SO1	0.007	7.29	56.87018	71	3MK4
0.003	334.83	16.13910	23	O01	0.012	12.40	56.95231	72	3MS4
0.012	256.57	27.34170	24	OQ2	0.005	65.20	57.88607	73	2MSK4
0.009	85.12	27.42383	25	MNS2	0.005	232.60	73.00928	76	3MO5
0.079	278.81	27.89535	26	2N2	0.003	316.39	86.48079	82	2MV6
0.023	67.27	27.96821	27	MU2	0.003	257.57	88.51258	85	3MSN6
0.600	301.63	28.43973	28	N2	0.004	177.02	114.84767	87	2(MN)8
0.137	300.84	28.51258	29	NU2	0.011	200.27	115.39204	88	3MN8
0.012	293.89	28.90197	30	OP2	0.015	225.39	115.93642	89	M8
3.150	325.31	28.98410	31	M2	0.009	237.85	116.40794	90	2MSN8
0.010	138.55	29.06624	32	MKS2	0.021	271.61	116.95231	91	3MS8
0.058	337.02	29.45563	33	LAMDA2	0.005	275.93	117.03445	92	3MK8
0.141	343.50	29.52848	34	L2	0.008	301.87	117.96821	94	2(MS)8
0.057	358.25	29.95893	35	T2	0.004	314.79	118.05035	95	2MSK8
1.026	7.73	30.00000	36	S2	0.003	28.91	145.93642	96	4MS10
0.011	9.92	30.04107	37	R2	0.008	71.71	27.49669	101	MVS2
0.294	6.74	30.08214	38	K2	0.032	97.72	27.88607	102	2MK2
0.031	212.71	30.54437	39	MSN2	0.021	277.82	28.94304	103	MA2
0.007	222.44	30.62651	40	KJ2	0.009	9.09	29.02517	104	MA2*
0.035	232.46	31.01590	41	2SM2	0.016	229.98	31.09803	106	SKM2
0.013	275.99	42.92714	42	MO3	0.006	335.36	56.40794	107	2MNS4
0.036	311.99	43.47616	43	M3	0.021	220.30	57.49669	108	MV4
0.010	340.81	43.94304	44	SO3	0.017	91.94	58.51258	109	3MN4
0.013	54.80	44.02517	45	MK3	0.011	331.39	59.52848	110	2MSN4
0.014	100.64	45.04107	46	SK3	0.008	147.94	28.39866	111	NA2
0.072	214.99	57.42383	47	MN4	0.003	333.39	28.48080	112	NA2*
0.195	243.90	57.96821	48	M4					

Table 4

MEAN SEA LEVEL PRINT-OUT  
-----

PORT - PORTPATRICK                      YEAR - 86                      UNITS - M

DATUM = DATUM OF DATA

JANUARY														
5.308	5.186	4.999	5.311	5.221	5.004	5.217	5.197	5.229	5.572	5.357	5.136	5.345	5.317	4.866
4.912	5.053	5.199	5.273	5.337	5.326	5.505	5.302	4.835	4.958	5.128	5.056	5.168	5.083	4.787
4.754														
MONTHLY MEAN SEA LEVEL	5.159				NO OF DAYS	31								
FEBRUARY														
4.621	4.598	4.835	4.918	4.944	4.890	4.859	4.946	4.981	5.080	5.102	5.051	5.095	5.110	5.153
5.091	5.064	5.085	5.104	5.117	5.186	5.087	4.997	5.009	5.024	4.957	4.855	4.781		
MONTHLY MEAN SEA LEVEL	4.984				NO OF DAYS	28								
MARCH														
4.738	4.910	5.147	5.368	5.349	5.216	5.064	5.202	5.100	4.971	5.010	5.072	5.113	5.163	5.181
5.154	5.086	5.127	5.040	5.372	4.988	5.288	5.211	5.191	4.980	5.102	5.364	5.299	5.104	5.097
5.146														
MONTHLY MEAN SEA LEVEL	5.134				NO OF DAYS	31								
APRIL														
5.054	4.998	4.905	4.855	4.790	4.729	4.634	4.615	4.655	4.646	4.823	4.929	5.050	5.133	5.060
4.914	4.845	5.040	5.162	5.247	5.219	5.193	5.155	5.103	5.045	5.081	5.075	5.202	5.125	5.170
MONTHLY MEAN SEA LEVEL	4.982				NO OF DAYS	30								
MAY														
5.120	5.066	5.047	5.107	5.166	5.179	5.193	5.145	5.175	5.387	5.242	5.427	5.280	5.219	5.133
5.082	5.297	5.293	5.033	5.163	5.374	5.260	5.203	5.188	5.260	5.180	5.259	4.992	4.904	4.978
4.982														
MONTHLY MEAN SEA LEVEL	5.172				NO OF DAYS	31								
JUNE														
4.954	4.981	5.014	4.979	4.975	5.007	5.062	5.164	5.318	5.156	5.010	5.062	5.016	4.932	4.944
5.042	5.013	4.981	5.027	4.975	4.994	5.060	5.084	5.149	5.092	5.012	5.025	5.002	4.998	5.054
MONTHLY MEAN SEA LEVEL	5.036				NO OF DAYS	30								
JULY														
5.078	5.125	5.127	5.176	5.185	5.161	5.105	5.057	5.065	5.033	5.005	5.005	5.016	5.025	5.038
5.191	5.037	4.959	4.999	5.054	5.064	5.044	5.035	5.075	5.140	5.201	5.237	5.220	5.150	5.207
5.165														
MONTHLY MEAN SEA LEVEL	5.096				NO OF DAYS	31								
AUGUST														
(INCOMPLETE)														
5.191	5.352	5.069	5.096	5.111	5.279	5.073	5.010	5.008	4.998	4.975	5.014	5.141	5.237	5.289
5.160	5.083	5.045	5.010	5.003	5.096	5.078	0.000	0.000	0.000	0.000	0.000	0.000	0.000	0.000
0.000														
MONTHLY MEAN SEA LEVEL	5.105				NO OF DAYS	22								
SEPTEMBER														
(INCOMPLETE)														
0.000	0.000	0.000	4.947	4.981	5.012	5.001	4.978	5.006	5.022	5.033	5.048	5.111	5.059	4.964
4.938	4.880	4.792	4.890	4.967	5.023	5.037	5.022	5.007	5.044	5.100	5.137	5.130	5.035	5.055
MONTHLY MEAN SEA LEVEL	5.008				NO OF DAYS	27								
OCTOBER														
5.090	4.993	4.970	5.002	5.060	5.034	5.056	5.085	5.231	5.163	5.069	5.119	5.154	5.143	5.014
4.955	5.087	5.287	5.295	5.303	5.322	5.401	5.199	5.563	5.399	5.100	5.353	5.262	5.264	5.396
5.094														
MONTHLY MEAN SEA LEVEL	5.176				NO OF DAYS	31								
NOVEMBER														
4.936	5.019	5.006	4.977	5.126	5.021	5.283	5.194	5.659	5.554	5.217	5.306	5.483	5.386	5.352
5.501	5.302	5.321	5.207	5.170	5.238	5.722	5.225	5.280	5.434	5.211	5.085	5.109	5.029	5.073
MONTHLY MEAN SEA LEVEL	5.248				NO OF DAYS	30								
DECEMBER														
5.177	5.218	5.484	5.375	5.373	5.248	5.523	5.293	5.148	5.317	5.411	5.445	5.413	5.236	5.542
5.233	5.299	5.356	5.132	4.949	4.868	4.802	4.878	5.063	5.059	5.084	5.043	5.211	5.268	5.423
5.229														
MONTHLY MEAN SEA LEVEL	5.229				NO OF DAYS	31								
ANNUAL MEAN SEA LEVEL	5.111				NO OF DAYS	353								

Table 5

EXTREME HOURLY ELEVATIONS PRINT-OUT  
-----

PORT - PORTPATRICK                      YEAR - 86                      UNITS - M

DATUM = DATUM OF DATA

MONTH	I	MINIMA			I	MAXIMA		
		HEIGHT	DAY	HR.		HEIGHT	DAY	HR.
JANUARY	I	3.059	30	21	I	7.439	10	11
FEBRUARY	I	2.959	28	20	I	7.048	11	13
MARCH	I	3.036	1	21	I	7.413	27	12
APRIL	I	2.914	7	17	I	7.037	26	13
MAY	I	3.196	28	9	I	7.111	25	0
JUNE	I	3.185	26	9	I	7.006	25	1
JULY	I	3.061	23	7	I	7.120	25	2
AUGUST	I	3.060	20	6	I	7.103	22	1
SEPTEMBER	I	2.942	18	5	I	6.970	21	1
OCTOBER	I	3.159	6	7	I	7.192	19	0
NOVEMBER	I	3.090	4	6	I	7.150	16	11
DECEMBER	I	3.182	2	5	I	7.373	12	21
ANNUAL	I	2.914	7	17	I	7.439	10	11

DATUM = ORDNANCE DATUM (NEWLYN)

MONTH	I	MINIMA			I	MAXIMA		
		HEIGHT	DAY	HR.		HEIGHT	DAY	HR.
JANUARY	I	-1.741	30	21	I	2.639	10	11
FEBRUARY	I	-1.841	28	20	I	2.248	11	13
MARCH	I	-1.764	1	21	I	2.613	27	12
APRIL	I	-1.886	7	17	I	2.237	26	13
MAY	I	-1.604	28	9	I	2.311	25	0
JUNE	I	-1.615	26	9	I	2.206	25	1
JULY	I	-1.739	23	7	I	2.320	25	2
AUGUST	I	-1.740	20	6	I	2.303	22	1
SEPTEMBER	I	-1.858	18	5	I	2.170	21	1
OCTOBER	I	-1.641	6	7	I	2.392	19	0
NOVEMBER	I	-1.710	4	6	I	2.350	16	11
DECEMBER	I	-1.618	2	5	I	2.573	12	21
ANNUAL	I	-1.886	7	17	I	2.639	10	11

Table 6

## PORT TITLE : SCOTLAND, WEST COAST - PORTPATRICK

IOS PORT NO	ATT PORT NO	IHB SHEET NO	COUNTRY CODE	SEA CODE	LATITUDE	LONGITUDE
63	415		74	18	54 50' 32.7" N	5 7' 8.0" W

DATA LENGTH (DAYS)	TYP	D	M	YEAR	CONSTANTS NDC OTH SWC	UNIT	TIME ZONE	TIME STEP	SOURCE	RECORD NUMBER
3287	0	2	1	1968	93 0 0	m	GMT	3.0	IOS	160

TIDE GAUGE ZERO (TGZ)	OBSERVATION DATUM (OBD)	ADMIRALTY CHART DATUM (ACD)	SO (TO OBD)
ODN - 4.800 m ACD - 3.000 m TGEM - 9.820 m	TGZ + 0.000 m	ODN - 1.80 m	5.115 m

MSL IS THE MEAN OF NINE YEARS - 1968 - 1976 (INCLUSIVE)  
 TGBM: OSBM (BOLT) ON TOP OF HARBOUR WALL (NW99765421)

## \*\*\* CONSTITUENTS \*\*\*

## \*\*\* CONSTITUENTS \*\*\*

H	G	SIG	NO	NAME	H	G	SIG	NO	NAME
0.082	238.07	0.04107	1	SA	0.003	92.09	59.06624	51	MK4
0.032	180.15	0.08214	2	SSA	0.003	227.71	60.00000	52	S4
0.020	209.89	0.54437	3	MM	0.002	225.97	60.08214	53	SK4
0.011	226.37	1.01590	4	MSF	0.002	221.09	86.40794	54	2MN6
0.020	183.06	1.09803	5	MF	0.003	231.36	86.95231	55	M6
0.007	286.47	12.85429	6	ZQ1	0.001	237.15	87.42383	56	MSN6
0.001	184.17	12.92714	7	SIGMA1	0.005	257.66	87.96821	57	2MS6
0.033	341.83	13.39866	8	Q1	0.001	257.07	88.05035	58	2MK6
0.007	351.01	13.47151	9	RH01	0.003	203.91	26.40794	61	2MN2S2
0.100	42.77	13.94304	10	O1	0.005	255.41	26.87018	62	3M(SK)2
0.008	285.59	14.02517	11	MP1	0.011	242.21	26.95231	63	3M2S2
0.001	132.82	14.56955	13	CHI1	0.002	246.68	28.35759	65	SNK2
0.002	155.46	14.91786	14	PI1	0.001	334.56	29.91786	66	2SK2
0.037	184.75	14.95893	15	P1	0.002	0.17	42.38277	68	MQ3
0.015	104.47	15.00000	16	S1	0.003	350.96	43.00928	69	2MP3
0.106	190.11	15.04107	17	K1	0.001	334.62	44.56955	70	2MQ3
0.004	147.55	15.08214	18	PSI1	0.003	149.13	56.95231	72	3MS4
0.003	247.52	15.51259	20	THETA1	0.001	269.65	72.46026	75	M5
0.003	295.41	15.58544	21	J1	0.001	322.58	85.39204	78	3MNS6
0.004	52.05	16.05696	22	SO1	0.001	348.85	85.93642	80	4MS6
0.001	359.34	16.13910	23	OO1	0.001	223.47	86.48079	82	2MV6
0.008	270.31	27.34170	24	OQ2	0.001	23.14	86.87018	83	3MSK6
0.011	118.76	27.42383	25	MNS2	0.001	73.01	87.49669	84	4MN6
0.033	280.45	27.89535	26	2N2	0.001	104.34	88.51258	85	3MSN6
0.034	129.61	27.96821	27	MU2	0.001	187.45	114.84767	87	2(MN)8
0.253	305.98	28.43973	28	N2	0.001	215.78	115.39204	88	3MN8
0.064	310.33	28.51258	29	NU2	0.002	257.49	115.93642	89	M8
0.008	339.44	28.90197	30	OP2	0.001	294.46	116.40794	90	2MSN8
1.332	332.43	28.98410	31	M2	0.003	326.24	116.95231	91	3MS8
0.007	155.89	29.06624	32	MKS2	0.001	333.58	117.03445	92	3MK8
0.034	352.45	29.45563	33	LAMDA2	0.001	13.52	117.96821	94	2(MS)8
0.064	357.65	29.52848	34	L2	0.001	39.15	118.05035	95	2MSK8
0.023	8.12	29.95893	35	T2	0.002	352.47	145.93642	96	4MS10
0.375	16.32	30.00000	36	S2	0.001	35.35	146.95231	97	3M2S10
0.002	36.59	30.04107	37	R2	0.001	233.41	174.92052	99	5MS12
0.108	15.02	30.08214	38	K2	0.001	265.58	175.93642	100	4M2S12
0.019	234.57	30.54437	39	MSN2	0.007	93.94	27.49669	101	MVS2
0.002	187.78	30.62651	40	KJ2	0.021	120.77	27.88607	102	2MK2
0.024	258.29	31.01590	41	2SM2	0.009	292.04	28.94304	103	MA2
0.006	26.98	42.92714	42	MO3	0.003	13.01	29.02517	104	MA2*
0.020	98.95	43.47616	43	M3	0.002	50.31	30.47152	105	MSV2
0.003	120.60	43.94304	44	SO3	0.011	252.24	31.09803	106	SKM2
0.008	194.98	44.02517	45	MK3	0.001	127.20	56.40794	107	2MNS4
0.006	274.38	45.04107	46	SK3	0.002	165.76	58.51258	109	3MN4
0.003	153.69	57.42383	47	MN4	0.001	116.30	59.52848	110	2MSN4
0.003	305.13	57.96821	48	M4	0.004	188.15	28.39866	111	NA2
0.008	87.96	58.98410	50	MS4					

Table 7



MEAN SEA LEVEL PRINT-OUT  
-----

PORT - HOLYHEAD

YEAR - 86

UNITS - M

DATUM = DATUM OF DATA

## JANUARY

3.437 3.340 3.154 3.397 3.329 3.150 3.359 3.302 3.260 3.497 3.349 3.169 3.341 3.378 3.037  
3.046 3.162 3.289 3.403 3.396 3.390 3.569 3.417 3.052 3.107 3.204 3.143 3.248 3.211 2.960  
2.911

MONTHLY MEAN SEA LEVEL 3.258 NO OF DAYS 31

## FEBRUARY

2.795 2.790 3.007 3.075 3.098 3.031 2.997 3.058 3.054 3.121 3.124 3.120 3.187 3.211 3.270  
3.246 3.229 3.246 3.252 3.260 3.314 3.212 3.124 3.135 3.132 3.044 2.936 2.891

MONTHLY MEAN SEA LEVEL 3.106 NO OF DAYS 28

## MARCH

2.864 3.029 3.216 3.418 3.405 3.320 3.170 3.227 3.174 3.069 3.083 3.153 3.169 3.182 3.219  
3.220 3.186 3.215 3.149 3.350 3.090 3.330 3.312 3.350 3.097 3.204 3.394 3.343 3.170 3.198  
3.275

MONTHLY MEAN SEA LEVEL 3.212 NO OF DAYS 31

## APRIL

3.211 3.156 3.080 3.022 2.957 2.888 2.809 2.812 2.811 2.800 2.932 3.048 3.169 3.298 3.335  
3.210 3.088 3.218 3.295 3.353 3.382 3.324 3.277 3.222 3.137 3.144 3.154 3.257 3.187 3.199

MONTHLY MEAN SEA LEVEL 3.126 NO OF DAYS 30

## MAY

3.183 3.220 3.238 3.294 3.313 3.306 3.290 3.229 3.248 3.398 3.306 3.445 3.336 3.329 3.268  
3.237 3.428 3.323 3.140 3.253 3.393 3.259 3.222 3.206 3.253 3.209 3.268 3.082 3.018 3.074  
3.101

MONTHLY MEAN SEA LEVEL 3.254 NO OF DAYS 31

## JUNE

3.091 3.108 3.147 3.128 3.131 3.153 3.200 3.259 3.380 3.279 3.140 3.150 3.114 3.058 3.105  
3.192 3.152 3.118 3.171 3.130 3.147 3.185 3.201 3.241 3.166 3.133 3.154 3.129 3.158 3.183

MONTHLY MEAN SEA LEVEL 3.163 NO OF DAYS 30

## JULY

3.203 3.236 3.235 3.278 3.292 3.261 3.205 3.174 3.159 3.136 3.116 3.109 3.115 3.127 3.136  
3.235 3.116 3.069 3.095 3.145 3.152 3.136 3.130 3.163 3.228 3.270 3.301 3.349 3.290 3.361  
3.300

MONTHLY MEAN SEA LEVEL 3.197 NO OF DAYS 31

## AUGUST

3.379 3.424 3.183 3.222 3.228 3.389 3.180 3.118 3.124 3.125 3.109 3.147 3.268 3.347 3.372  
3.263 3.213 3.161 3.116 3.109 3.213 3.218 3.145 3.130 3.297 3.139 3.173 3.226 3.183 3.157  
3.202

MONTHLY MEAN SEA LEVEL 3.212 NO OF DAYS 31

## SEPTEMBER

3.219 3.214 3.108 3.086 3.094 3.124 3.123 3.123 3.144 3.171 3.206 3.225 3.287 3.244 3.163  
3.103 3.038 2.938 2.993 3.051 3.103 3.141 3.169 3.185 3.213 3.270 3.285 3.240 3.165 3.170

MONTHLY MEAN SEA LEVEL 3.153 NO OF DAYS 30

## OCTOBER

3.201 3.126 3.114 3.136 3.148 3.114 3.165 3.197 3.333 3.310 3.220 3.262 3.296 3.265 3.134  
3.084 3.167 3.360 3.404 3.414 3.443 3.521 3.357 3.662 3.506 3.273 3.470 3.407 3.338 3.429  
3.273

MONTHLY MEAN SEA LEVEL 3.295 NO OF DAYS 31

## NOVEMBER

3.139 3.120 3.098 3.066 3.197 3.130 3.359 3.324 3.652 3.584 3.371 3.418 3.564 3.521 3.433  
3.518 3.392 3.449 3.363 3.324 3.387 3.657 3.312 3.416 3.548 3.315 3.163 3.179 3.125 3.143

MONTHLY MEAN SEA LEVEL 3.342 NO OF DAYS 30

## DECEMBER

3.233 3.253 3.482 3.466 3.448 3.329 3.557 3.494 3.319 3.444 3.494 3.505 3.491 3.371 3.587  
3.323 3.394 3.466 3.262 3.143 3.081 2.990 3.042 3.165 3.186 3.214 3.169 3.300 3.390 3.543  
3.358

MONTHLY MEAN SEA LEVEL 3.339 NO OF DAYS 31

ANNUAL MEAN SEA LEVEL 3.221 NO OF DAYS 365

Table 8

EXTREME HOURLY ELEVATIONS PRINT-OUT  
-----

PORT - HOLYHEAD

YEAR - 86

UNITS - M

DATUM = DATUM OF DATA

MONTH	I	MINIMA			I	MAXIMA		
		HEIGHT	DAY	HR.		HEIGHT	DAY	HR.
JANUARY	I	0.442	12	18	I	6.141	10	10
FEBRUARY	I	0.219	27	18	I	5.791	11	12
MARCH	I	0.413	29	6	I	6.227	27	11
APRIL	I	0.265	25	17	I	5.912	24	10
MAY	I	0.503	25	17	I	5.906	25	11
JUNE	I	0.632	23	5	I	5.770	23	23
JULY	I	0.442	24	6	I	5.789	25	1
AUGUST	I	0.461	21	5	I	5.931	21	23
SEPTEMBER	I	0.292	18	4	I	5.710	19	23
OCTOBER	I	0.428	5	5	I	5.915	18	23
NOVEMBER	I	0.297	4	5	I	5.798	2	22
DECEMBER	I	0.452	2	4	I	6.051	3	11
ANNUAL	I	0.219	27	18	I	6.227	27	11

DATUM = ORDNANCE DATUM (NEWLYN)

MONTH	I	MINIMA			I	MAXIMA		
		HEIGHT	DAY	HR.		HEIGHT	DAY	HR.
JANUARY	I	-2.608	12	18	I	3.091	10	10
FEBRUARY	I	-2.831	27	18	I	2.741	11	12
MARCH	I	-2.637	29	6	I	3.177	27	11
APRIL	I	-2.785	25	17	I	2.862	24	10
MAY	I	-2.547	25	17	I	2.856	25	11
JUNE	I	-2.418	23	5	I	2.720	23	23
JULY	I	-2.608	24	6	I	2.739	25	1
AUGUST	I	-2.589	21	5	I	2.881	21	23
SEPTEMBER	I	-2.758	18	4	I	2.660	19	23
OCTOBER	I	-2.622	5	5	I	2.865	18	23
NOVEMBER	I	-2.753	4	5	I	2.748	2	22
DECEMBER	I	-2.598	2	4	I	3.001	3	11
ANNUAL	I	-2.831	27	18	I	3.177	27	11

Table 9

## PORT TITLE : WALES - HOLYHEAD

IOS PORT NO	ATT PORT NO	IHB SHEET NO	COUNTRY CODE	SEA CODE	LATITUDE	LONGITUDE
54	478		74	19	53 18' 27.1" N	4 37' 48.0" W

DATA LENGTH (DAYS)	TYP	D	M	YEAR	CONSTANTS NDC OTH SWC	UNIT	TIME ZONE	TIME STEP	SOURCE	RECORD NUMBER
2918	0	01	01	1964	107 0 0	m	GMT	3.0	IOS	20

TIDE GAUGE ZERO (TGZ)	OBSERVATION DATUM (OBD)	ADMIRALTY CHART DATUM (ACD)	SO (TO OBD)
ODN - 6.831 m ACD - 3.783 m TGEM - 11.573 m	TGZ + 0.000 m	ODN - 3.05 m	6.990 m

CONSTANTS : FROM ANALYSIS OF DATA 1964-71      ZO : AVERAGE OF M.S.L. 1961-71  
 TGBM : O.S.B.M. (BOLT) SH 24798221 SITED AT S.W. ANGLE OF ATR HUT

## \*\*\* CONSTITUENTS \*\*\*

## \*\*\* CONSTITUENTS \*\*\*

H	G	SIG	NO	NAME	H	G	SIG	NO	NAME
0.069	230.61	0.04107	1	SA	0.020	264.07	87.96821	57	2MS6
0.011	121.90	0.08214	2	SSA	0.006	263.72	88.05035	58	2MK6
0.027	238.77	0.54437	3	MM	0.004	322.42	88.98410	59	2SM6
0.030	211.23	1.01590	4	MSF	0.002	292.64	89.06624	60	MSK6
0.024	205.11	1.09803	5	MF	0.005	183.07	26.40794	61	2MN2S2
0.006	279.43	12.85429	6	2Q1	0.003	234.94	26.87018	62	3M(SK)2
0.001	153.37	12.92714	7	SIGMA1	0.009	218.67	26.95231	63	3M2S2
0.033	334.90	13.39866	8	Q1	0.002	200.11	28.35759	65	SNK2
0.007	349.91	13.47151	9	RHO1	0.001	106.89	29.91786	66	2SK2
0.098	29.73	13.94304	10	O1	0.001	189.42	42.38277	68	MQ3
0.010	288.09	14.02517	11	MP1	0.003	275.73	43.00928	69	2MP3
0.002	95.45	14.56955	13	CHI1	0.001	145.93	44.56955	70	2MQ3
0.002	126.40	14.91786	14	PI1	0.002	165.09	56.87018	71	3MK4
0.038	169.68	14.95893	15	P1	0.004	186.73	56.95231	72	3MS4
0.013	118.86	15.00000	16	S1	0.001	210.22	57.88607	73	2MSK4
0.101	175.26	15.04107	17	K1	0.002	300.13	71.91124	74	3MK5
0.006	136.35	15.08214	18	PSI1	0.001	39.28	72.46026	75	M5
0.002	191.97	15.12321	19	PHI1	0.002	72.39	73.00928	76	3MO5
0.002	84.35	15.51259	20	THETA1	0.001	329.17	84.84767	77	2(MN)S6
0.004	275.72	15.58544	21	J1	0.003	355.32	85.39204	78	3MNS6
0.005	18.25	16.05696	22	SO1	0.001	6.48	85.85428	79	4MK6
0.003	334.14	16.13910	23	OO1	0.003	40.24	85.93642	80	4MS6
0.006	240.83	27.34170	24	OQ2	0.001	24.55	86.32580	81	2MSNK6
0.011	129.10	27.42383	25	MNS2	0.004	214.19	86.48079	82	2MV6
0.048	241.87	27.89535	26	2N2	0.002	47.16	86.87018	83	3MSK6
0.038	181.40	27.96821	27	MU2	0.004	81.64	87.49669	84	4MN6
0.360	265.90	28.43973	28	N2	0.005	118.57	88.51258	85	3MSN6
0.073	274.13	28.51258	29	NU2	0.001	306.39	88.59472	86	MKL6
0.008	305.00	28.90197	30	OP2	0.001	14.20	115.39204	88	3MN8
1.810	291.88	28.98410	31	M2	0.002	31.66	115.93642	89	M8
0.005	195.23	29.06624	32	MKS2	0.001	18.22	116.40794	90	2MSN8
0.025	326.79	29.45563	33	LAMDA2	0.002	61.67	116.95231	91	3MS8
0.047	312.02	29.52848	34	L2	0.001	101.27	117.96821	94	2(MS)8
0.032	320.66	29.95893	35	T2	0.001	75.77	118.05035	95	2MSK8
0.596	327.81	30.00000	36	S2	0.002	178.64	145.93642	96	4MS10
0.006	3.79	30.04107	37	R2	0.002	211.22	146.95231	97	3M2S10
0.172	326.53	30.08214	38	K2	0.001	327.65	174.37615	98	4MSN12
0.010	209.06	30.54437	39	MSN2	0.001	6.47	174.92052	99	5MS12
0.008	155.14	30.62651	40	KJ2	0.001	46.82	175.93642	100	4M2S12
0.016	221.74	31.01590	41	2SM2	0.007	110.62	27.49669	101	MVS2
0.003	255.24	42.92714	42	MO3	0.017	104.78	27.88607	102	2MK2
0.019	246.05	43.47616	43	M3	0.011	246.35	28.94304	103	MA2
0.003	299.26	43.94304	44	SO3	0.001	345.80	29.02517	104	MA2*
0.001	91.34	44.02517	45	MK3	0.003	334.96	30.47152	105	MSV2
0.002	47.78	45.04107	46	SK3	0.006	224.57	31.09803	106	SKM2
0.015	8.47	57.42383	47	MN4	0.003	137.02	56.40794	107	2MNS4
0.034	41.97	57.96821	48	M4	0.004	20.02	57.49669	108	MV4
0.001	121.25	58.43973	49	SN4	0.004	251.78	58.51258	109	3MN4
0.010	95.26	58.98410	50	MS4	0.001	82.99	59.52848	110	2MSN4
0.003	72.25	59.06624	51	MK4	0.002	118.77	28.39866	111	NA2
0.001	189.50	60.00000	52	S4	0.002	99.48	72.92714	113	MSO5
0.013	197.97	86.40794	54	2MN6	0.002	8.88	74.02517	114	MSK5
0.023	225.02	86.95231	55	M6	0.026	356.73	29.52848	115	2MN2
0.005	224.12	87.42383	56	MSN6					

Table 10

PROUDMAN OCEANOGRAPHIC LABORATORY (BIDSTON OBSERVATORY)  
HARMONIC TIDAL ANALYSIS.

PORT: BARROW : RAMSDEN DOCK

LATITUDE: 54 06' N

LONGITUDE: 3 12' W

TIME ZONE: GMT

LENGTH: 2 YEARS

FROM: 7TH JANUARY,1985

TO: 11TH FEBRUARY,1987

UNITS: METRES

AO: 5.004

FILTERED HOURLY DATA FROM 15 MINUTE OBSERVATIONS RECORDED BY AANDERAA WLR5.

DATUM OF OBSERVATIONS = CHART DATUM = 4.75 METRES BELOW ORDNANCE DATUM (NEWLYN)

OBSERVATION MEAN = 0.5007D+01 RESIDUAL MEAN = -0.8764D-04  
STD = 0.2303D+01 STD = 0.2210D+00

	H	G		SIGMA	H	G
SA	0.051	227.67	2MN2S2	26.40794	0.006	225.06
SSA	0.056	132.47	3M(SK)2	26.87018	0.010	227.67
MM	0.058	226.51	3M2S2	26.95231	0.017	208.43
MSF	0.028	220.10	SNK2	28.35759	0.001	39.93
MF	0.043	204.03	MQ3	42.38277	0.007	242.18
ZQ1	0.012	266.37	2MP3	43.00928	0.002	36.31
SIGMA1			2MQ3	44.56955	0.006	97.88
Q1	0.042	346.43	3MK4	56.87018	0.013	70.50
RHO1	0.008	350.98	3MS4	56.95231	0.004	65.71
O1	0.110	45.02	2MSK4	57.88607	0.002	115.22
MP1	0.014	288.10	3MK5	71.91124	0.005	77.29
M1	0.006	147.67	M5	72.46026	0.001	133.79
CHI1	0.004	110.56	3MOS	73.00928	0.007	257.61
PI1	0.003	226.43	2(MN)56	84.84767	0.001	336.58
P1	0.046	184.38	3MNS6	85.39204	0.003	9.92
S1	0.008	107.38	4MK6	85.85428	0.003	268.23
K1	0.119	195.46	4MS6	85.93642	0.005	32.37
PSI1	0.002	127.78	2MSNK6	86.32580	0.001	64.47
PHI1	0.004	171.63	2MV6	86.48079	0.002	47.42
THETA1	0.007	236.99	3MSK6	86.87018	0.001	24.53
J1	0.005	325.34	4MN6	87.49669	0.003	337.88
SO1	0.008	14.27	MKL6	88.59472	0.001	289.40
OO1	0.004	341.76	2(MN)8	114.84767	0.003	152.19
OQ2	0.014	260.46	3MN8	115.39204	0.007	174.10
MNS2	0.015	60.83	MB	115.93642	0.010	192.26
2N2	0.083	267.73	2MSN8	116.40794	0.008	220.67
MU2	0.052	42.84	3MS8	116.95231	0.012	241.95
N2	0.588	308.20	3MK8	117.03445	0.004	246.38
NU2	0.133	306.34	MSNK8	117.50597	0.001	276.45
OP2	0.022	278.98	2(MS)8	117.96821	0.006	291.27
M2	3.077	330.90	2MSK8	118.05035	0.004	292.28
MKS2	0.014	118.61	4MS10	145.93642	0.003	129.60
LAMDA2	0.065	333.89	3M2S10	146.95231	0.001	188.23
L2	0.111	337.17	MVS2	27.49669	0.009	52.32
T2	0.059	8.47	MA2	28.94304	0.009	249.93
S2	0.998	15.05	MB2	29.02517	0.010	8.98
R2	0.013	26.27	MSV2	30.47152	0.002	16.92
K2	0.287	13.60	SKM2	31.09803	0.019	220.54
MSN2	0.037	208.40	2MNS4	56.40794	0.002	73.67
KJ2	0.011	245.23	MV4	57.49669	0.022	227.73
2SM2	0.038	229.44	3MN4	58.51258	0.015	127.76
MO3	0.013	266.05	2MSN4	59.52848	0.008	357.53
M3	0.037	313.49	M5O5	72.92714	0.003	252.47
SO3	0.011	347.74	MSK5	74.02517	0.003	222.42
MK3	0.016	63.32				
SK3	0.015	109.33				
MN4	0.084	218.14				
M4	0.211	247.36				
SN4	0.019	267.83				
MS4	0.128	294.95				
MK4	0.039	290.81				
S4	0.020	328.47				
SK4	0.012	325.02				
2MN6	0.016	35.68				
M6	0.026	56.10				
MSN6	0.011	81.92				
2MS6	0.025	98.21				
2MK6	0.008	91.03				
2SM6	0.009	149.34				
MSK6	0.006	136.34				

Table 11

PROUDMAN OCEANOGRAPHIC LABORATORY (BIDSTON OBSERVATORY)  
HARMONIC TIDAL ANALYSIS.

PORT: LOWSY POINT

LATITUDE: 54 09.5' N

LONGITUDE: 3 14.5' W

TIME ZONE: GMT

LENGTH: 15 MONTHS

FROM: 14TH SEPTEMBER,1985 TO: 7TH FEBRUARY,1987

UNITS: METRES A0: 2.809

15 MINUTE OBSERVATIONS RECORDED BY AANDERAA WLR5.

DATUM OF OBSERVATIONS = TIDE GAUGE ZERO = 8.54 METRES BELOW LOCAL BM

OBSERVATION MEAN = 0.3648D+01  
STD = 0.1506D+01

N.B. DRIES OUT AT LOW WATER. DATA HAS BEEN CLIPPED FOR ANALYSIS.

	H	G		SIGMA	H	G
SA	0.071	235.01				
SSA	0.076	133.19	MA2	28.94304	0.026	251.97
MM	0.090	307.65	MB2	29.02517	0.015	39.78
MSF	0.140	58.69				
MF	0.022	155.05				
ZQ1	0.019	253.76				
SIGMA1	0.008	318.83				
Q1	0.040	354.66				
RHO1	0.008	265.05				
O1	0.093	49.32				
MP1	0.011	322.42				
M1	0.012	172.34				
CHI1	0.006	119.92				
PI1	0.008	311.84				
P1	0.033	174.56				
S1	0.007	106.10				
K1	0.114	203.42				
PSI1	0.005	158.68				
PHI1	0.011	173.24				
THETA1	0.012	275.44				
J1	0.005	332.17				
SO1	0.006	5.10				
OO1	0.003	39.95				
OO2	0.031	265.14				
MNS2	0.023	36.84				
2N2	0.098	250.29				
MU2	0.094	73.65				
N2	0.448	307.20				
NU2	0.138	312.94				
OP2	0.014	301.83				
M2	2.359	335.32				
MKS2	0.019	54.89				
LAMDA2	0.013	31.28				
L2	0.130	320.54				
T2	0.030	339.77				
S2	0.746	18.44				
R2	0.005	12.19				
K2	0.225	21.51				
MSN2	0.040	194.53				
KJ2	0.012	9.20				
2SM2	0.033	222.06				
MO3	0.017	311.17				
M3	0.030	300.57				
SO3	0.005	14.13				
MK3	0.027	85.15				
SK3	0.013	99.30				
MN4	0.149	233.28				
M4	0.453	261.70				
SN4	0.042	183.31				
MS4	0.266	301.81				
MK4	0.098	292.37				
S4	0.035	321.93				
SK4	0.021	296.74				
2MN6	0.049	70.81				
M6	0.111	92.36				
MSN6	0.027	11.09				
2MS6	0.084	128.56				
2MK6	0.034	118.85				
2SM6	0.023	145.11				
MSK6	0.015	104.67				

Table 12

PROUDMAN OCEANOGRAPHIC LABORATORY (BIDSTON OBSERVATORY)  
HARMONIC TIDAL ANALYSIS.

PORT: ROA ISLAND  
LATITUDE: 54 04' N  
LONGITUDE: 3 10' W  
TIME ZONE: GMT  
LENGTH: 11.5 MONTHS  
FROM: 16TH SEPTEMBER,1985 TO: 12TH FEBRUARY,1987  
UNITS: METRES AO: 4.623

FILTERED HOURLY DATA FROM 15 MINUTE OBSERVATIONS RECORDED BY AANDERAA WLR5.  
DATUM OF OBSERVATIONS = CHART DATUM = 4.373 METRES BELOW ORDNANCE DATUM (NEWLYN)  
OBSERVATION MEAN = 0.4623D+01 RESIDUAL MEAN = 0.4276D-06  
STD = 0.2298D+01 STD = 0.2432D+00

	H	G		SIGMA	H	G
SA	0.060	158.33	2MN2S2	26.40794	0.006	224.38
SSA	0.117	150.55	3M(SK)2	26.87018	0.009	225.85
MM	0.062	219.18	3M2S2	26.95231	0.013	230.31
MSF	0.039	212.34	SNK2	28.35759	0.003	249.44
MF	0.050	200.39	2SK2	29.91786	0.008	347.57
2Q1	0.021	261.14	MQ3	42.38277	0.007	241.01
SIGMA1	0.008	343.87	2MP3	43.00928	0.002	22.50
Q1	0.046	358.73	2MQ3	44.56955	0.005	77.83
RH01	0.006	328.65	3MK4	56.87018	0.016	53.92
O1	0.109	44.42	3MS4	56.95231	0.006	17.17
MP1	0.020	309.80	2MSK4	57.88607	0.001	324.43
M1	0.005	150.36	3MK5	71.91124	0.005	74.71
CHI1	0.007	102.21	3MO5	73.00928	0.006	250.64
PI1	0.011	291.36	3MNS6	85.39204	0.001	26.29
P1	0.045	171.74	4MK6	85.85428	0.002	185.41
S1	0.014	99.80	4MS6	85.93642	0.003	22.75
K1	0.119	190.28	2MSNK6	86.32580	0.002	64.27
PSI1	0.009	228.88	2MV6	86.48079	0.003	27.77
PHI1	0.008	206.70	3MSK6	86.87018	0.002	163.97
THETA1	0.007	237.80	4MN6	87.49669	0.003	250.25
J1	0.004	339.00	3MSN6	88.51258	0.003	241.25
SO1	0.009	9.12	MK16	88.59472	0.001	291.36
OO1	0.004	8.65	2(MN)8	114.84767	0.003	173.29
OQ2	0.016	254.08	3MN8	115.39204	0.007	198.74
MNS2	0.012	49.31	M8	115.93642	0.009	213.81
2N2	0.099	268.66	2MSN8	116.40794	0.007	236.43
MU2	0.045	50.74	3MS8	116.95231	0.012	262.95
N2	0.579	306.24	3MK8	117.03445	0.004	262.89
NU2	0.129	305.73	MSNK8	117.50597	0.002	277.06
OP2	0.017	256.67	2(MS)8	117.96821	0.006	305.29
M2	3.059	328.58	2MSK8	118.05035	0.003	302.07
MKS2	0.018	103.08	4MS10	145.93642	0.002	125.86
LAMDA2	0.072	331.85	3M2S10	146.95231	0.001	183.96
L2	0.103	341.82	MVS2	27.49669	0.010	77.42
T2	0.067	7.01	MA2	28.94304	0.006	218.66
S2	0.984	11.78	MB2	29.02517	0.020	346.33
R2	0.008	315.86	MSV2	30.47152	0.003	112.87
K2	0.289	11.30	SKM2	31.09803	0.020	221.06
MSN2	0.040	209.12	2MNS4	56.40794	0.004	39.53
KJ2	0.009	245.92	MV4	57.49669	0.023	226.80
2SM2	0.040	231.70	3MN4	58.51258	0.019	117.63
MO3	0.011	267.68	2MSN4	59.52848	0.010	338.04
M3	0.035	308.91	MSO5	72.92714	0.003	257.19
SO3	0.010	346.18	MSK5	74.02517	0.003	201.63
MK3	0.015	58.43				
SK3	0.013	96.08				
MN4	0.081	215.82				
M4	0.214	244.08				
SN4	0.019	274.46				
MS4	0.132	291.87				
MK4	0.039	286.30				
S4	0.018	327.89				
SK4	0.010	320.59				
2MN6	0.014	1.74				
M6	0.023	24.07				
MSN6	0.009	58.96				
2MS6	0.021	64.69				
2MK6	0.008	66.12				
2SM6	0.006	116.58				
MSK6	0.005	108.70				

Table 13

PROUDMAN OCEANOGRAPHIC LABORATORY (BIDSTON OBSERVATORY)  
HARMONIC TIDAL ANALYSIS.

PORT: HAWES POINT

LATITUDE: 54 03' N

LONGITUDE: 3 10' W

TIME ZONE: GMT

LENGTH: 11 MONTHS

FROM: 20TH OCTOBER, 1985

TO: 30TH APRIL, 1987

UNITS: METRES

A0: 2.465

15 MINUTE OBSERVATIONS RECORDED BY AANDERAA WLR5.

DATUM OF OBSERVATIONS = TGZ = 2.81 METRES BELOW ORDNANCE DATUM (NEWLYN)

OBSERVATION MEAN = 0.3359D+01

STD = 0.1742D+01

N.B. DRIES OUT AT LOW WATER. DATA HAS BEEN CLIPPED FOR ANALYSIS.

	H	G		SIGMA	H	G
SA	0.070	330.02	MA2	28.94304	0.048	237.36
SSA	0.098	188.00	MB2	29.02517	0.037	34.42
MM	0.080	248.99				
MSF	0.041	240.79				
MF	0.044	230.53				
ZQ1	0.017	280.08				
SIGMA1	0.003	206.09				
Q1	0.040	341.55				
RHO1	0.003	315.41				
O1	0.105	42.66				
MP1	0.007	299.26				
M1	0.006	183.22				
CHI1	0.002	106.17				
PI1	0.004	151.25				
P1	0.040	181.17				
S1	0.021	126.58				
K1	0.112	193.34				
PSI1	0.006	136.87				
PHI1	0.002	212.22				
THETA1	0.004	19.42				
J1	0.006	359.84				
SO1	0.002	107.80				
OO1	0.005	338.38				
OO2	0.022	252.51				
MNS2	0.011	43.96				
2N2	0.110	263.58				
MU2	0.036	103.62				
N2	0.559	302.36				
NU2	0.139	310.95				
OP2	0.005	329.97				
M2	2.918	327.25				
MKS2	0.007	27.92				
LAMDA2	0.038	348.66				
L2	0.113	329.86				
T2	0.035	335.21				
S2	0.948	11.46				
R2	0.023	337.17				
K2	0.276	8.38				
MSN2	0.049	193.56				
KJ2	0.009	264.56				
2SM2	0.038	199.44				
MO3	0.007	285.46				
M3	0.034	297.64				
SO3	0.007	298.87				
MK3	0.010	74.55				
SK3	0.009	98.39				
MN4	0.076	212.98				
M4	0.238	249.83				
SN4	0.022	113.81				
MS4	0.152	290.21				
MK4	0.047	286.58				
S4	0.032	298.39				
SK4	0.010	293.76				
2MN6	0.009	300.21				
M6	0.019	17.94				
MSN6	0.020	282.17				
2MS6	0.025	28.37				
2MK6	0.003	309.54				
2SM6	0.018	63.57				
MSK6	0.009	7.60				

Table 14

PROUDMAN OCEANOGRAPHIC LABORATORY (BIDSTON OBSERVATORY)  
HARMONIC TIDAL ANALYSIS.

PORT: HALFWAY SHOALS

LATITUDE: 54 01.5' N

LONGITUDE: 3 11.5' W

TIME ZONE: GMT

LENGTH: 1 YEAR

FROM: 24TH SEPTEMBER,1985 TO: 24TH SEPTEMBER,1986

UNITS: METRES A0: 6.831

FILTERED HOURLY DATA FROM 15 MINUTE OBSERVATIONS RECORDED BY AANDERAA WLR5.

DATUM OF OBSERVATIONS = TIDE GAUGE ZERO

OBSERVATION MEAN = 0.6829D+01 RESIDUAL MEAN = 0.6913D-06  
STD = 0.2239D+01 STD = 0.2013D+00

	H	G		SIGMA	H	G
SA	0.033	280.90	2MN2S2	26.40794	0.006	222.10
SSA	0.053	145.84	3M(SK)2	26.87018	0.008	236.15
MM	0.092	241.02	3M2S2	26.95231	0.012	219.43
MSF	0.031	215.79	SNK2	28.35759	0.003	274.36
MF	0.046	199.60	2SK2	29.91786	0.002	356.93
2Q1	0.014	260.19	MQ3	42.38277	0.005	244.34
SIGMA1	0.005	318.01	2MP3	43.00928	0.001	56.87
Q1	0.041	343.16	2MQ3	44.56955	0.005	70.91
RHO1	0.002	228.89	3MK4	56.87018	0.016	41.79
O1	0.105	42.99	3MS4	56.95231	0.011	349.48
MP1	0.012	308.27	2MSK4	57.88607	0.004	37.12
M1	0.004	147.23	3MK5	71.91124	0.003	64.20
CHI1	0.003	191.63	M5	72.46026	0.001	148.29
PI1	0.004	267.03	3MO5	73.00928	0.004	236.58
P1	0.041	178.98	3MNS6	85.39204	0.001	171.93
S1	0.010	103.30	4MK6	85.85428	0.003	191.75
K1	0.121	193.70	4MS6	85.93642	0.001	180.12
PSI1	0.008	182.86	2MSNK6	86.32580	0.001	197.89
PHI1	0.005	183.17	2MV6	86.48079	0.002	12.28
THETA1	0.004	254.22	3MSK6	86.87018	0.002	206.20
J1	0.006	2.13	4MN6	87.49669	0.004	258.31
SO1	0.005	45.68	3MSN6	88.51258	0.003	256.63
OO1	0.006	351.24	2(MN)8	114.84767	0.002	157.12
OQ2	0.017	271.52	3MN8	115.39204	0.005	192.08
MNS2	0.007	99.48	MB8	115.93642	0.006	214.46
2N2	0.097	260.58	2MSN8	116.40794	0.005	235.05
MU2	0.024	79.16	3MS8	116.95231	0.009	262.48
N2	0.570	300.96	3MK8	117.03445	0.002	253.87
NU2	0.126	303.11	MSNK8	117.50597	0.001	248.56
OP2	0.016	274.04	2(MS)8	117.96821	0.004	308.35
M2	2.965	324.78	2MSK8	118.05035	0.002	302.09
MKS2	0.011	148.49	4MS10	145.93642	0.001	345.40
LAMDA2	0.062	331.61	3M2S10	146.95231	0.001	27.91
L2	0.101	336.05	MVS2	27.49669	0.008	88.92
T2	0.049	1.15	MA2	28.94304	0.013	224.19
S2	0.968	6.90	MB2	29.02517	0.022	332.98
R2	0.008	2.64	MSV2	30.47152	0.003	35.57
K2	0.279	5.19	SKM2	31.09803	0.016	226.64
MSN2	0.035	216.87	2MNS4	56.40794	0.006	343.48
KJ2	0.011	229.96	MV4	57.49669	0.020	211.91
2SM2	0.034	235.73	3MN4	58.51258	0.019	97.59
MO3	0.007	261.66	2MSN4	59.52848	0.011	309.99
M3	0.034	300.01	MSO5	72.92714	0.002	253.69
SO3	0.008	343.11	MSK5	74.02517	0.002	213.25
MK3	0.013	53.41				
SK3	0.012	101.10				
MN4	0.073	200.44				
M4	0.188	229.22				
SN4	0.013	260.16				
MS4	0.110	275.61				
MK4	0.033	270.74				
S4	0.012	312.08				
SK4	0.008	318.62				
2MN6	0.009	345.00				
M6	0.015	9.12				
MSN6	0.004	22.17				
2MS6	0.015	43.95				
2MK6	0.004	48.73				
2SM6	0.004	74.03				
MSK6	0.003	81.19				

Table 15



	Ramsden	Roa Is.	Halfway S.	P Patrick	Holyhead
Heysham	0.879	0.851	0.848	0.849	0.774
Ramsden Dock		0.856	0.946	0.904	0.882
Roa Is.			0.951	0.879	0.879
Halfway S.				0.852	0.842
P. Patrick					0.852

Table 16: Cross-correlation of observed surges of May-June 1987

	$P$ $\text{cm}(\text{mb})^{-1}$	coefficients of $u$ $\text{cm}(\text{ms}^{-1})^{-1}$	$v$ $\text{cm}(\text{ms}^{-1})^{-1}$
Jan-Feb 1985	-0.54(0.11)	0.99(0.22)	3.69(0.35)
Mar-Apr "	-0.82(0.11)	0.66(0.26)	3.28(0.32)
May-Jun "	-0.99(0.12)	0.31(0.17)	2.56(0.23)
Jul-Aug "	-0.69(0.12)	0.25(0.19)	2.81(0.24)
Sep-Oct "	-0.95(0.11)	0.36(0.26)	1.63(0.38)*
Nov-Dec "	-1.11(0.14)	0.08(0.28)*	3.44(0.37)
average	-0.83	0.52	2.89

\* These values are not included in average.

Table 17: Regression Coefficient of P, u and v (Squires Gate) for all surges at Ramsden Dock.

	A		B		C	
	Mean (cm)	Variance (cm <sup>2</sup> )	Mean (cm)	Variance (cm <sup>2</sup> )	Mean (cm)	Variance (cm <sup>2</sup> )
Oct 1985	-5.9	473.9	-0.5	110.1	-1.7	111.4
Nov 1985	-13.4	597.4	-13.0	105.1	-10.5	142.9
Dec 1985	5.7	509.5	-6.6	137.4	-5.9	196.2
Oct-Dec 1985	-4.3	595.8	-6.9	143.8	-6.2	163.9

Table 18: Means and variances of observed surges and unpredicted component.  
 A observed surge; B unpredicted when NM is used; C unpredicted when  
 RM is used.

Ramsden Dock

Period	$P$ $\text{cm mb}^{-1}$	$u$ $\text{cm}(\text{ms}^{-1})$	$v$ $\text{cm}(\text{ms}^{-1})$
2-9 Jan 1985	-1.07(0.25)	1.66(0.87)	5.15(0.88)
23-30 Jan	-0.83(0.19)	0.52(0.49)	3.61(0.60)
29 Jan-5 Feb	-0.72(0.32)	1.83(1.06)	5.16(1.44)
26 Feb-5 Mar	-0.20(0.39)*	1.18(0.90)	4.44(1.03)
4-11 Apr	-0.14(0.78)*	1.11(0.23)	2.28(1.29)
19-26 Aug	-0.67(0.47)	0.75(0.65)	4.81(1.32)
	-----	-----	-----
average	-0.82	1.22	4.24

Roa Island

2-9 Jan 1985	-1.10(0.25)	1.81(0.71)	5.15(0.92)
23-30 Jan	-0.77(0.19)	0.79(0.48)	3.73(0.60)
29 Jan-5 Feb	-0.79(0.31)	1.90(1.05)	5.11(1.41)
26 Feb-5 Mar	-0.14(0.37)*	1.30(0.85)	4.37(1.03)
4-11 Apr	-0.16(0.75)*	1.51(0.63)	2.28(1.24)
	-----	-----	-----
average	-0.88	1.46	4.10

Halfway Shoals

2-9 Jan 1985	-1.06(0.23)	1.95(0.65)	5.05(0.84)
23-30 Jan	-0.71(0.18)	1.02(0.47)	3.55(0.60)
29 Jan-5 Feb	-0.55(0.30)	1.24(1.00)	5.07(1.36)
26 Feb-5 Mar	-0.35(0.32)*	1.22(0.74)	4.44(0.89)
4-11 Apr	-0.18(0.72)*	1.62(0.60)	2.20(1.18)
19-26 Aug	-0.68(0.41)	0.67(0.61)	4.33(1.22)
	-----	-----	-----
average	-0.75	1.28	4.10

\* These values, when error is bigger than coefficient, are not included in averages.

Table 19: Regression coefficient (standard error) of meteorological inputs (P, u and v at Squires Gate) for negative surge output).

<u>Ramsden Dock</u>	A		B		C	
	m	var.	m	var.	m	var.
2-9 Jan 1985	-5.1	291.5	-10.0	123.1	-9.3	91.4
23-30 Jan	-4.1	601.1	-7.3	159.3	-6.8	140.3
29 Jan-5 Feb	-25.1	466.7	-3.7	57.2	-2.9	149.1
26 Feb-5 Mar	-2.1	677.6	8.1	82.0	5.0	186.6
4-11 Apr	-29.5	149.5	-0.4	44.2	3.7	101.7
19-26 Aug	1.8	268.9	6.7	216.3	12.1	115.4
<u>Roa Island</u>						
2-9 Jan 1985	-3.0	297.9	-7.9	131.6	-7.3	98.0
23-30 Jan	-3.3	604.0	-6.5	146.4	-6.0	125.4
29 Jan-5 Feb	-26.9	479.7	-5.5	53.9	-4.7	145.1
26 Feb-5 Mar	-0.3	664.8	9.8	74.4	6.8	180.6
4-11 Apr	-31.7	149.3	-2.6	41.1	1.5	95.4
<u>Halfway Shoals</u>						
2-9 Jan 1985	-3.9	272.9	08.8	121.3	-7.2	87.1
23-30 Jan	-7.9	565.6	-11.1	124.3	-10.0	111.8
29 Jan-5 Feb	-30.0	436.7	-9.0	55.5	-8.6	144.1
26 Feb-5 Mar	-6.5	764.0	3.8	41.6	0.4	89.4
4-11 Apr	28.1	147.3	0.5	527.3	2.8	85.3
19-26 Aug	3.3	228.2	8.2	185.2	13.3	88.6

Average air pressure (1013mb) is subtracted in calculation of surges with the regression formula.

Table 20: Means (cm) and variances (cm<sup>2</sup>) of negative surges.  
 A observed; B unpredicted component when NM is used;  
 and C unpredicted component when RM is used.

Day No	Ramsden Dock	Roa Island	Halfway Shoals
317-330	1.19(0.06)	1.17(0.07)	1.13(0.06)
2-9	0.98(0.11)	0.98(0.12)	0.94(0.11)
29-39	1.09(0.06)	1.09(0.06)	1.06(0.07)
94-101	0.98(0.09)	0.98(0.09)	0.98(0.10)
219-226	0.91(0.12)	---	0.98(0.11)
	-----	-----	-----
	1.03	1.03	1.01

Table 21: Regression coefficients with Heysham model surge as input  
(for optimisation of surge output).

	Model grid point (I,J)	Computed	Observed	Source
Heysham HY	32,23	313.8 cm 325.7°	315.6 cm 325.7°	Amin,1982 8 yrs analysis
Fleetwood FL	28,31	306.7 cm 324.0°	304.8 cm 326.4°	IOS 1 yr analysis
Morecambe MO	34,19	306.2 cm 330.5°	308.0 cm 326.1°	Doodson & Corkan, 1932
Glasson Docks GD	35,26	227.9 cm* 344.0°	338.0 cm 326.1°	Doodson & Corkan, 1932
Wyre Light WL	27,29	305.5 cm 323.8°	310.0 cm 324.0°	Doodson & Corkan, 1932
Barrow,Ramsden Dock RD	17,18	308.7 cm 331.0°	307.7 cm 330.9°	7/1/85-11/2/87, 2 yrs
Roa Island RI	19,20) 20,20)	305.8 cm 329.1°	305.9 cm 328.6°	16/9/85-12/2/87, 11½ mths
Halfway Shoals HS	18,23	295.6 cm 325.0°	296.5 cm 324.8°	24/9/85-24/9/86, 1 yr
Lowsy Point LP	15,13	207.4 cm* 338.7°	235.9 cm* 335.3°	14/9/85-7/2/87, 15 mths
Hawes Point HP	20,21) 20,22)	303.2 cm 327.9°	291.8 cm* 327.3°	20/10/85-30/4/86, 11 mths

\* location subject to drying or ponding

Table 22: Comparison between computed and observed amplitudes and phases of the  $M_2$  tide.

	Observed ATT	$2(M_2+S_2)$	Computed
Ramsden Dock	8.1	8.15	8.18
Roa Island	-	8.09	8.11
Halfway Shoals	-	7.87	7.87
Heysham	8.0	8.34	8.46
Fleetwood	8.2		8.32

Table 23: Comparison of observed and computed estimates of the mean spring tidal range (m) for locations not subject to drying or ponding. Observed values are taken from the Admiralty Tide Tables (ATT) or based on the sum of the amplitudes of the  $M_2$  and  $S_2$  constituents ( $2(M_2+S_2)$ ).

BARROW IN FURNESS

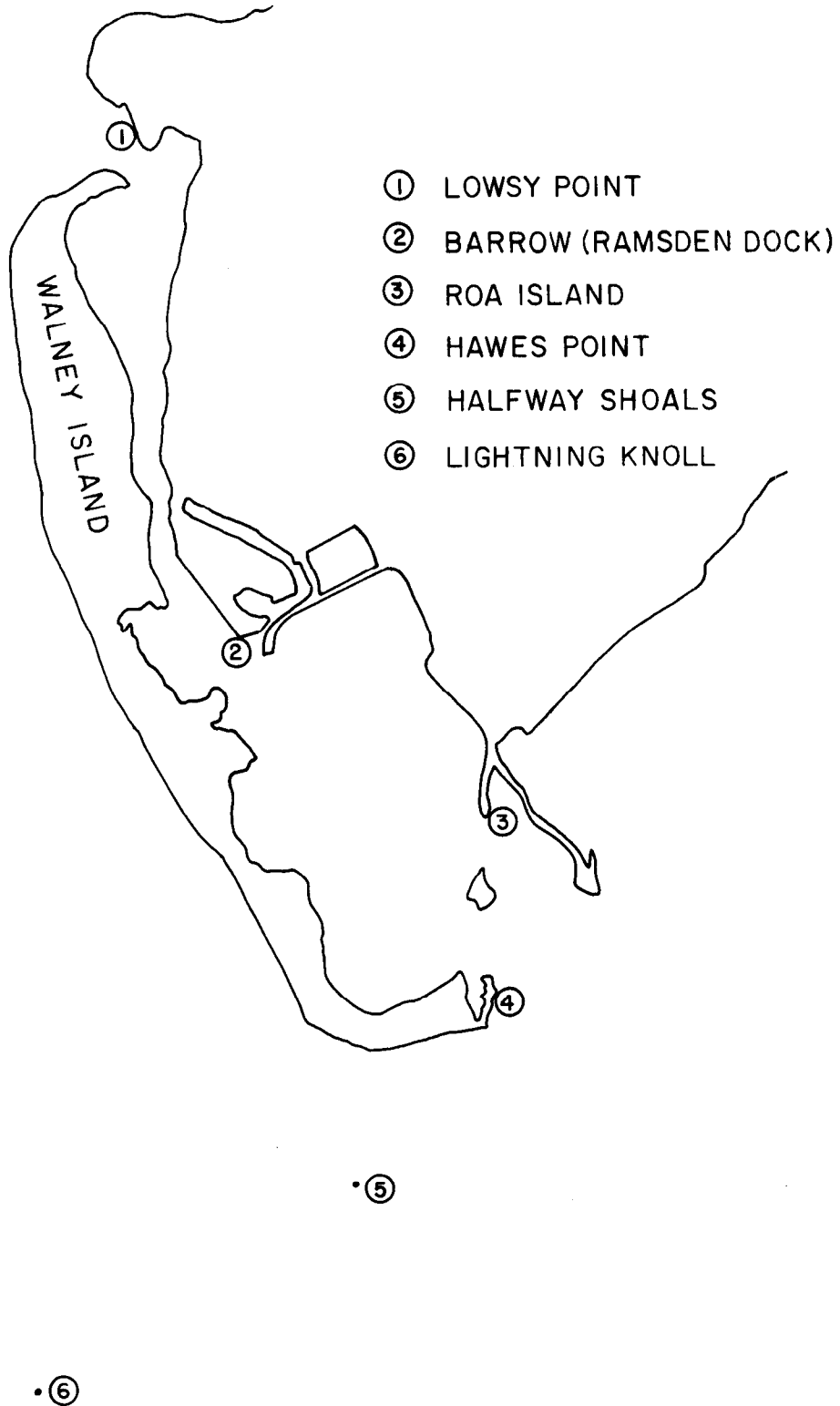
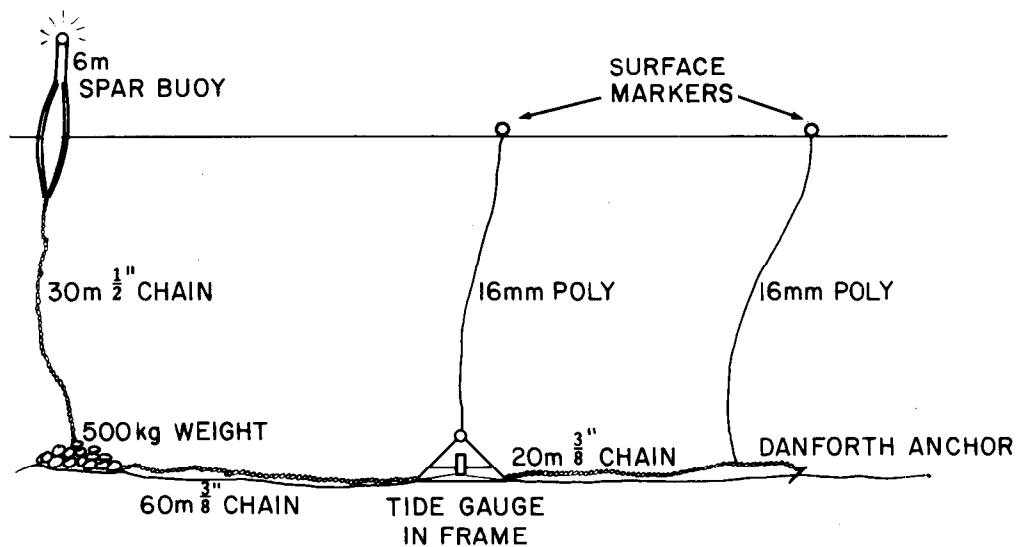
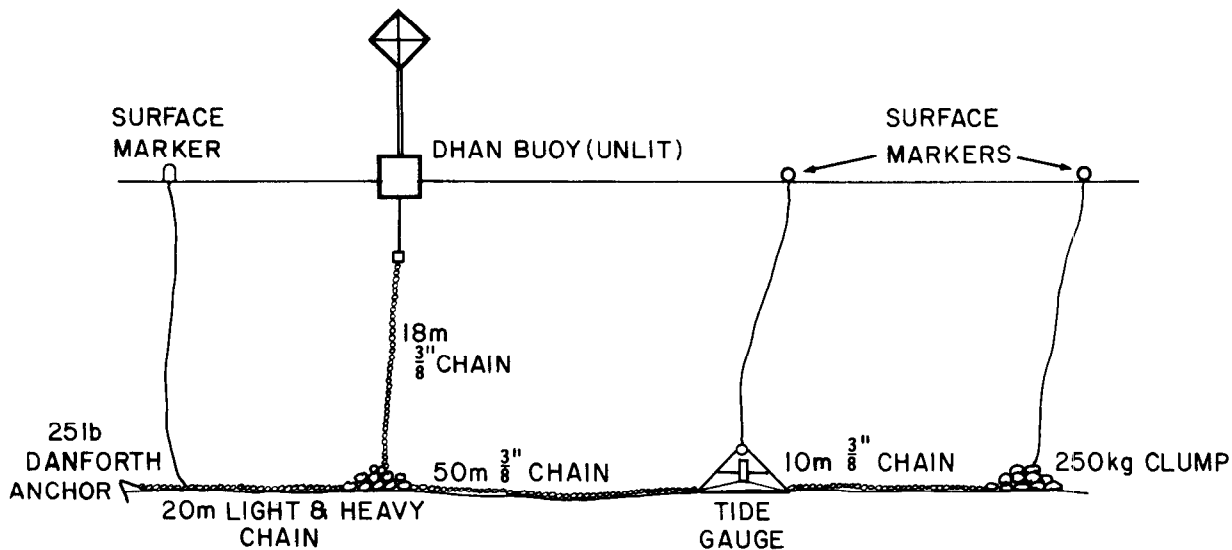


Figure 1: POL installed tide gauge positions





LIGHTNING KNOLL MOORING



HALFWAY SHOALS MOORING

Figure 2

# **NOTICE TO MARINERS**

## **WEST COAST - ENGLAND**

### **BARROW HARBOUR APPROACHES**

Notice is hereby given that commencing September 1985 a bottom mounted tide gauge will be sited in the following position which lies near Halfway Buoy:

Latitude  $54^{\circ} 01.5' N$  approximately

Longitude  $03^{\circ} 11.9' W$

The instrument will be marked by a yellow unlit buoy fitted with a radar reflector and will remain in position until October 1986.

Masters of vessels and small boats are requested to proceed with caution when in the vicinity of this buoy and give it a wide berth.

Institute of Oceanographic Sciences

Bidston, Birkenhead,

Merseyside L43 7RA

U. K.

( 051 - 653 8633 )

# **NOTICE TO MARINERS**

**WALNEY CHANNEL      BARROW - IN - FURNESS**  
**CUMBRIA**

Commencing mid September 1985, a bottom mounted tide gauge will be deployed in approximate position  $54^{\circ} 01.5'N$ ,  $3^{\circ} 11.9'W$ , approximately 1 cable North by West of the Halfway Shoal Buoy. This instrument will be in position until October 1986, and will be marked by a yellow Dhan buoy, with radar reflector, which will be unlit.

To avoid fouling the mooring the Institute would be grateful if ships and fishing boats keep clear of this Dhan buoy.

Institute of Oceanographic Sciences  
Bidston  
Merseyside L43 7RA  
UK.

( 051 - 653 - 8633 )

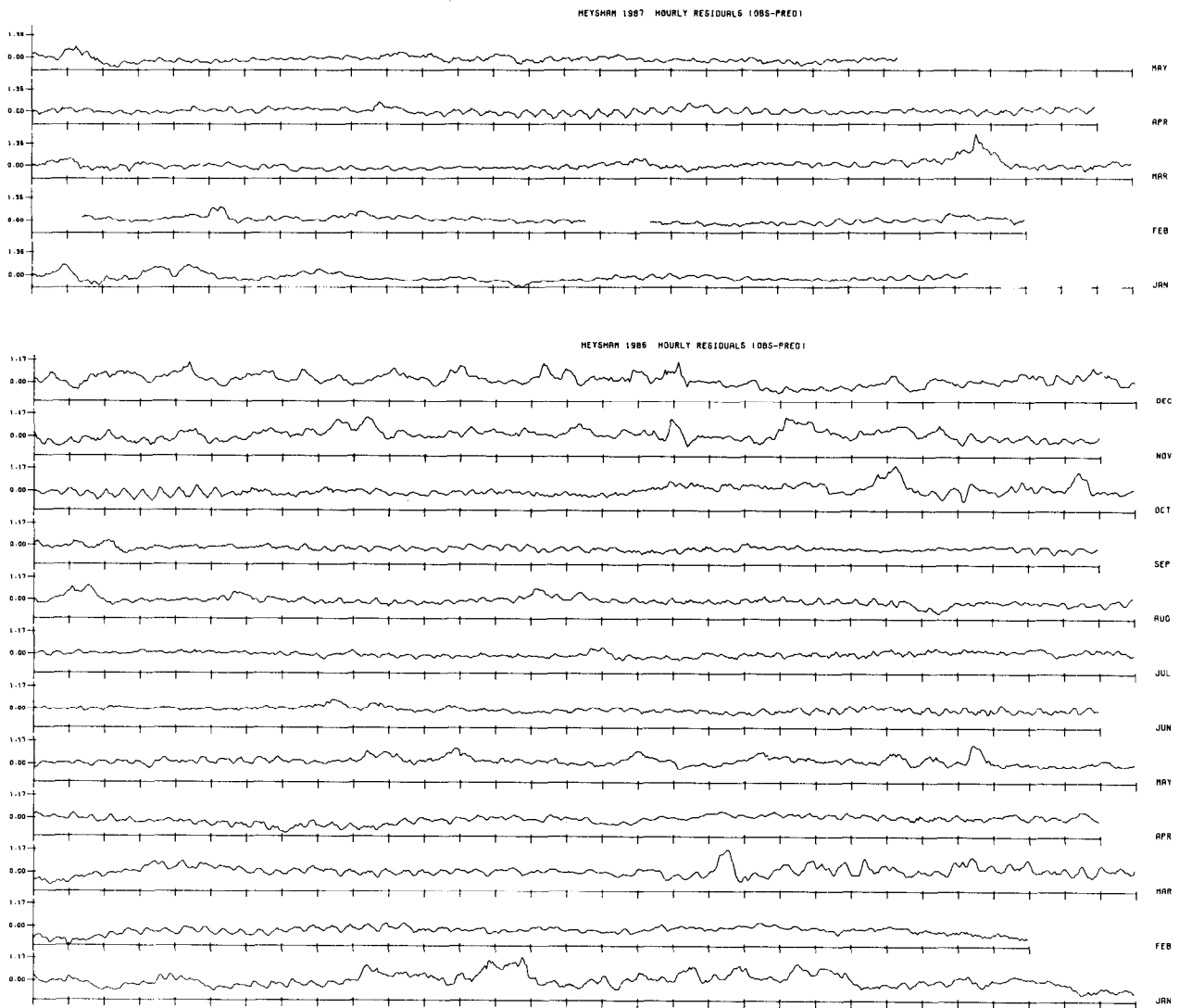


Figure 5: Heysham residuals January 1986 to May 1987

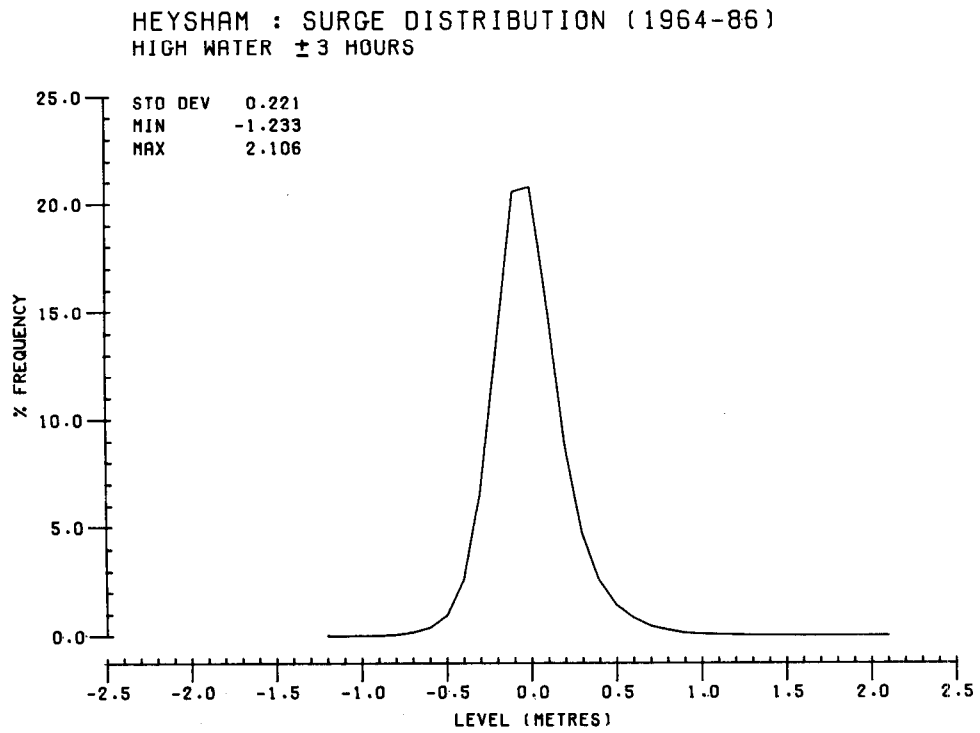


Figure 6

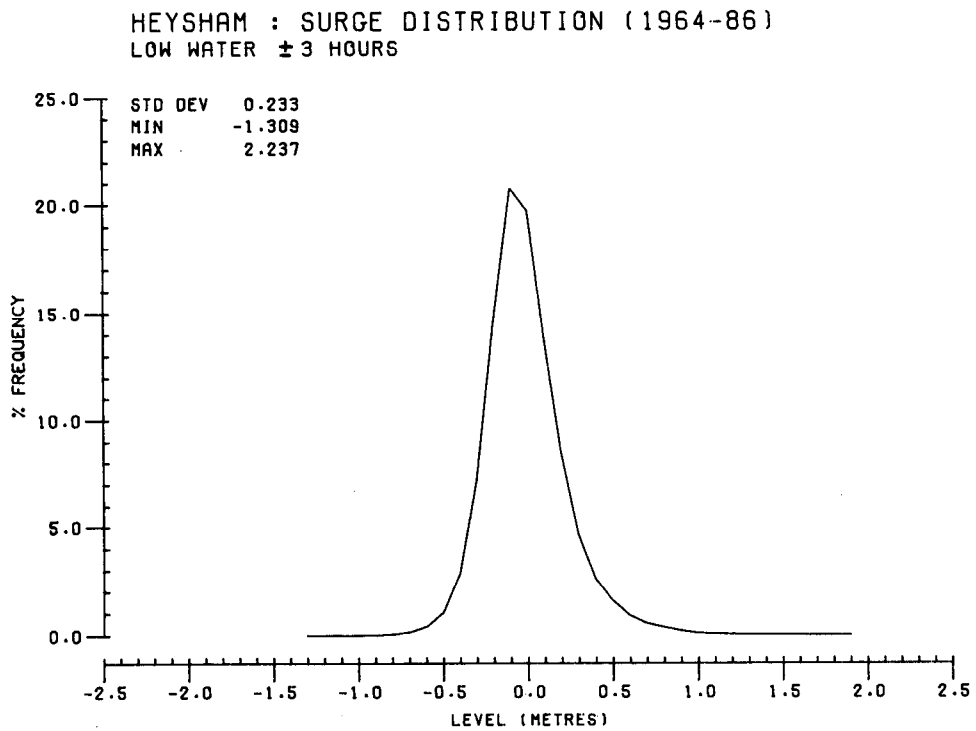


Figure 7

HEYSHAM : MONTHLY SURGE PROBABILITY ( 1964-1986 )

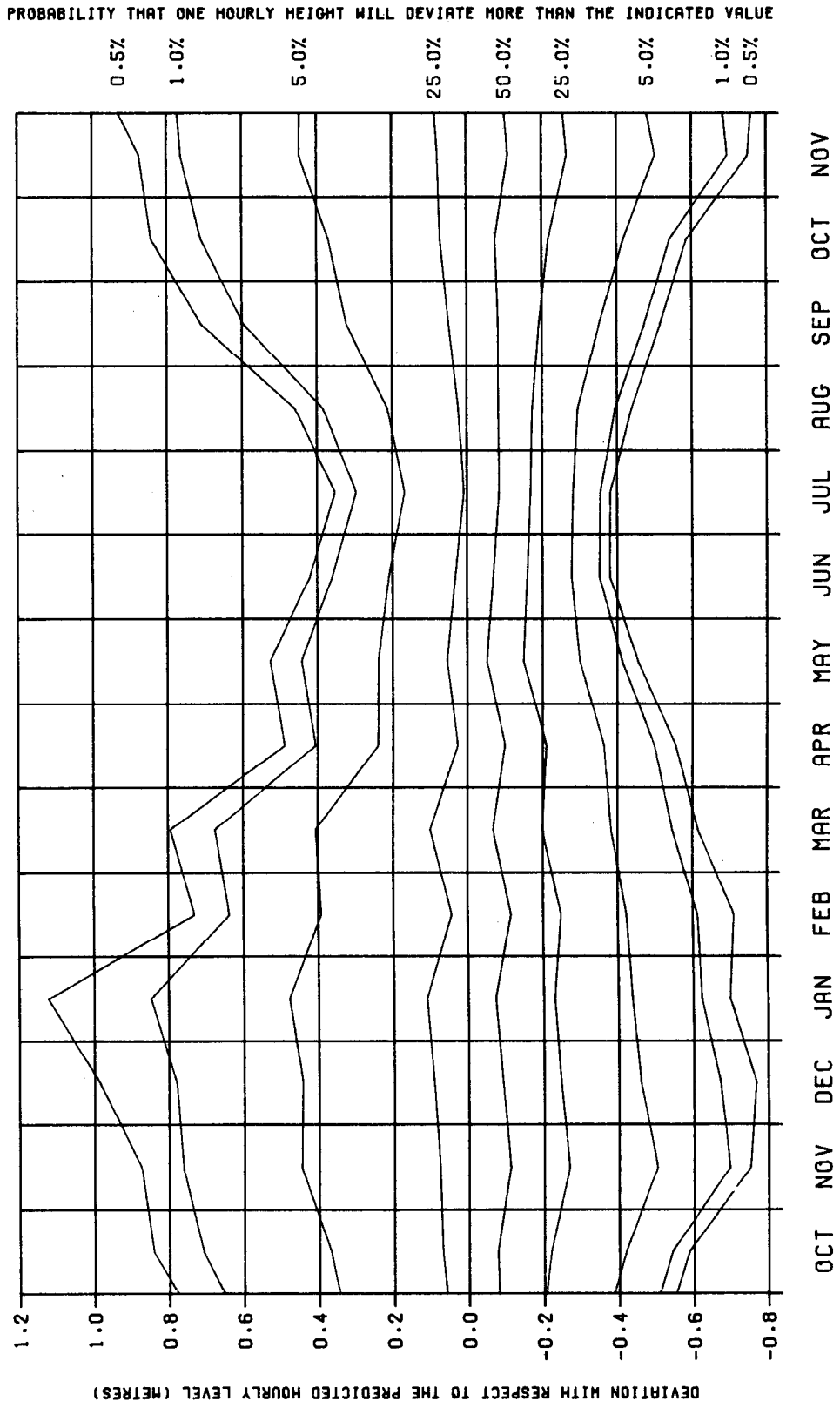


Figure 8

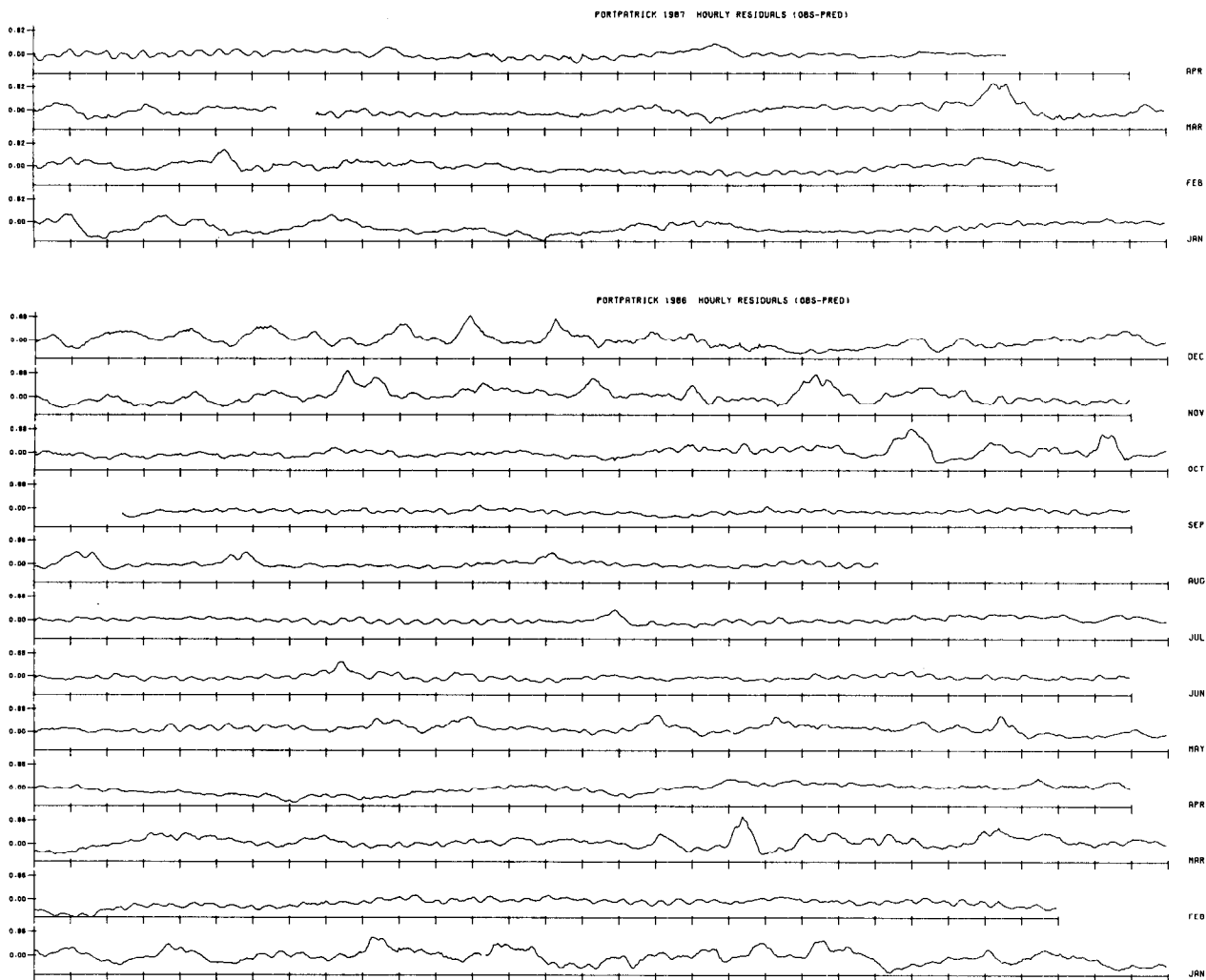


Figure 9: Port Patrick residuals January 1986 to April 1987

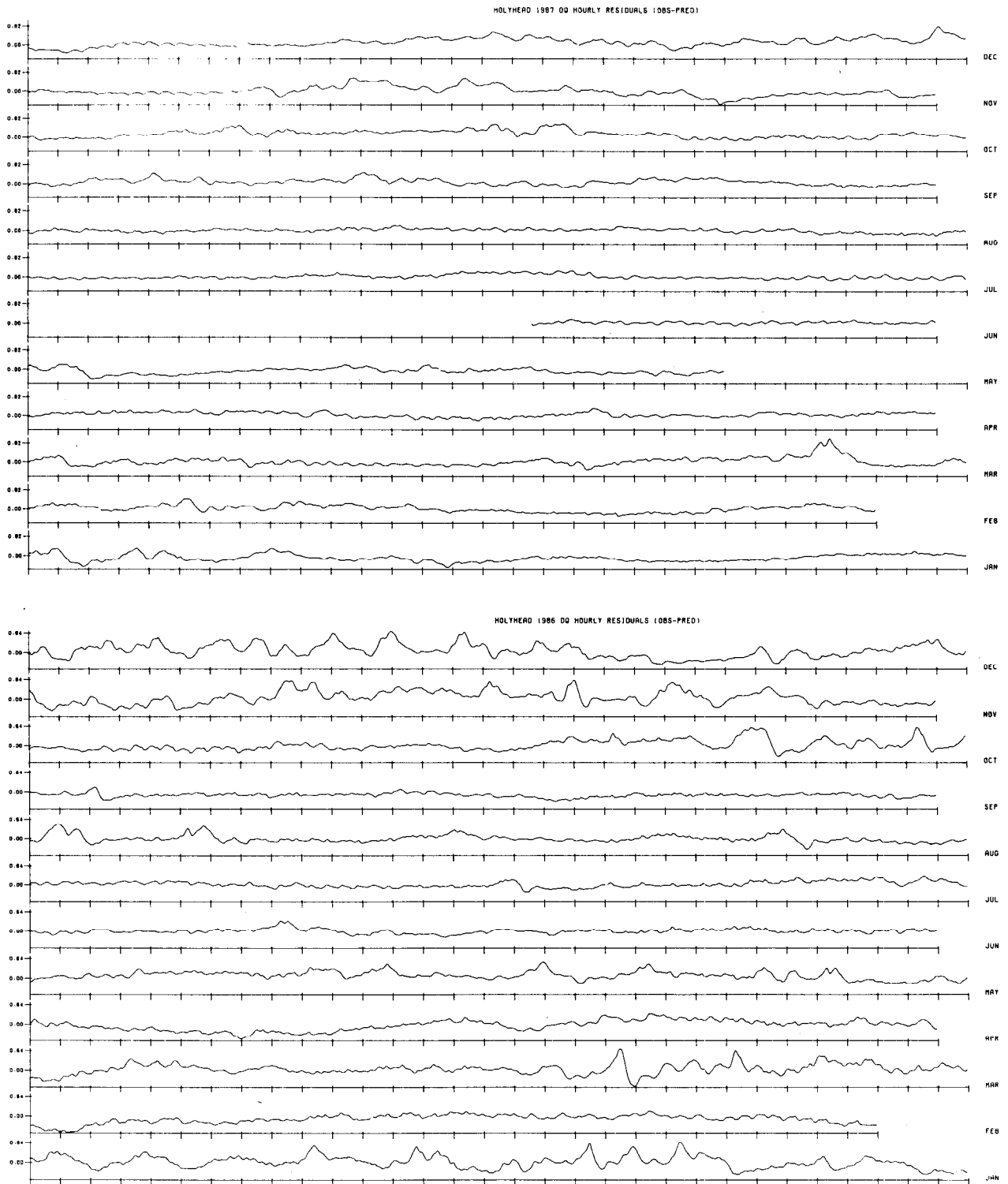


Figure 10: Holyhead residuals January 1986 to December 1987



BARROW : RAMSDEN DOCK  
ANALYSIS : JANUARY 1985 - FEBRUARY 1987

NOVEMBER 1985

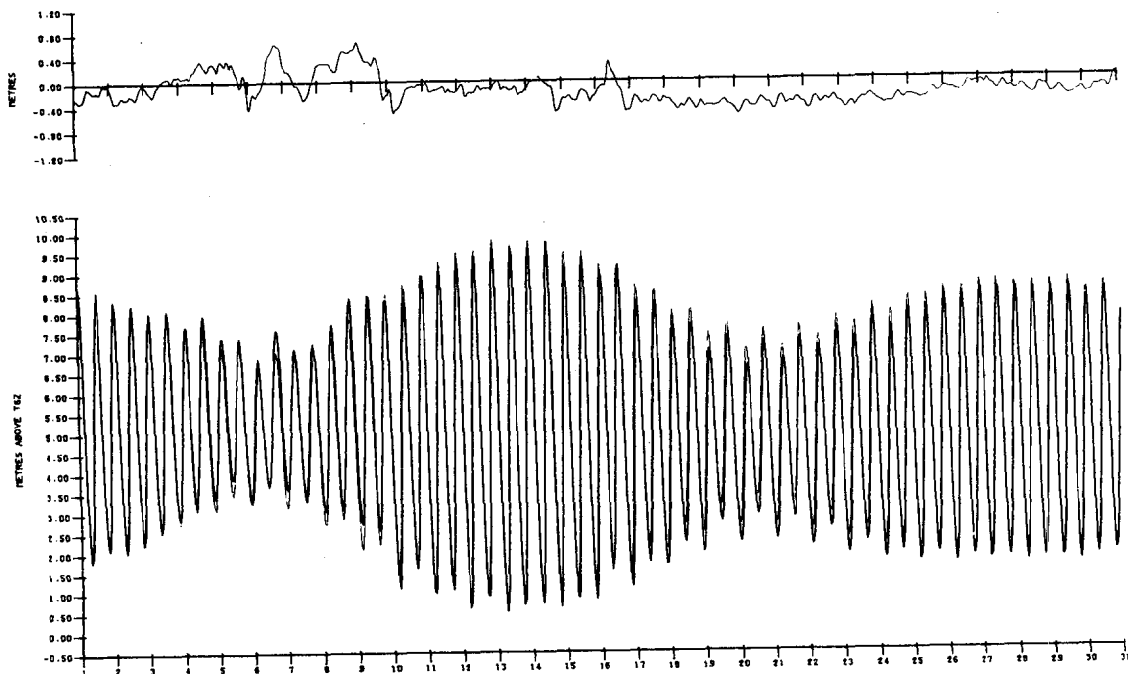


Figure 11

HALFWAY SHOALS  
ANALYSIS : SEPTEMBER 1985 - SEPTEMBER 1986

NOVEMBER 1985

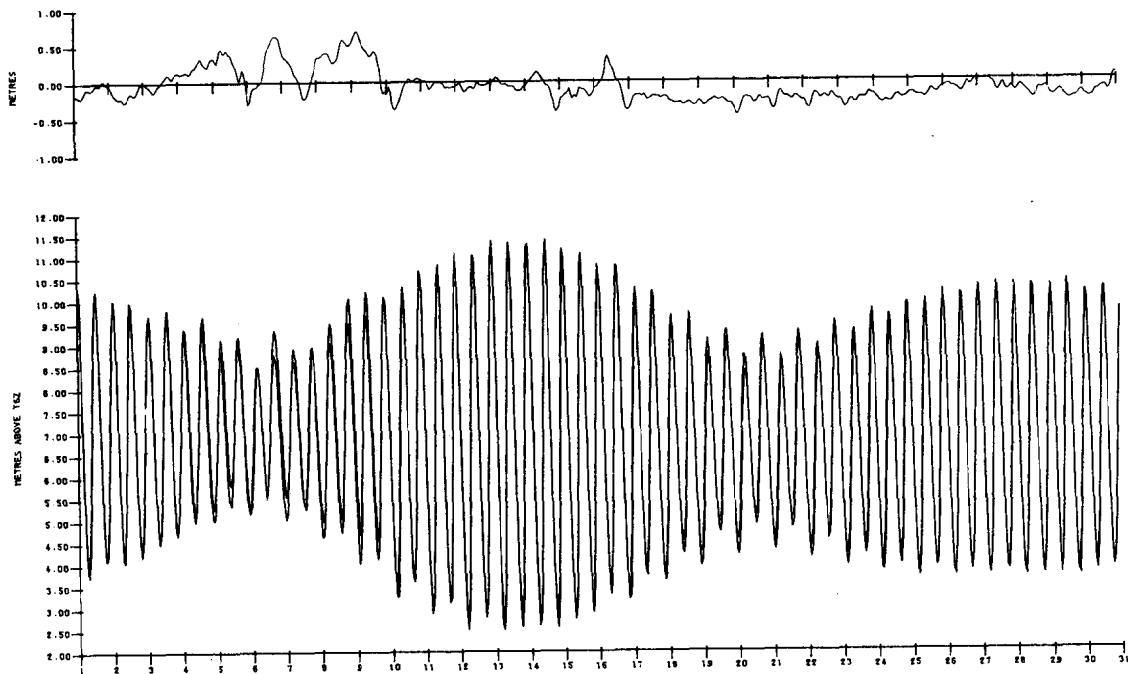


Figure 12

ROR ISLAND  
ANALYSIS : SEPTEMBER 1985 - FEBRUARY 1987

NOVEMBER 1985

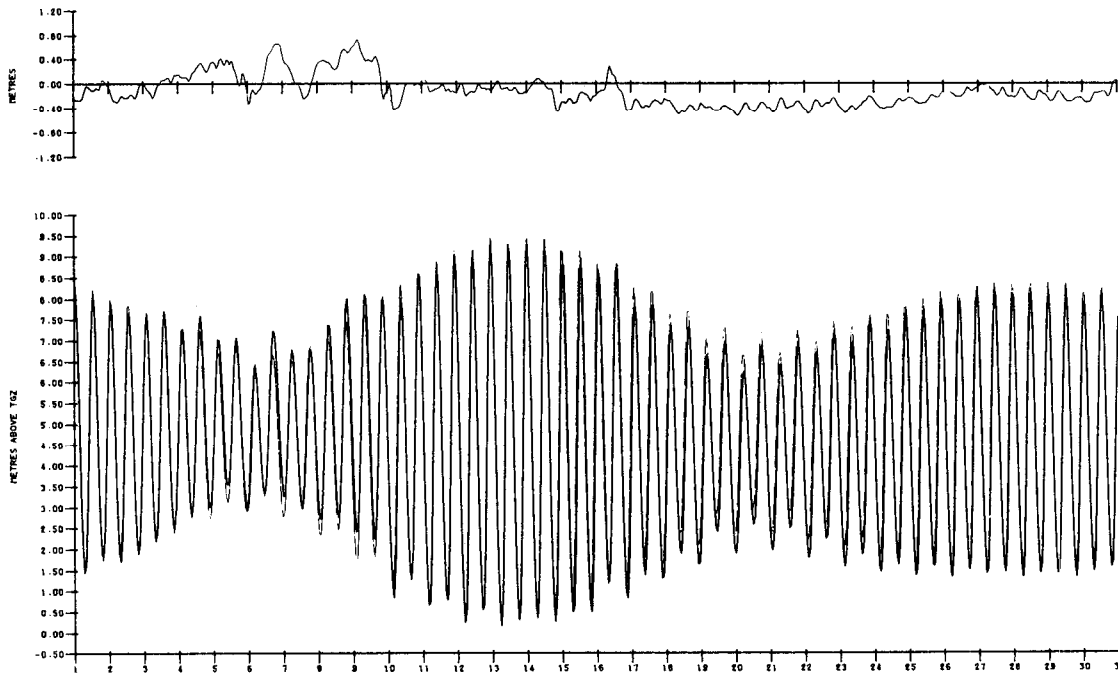


Figure 13

HAWES POINT  
ANALYSIS : OCTOBER 1985 - APRIL 1987

NOVEMBER 1985

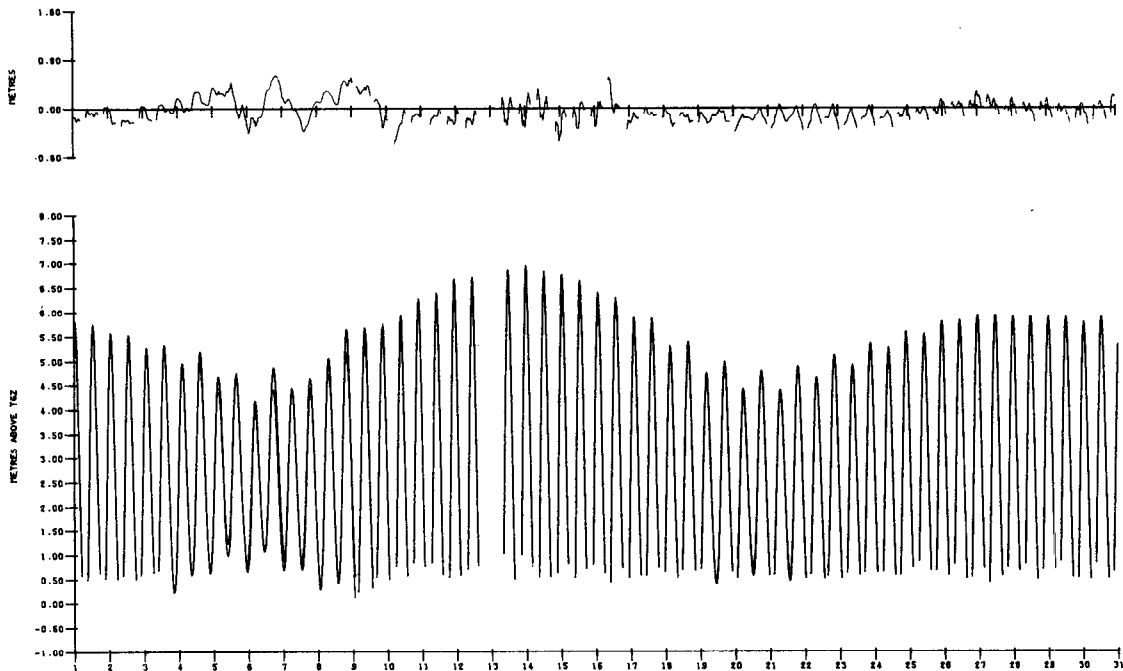


Figure 14

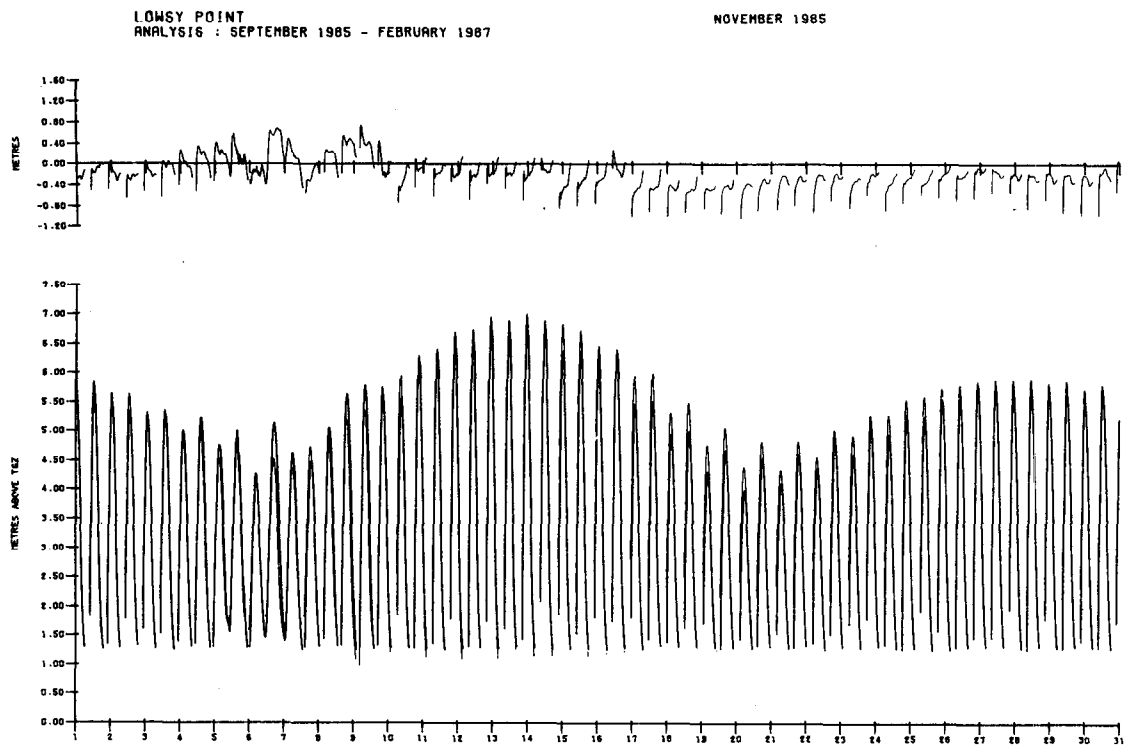


Figure 15

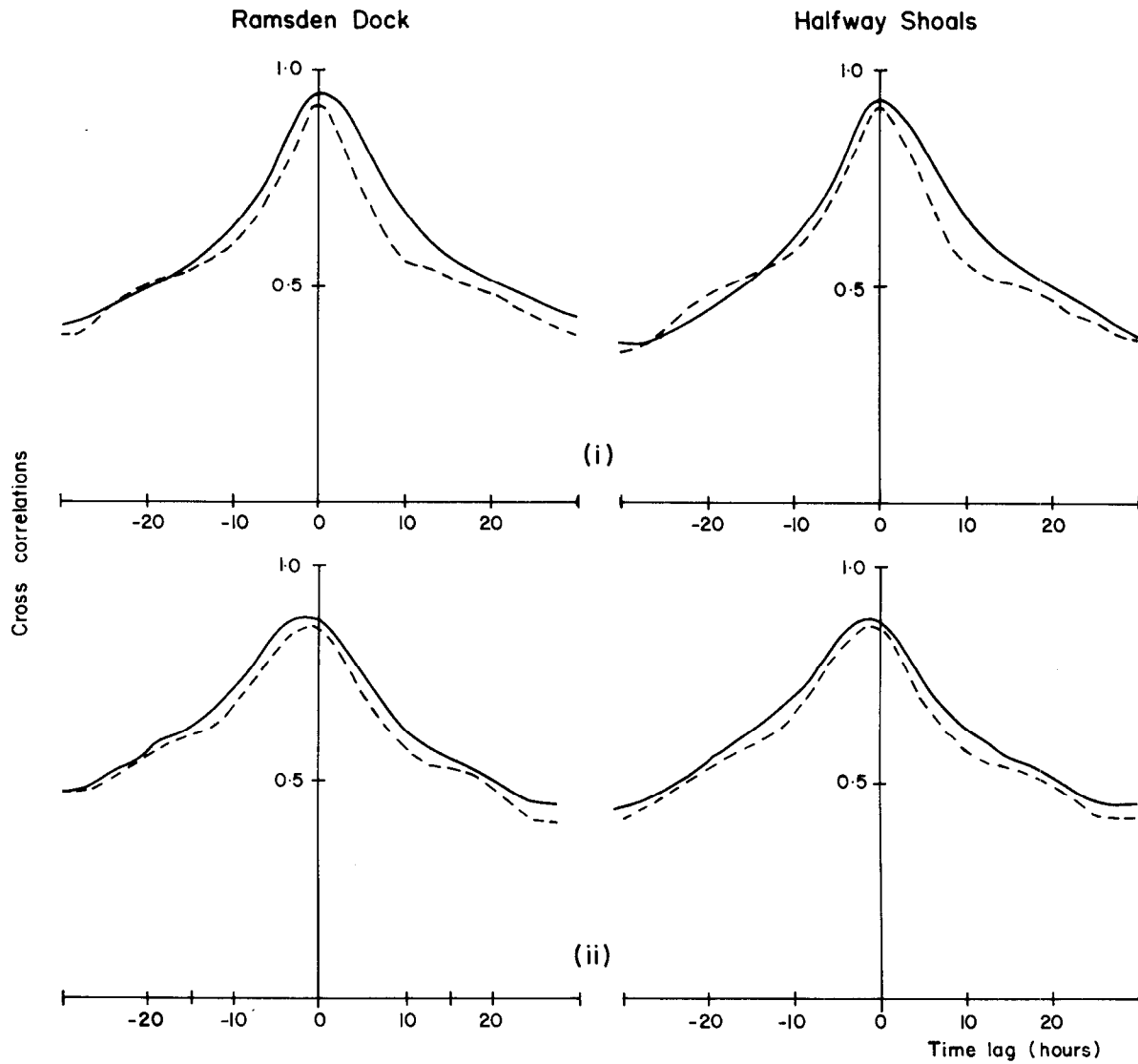


Figure 16a: Cross correlations between observed surges at Ramsden Dock and Halfway Shoals and  
 (i) observed surges at Heysham (—) and Portpatrick (----),  
 (ii) model (numerical) surges at Heysham and Portpatrick.

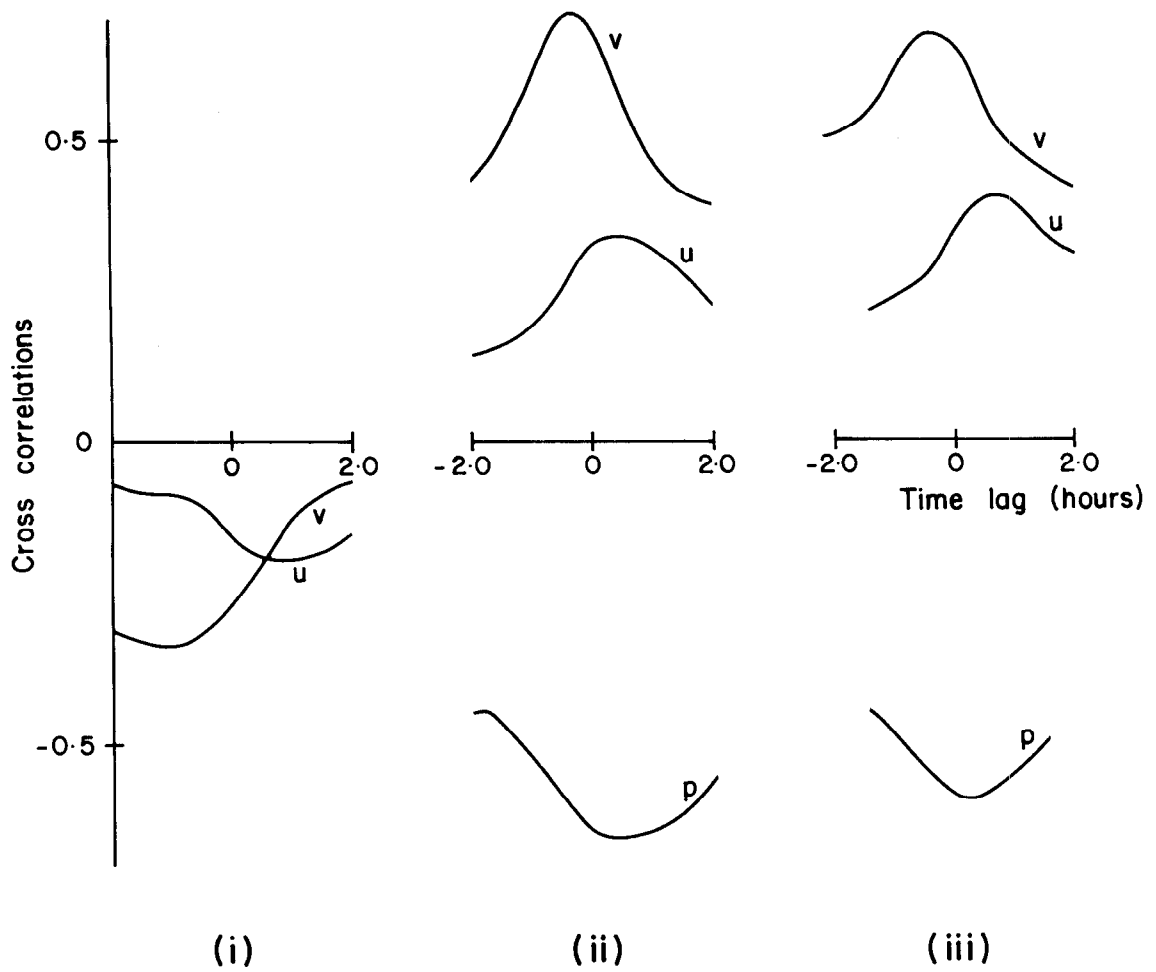


Figure 16b: Cross correlations between surge elevations at Ramsden Dock and air pressure, u-component and v-component of wind at Squires Gate:  
 (i) between air pressure and u- and v-component of winds of (Nov-Dec, 1985),  
 (ii) surge elevations and air pressure, u- and v-component of (Nov-Dec 1985),  
 (iii) between surge elevations and air pressure, u-component and v-component of wind (Nov-Dec, 1986).

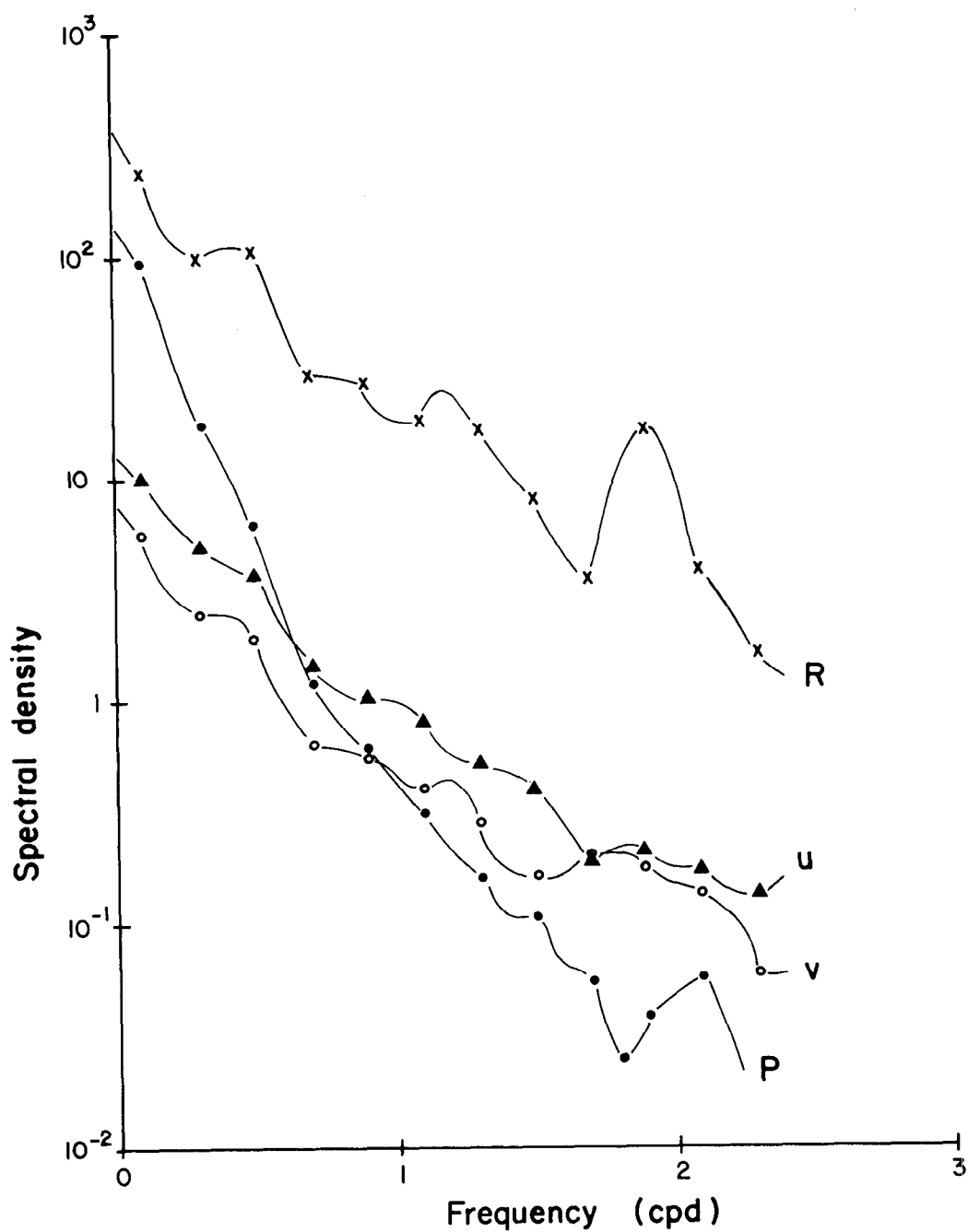


Figure 17: Spectral density of surge elevations at Ramsden Dock, air pressure, u-component and v-component of winds at Squires Gate from 3-hourly values of Oct-Dec 1986. Units are  $\text{cm}^2(\text{cpd})^{-1}$  for elevations,  $\text{mb}^2(\text{cpd})^{-1}$  for pressure and  $(\text{ms}^{-1})^2(\text{cpd})^{-1}$  for winds.

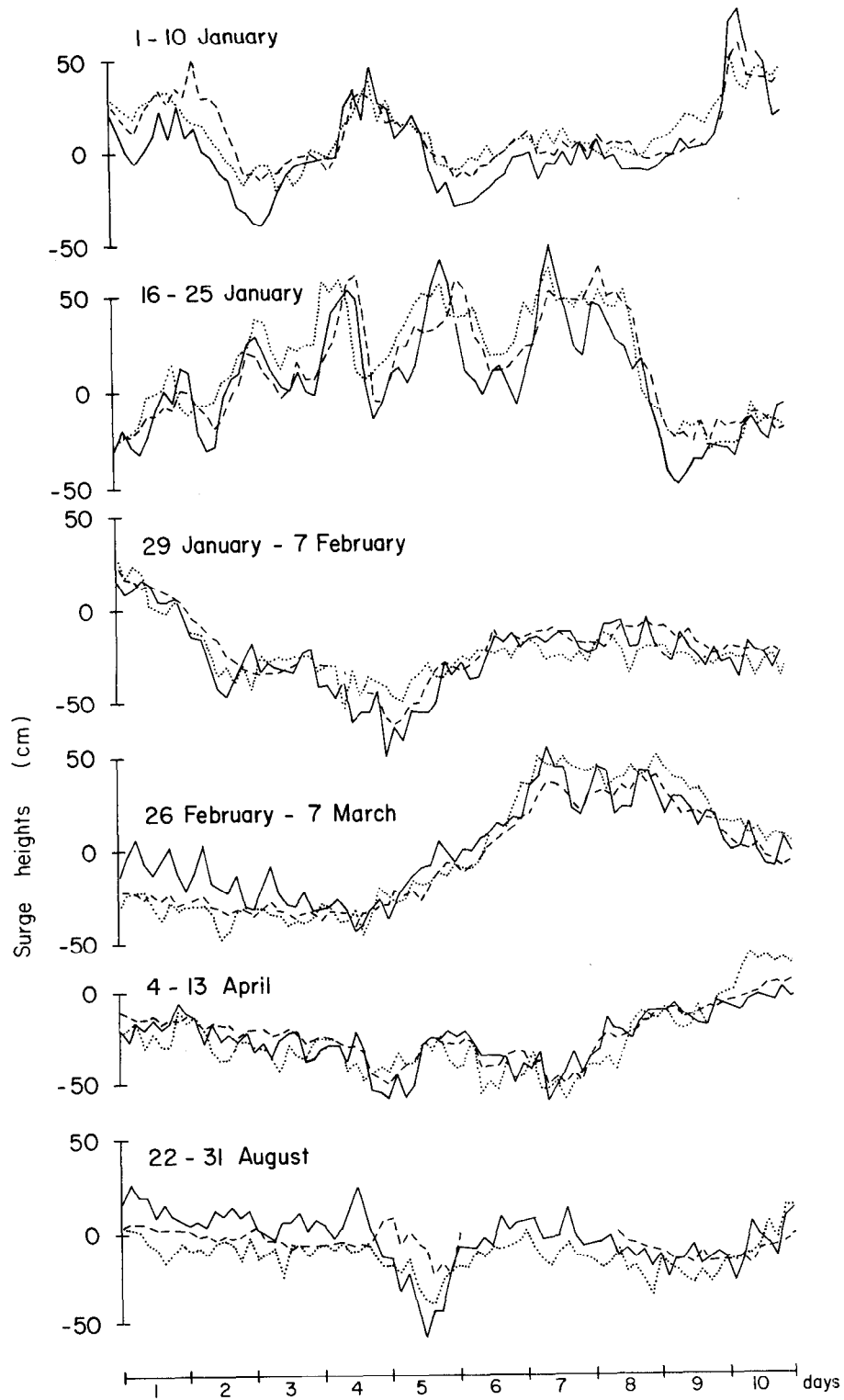


Figure 18: Observed and model surges at Ramsden Dock (3 hourly)  
 —, observed;  
 ----, numerical model;  
 ....., regression model.

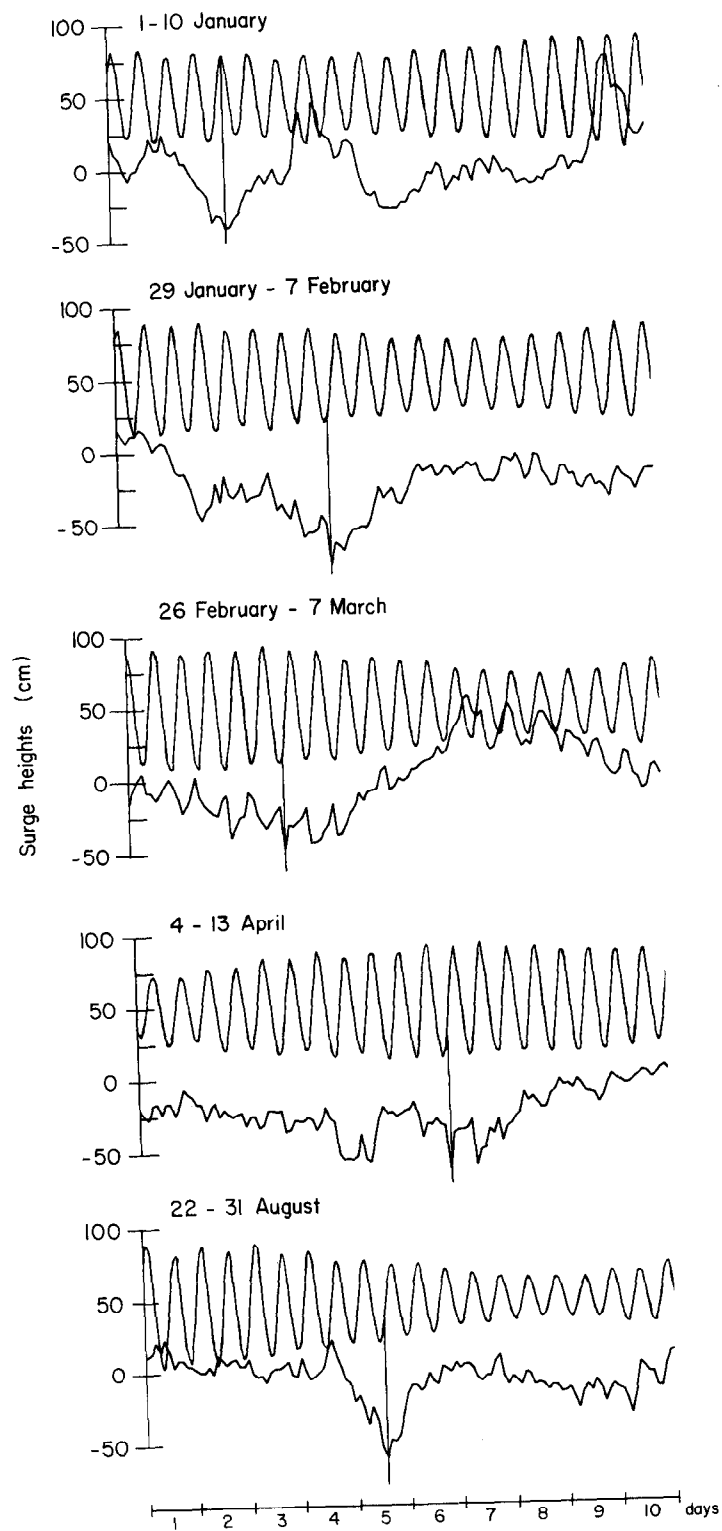


Figure 19: Relationship between the phase of the tide and minima of negative surges (hourly values)



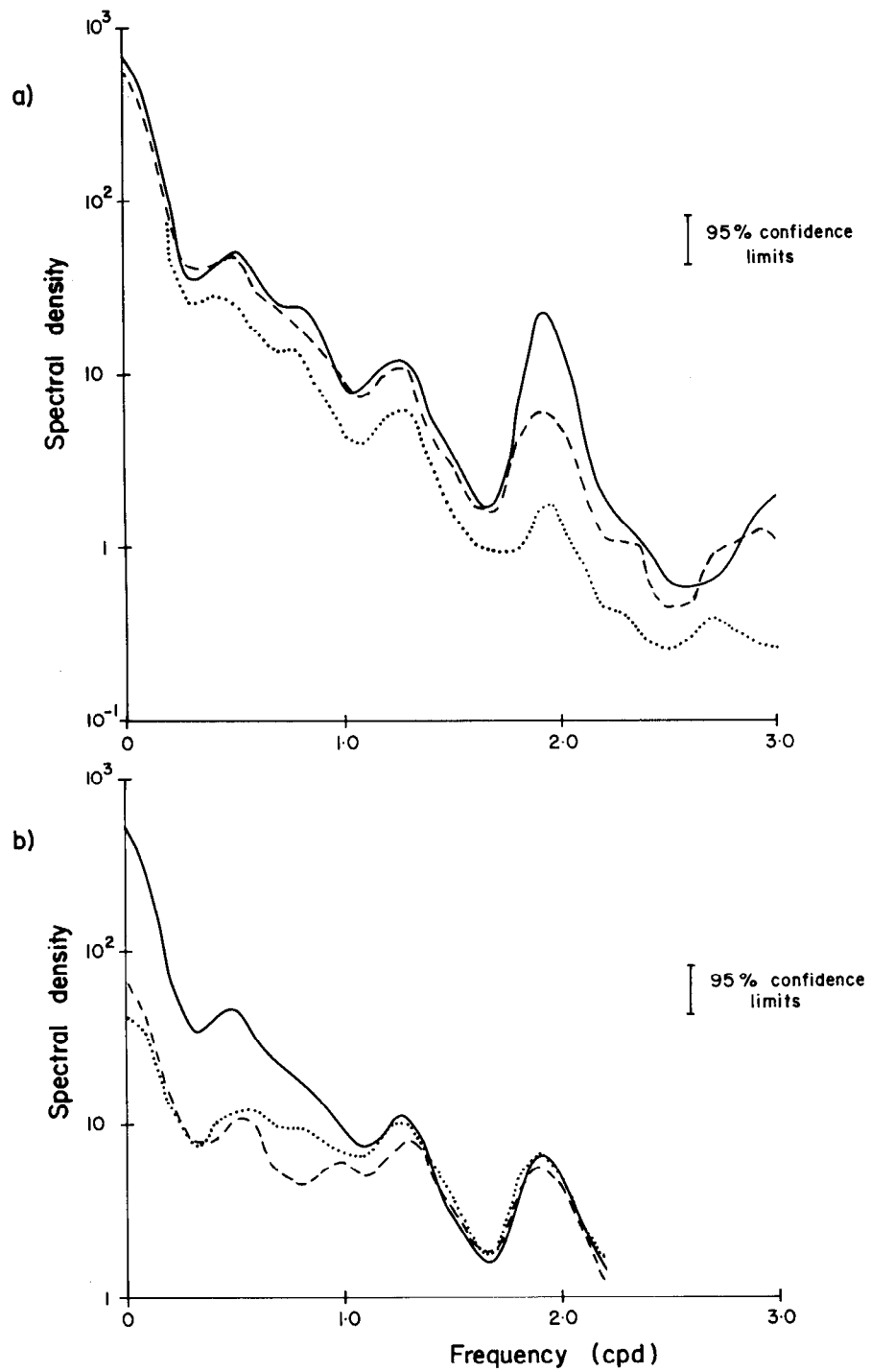


Figure 20: a) Spectral density of surges. Heysham (—), Ramsden Dock observed (----), and Heysham numerical model (....).  
 b) Spectral density functions. Observed surge elevations (—), unpredicted component of surge elevations when numerical model is used (----), and unpredicted component of surge elevations when regression model is used (....).

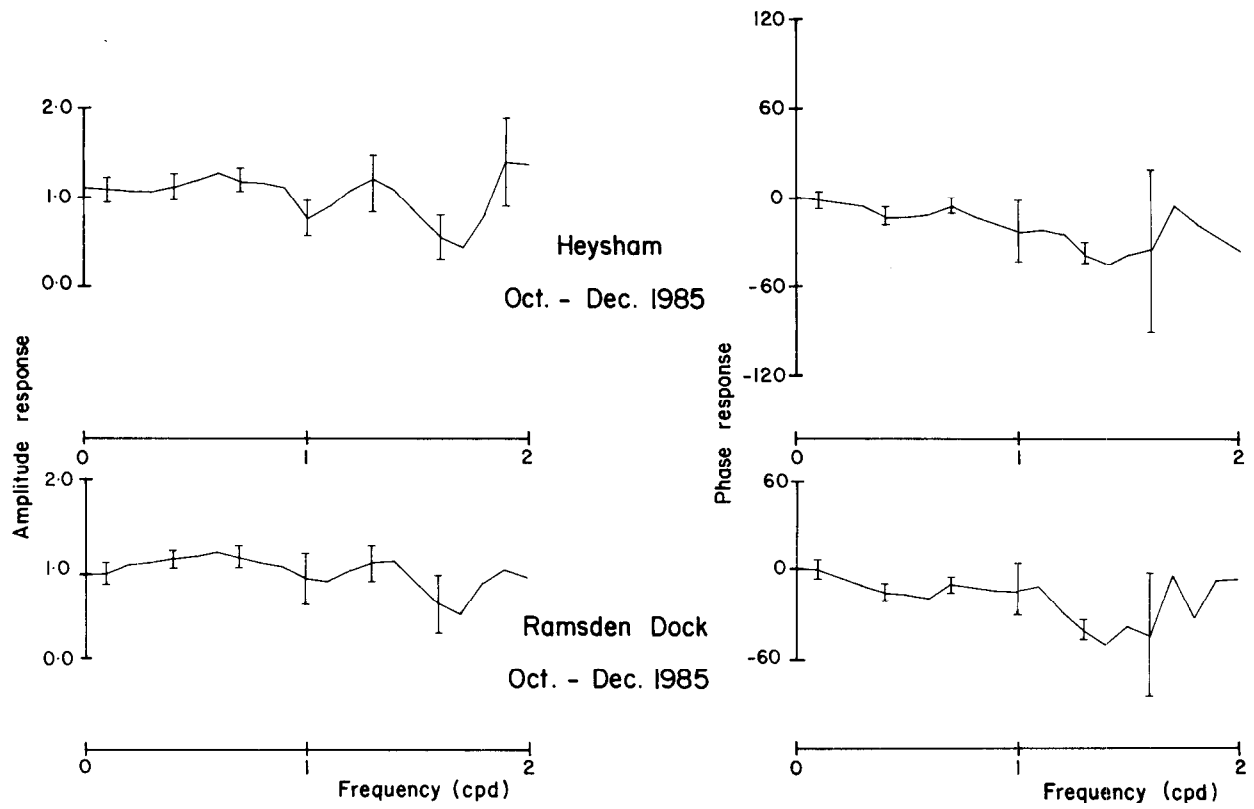


Figure 21: Transfer functions between the numerical model surge at Heysham (input) and observed surges at Heysham and Ramsden Dock (output).

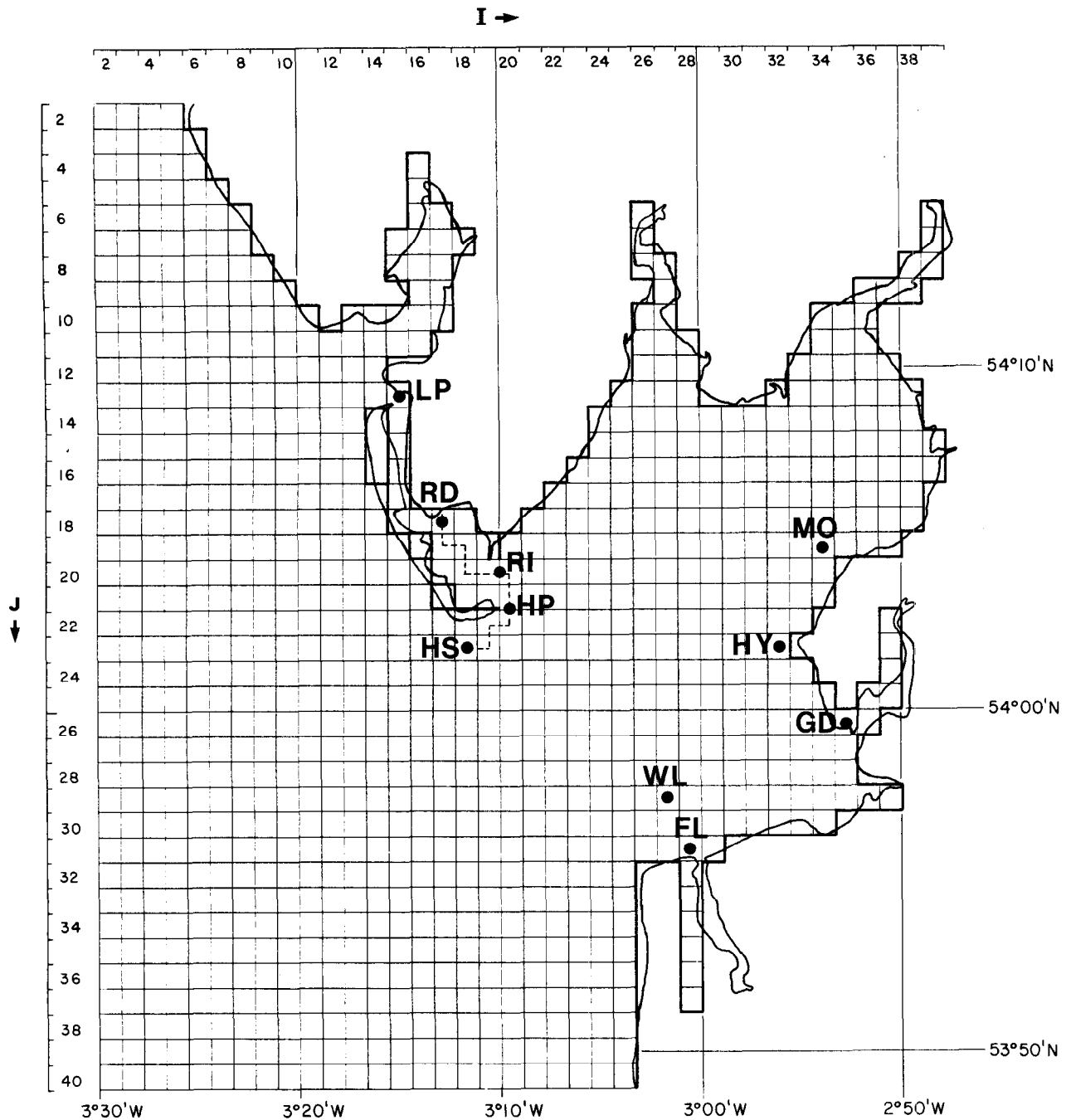


Figure 22: Computational grid for the Morecambe Bay model, with locations of points corresponding to tide gauges referred to in Table 22. The broken line indicates the approximation of the approach channel to Ramsden Dock. Grid points mentioned in the text may be identified by column (I) and row (J) numbers.

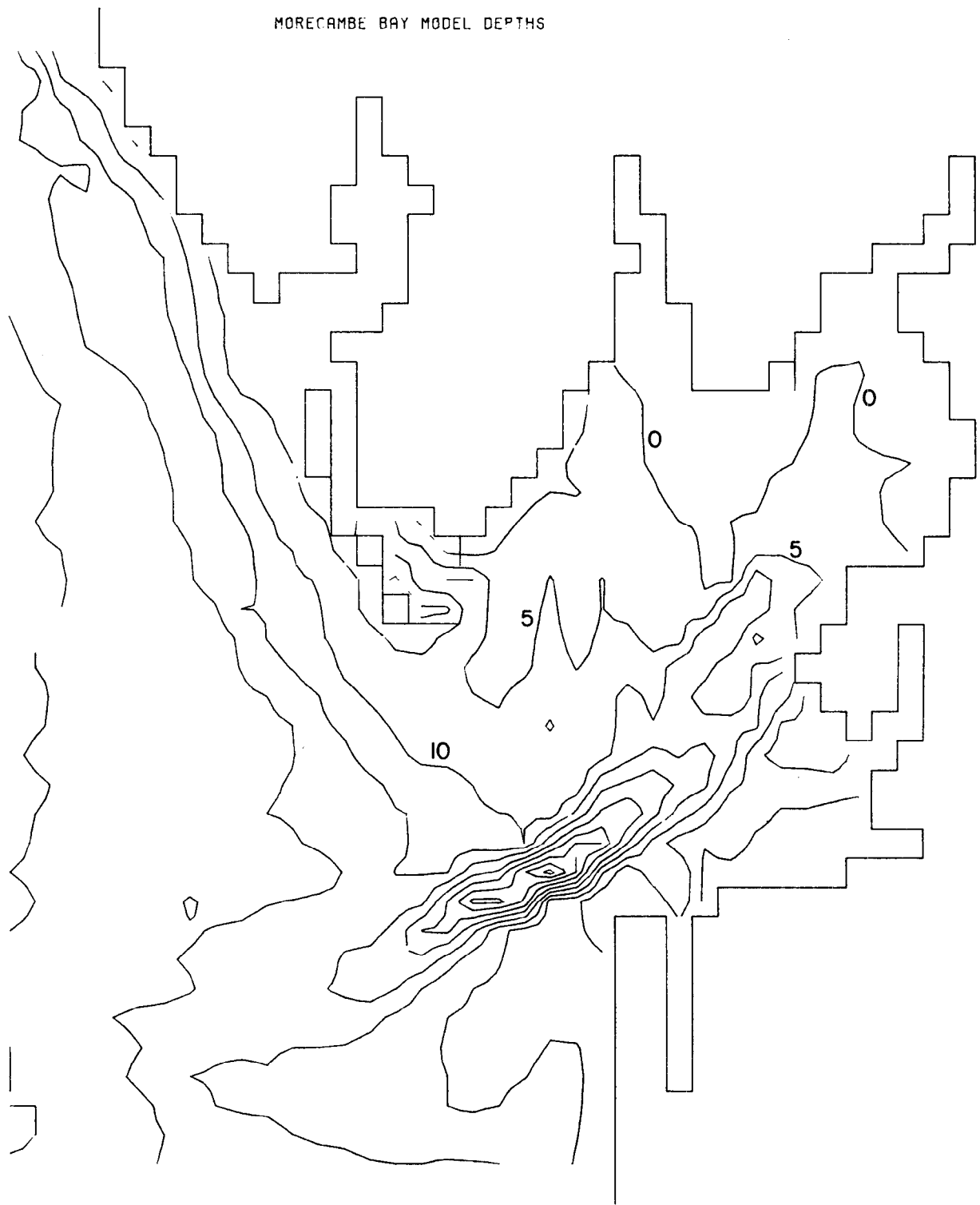


Figure 23: Bathymetry as represented in the Morecambe Bay model.

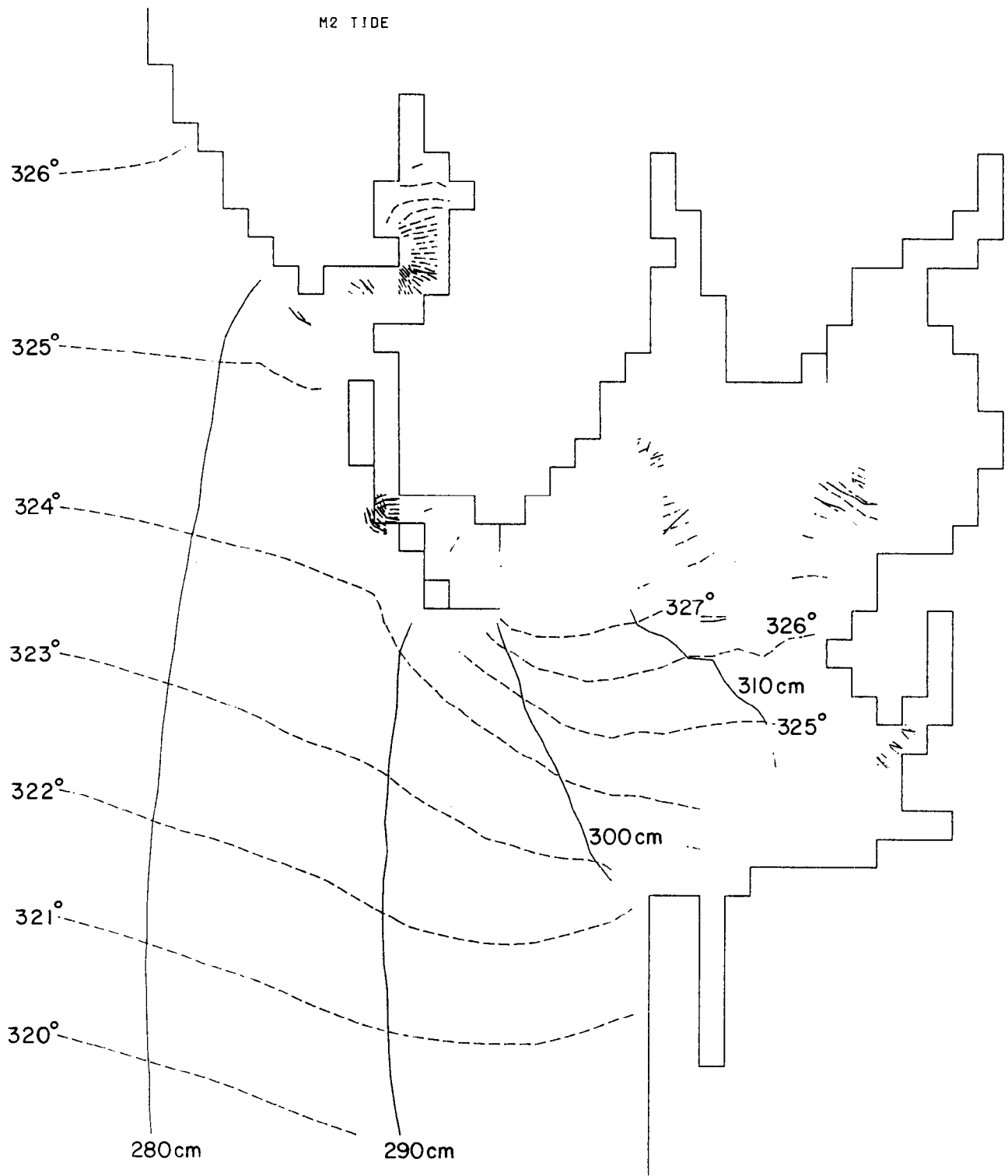


Figure 24: Chart of  $M_2$  tide computed using the Morecambe Bay model, showing contours of amplitude (cm : continuous lines), and phase (degrees : broken lines) for those parts of the Bay not subject to drying.

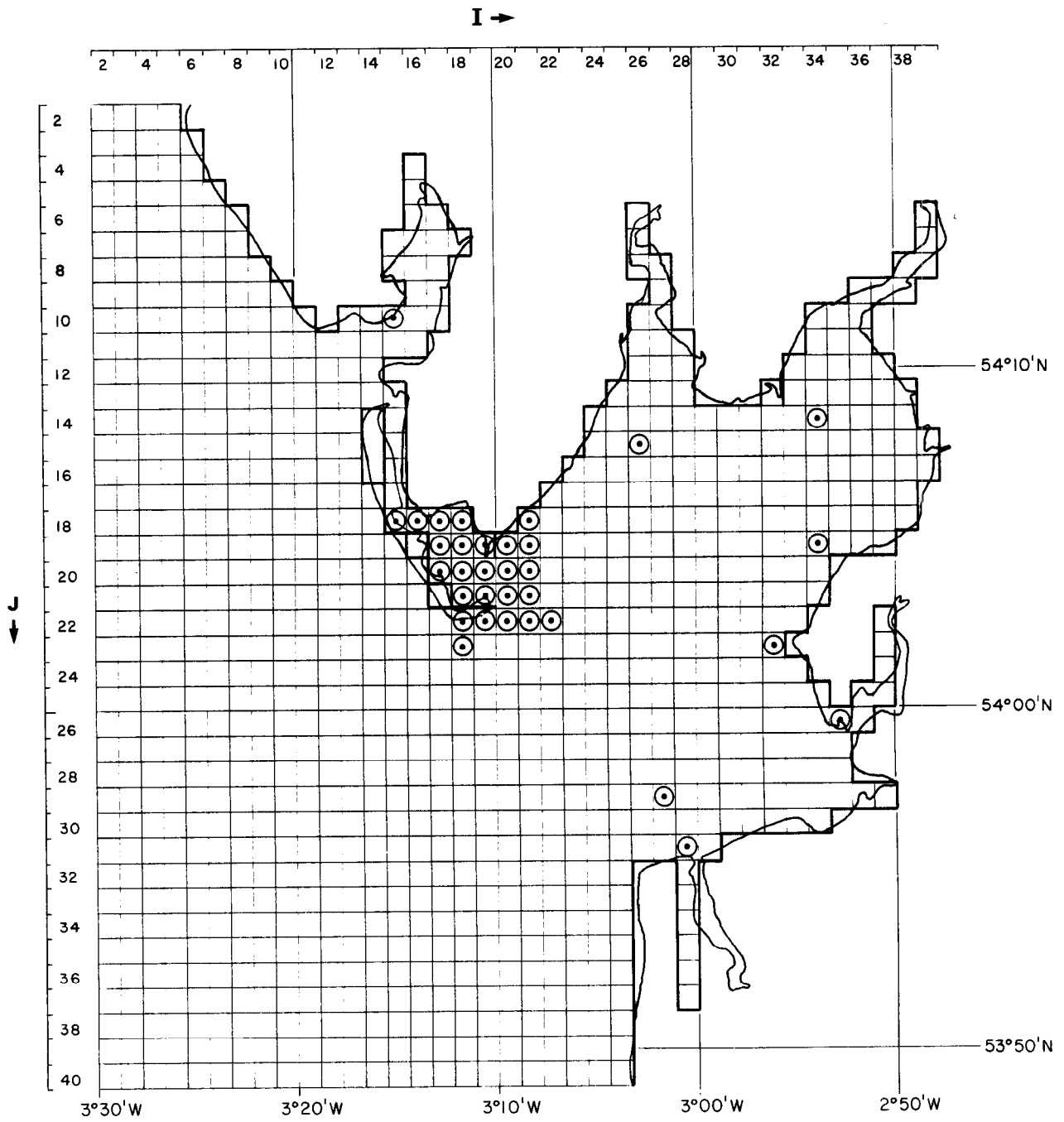


Figure 25: Locations of model grid points for which surge responses are plotted.

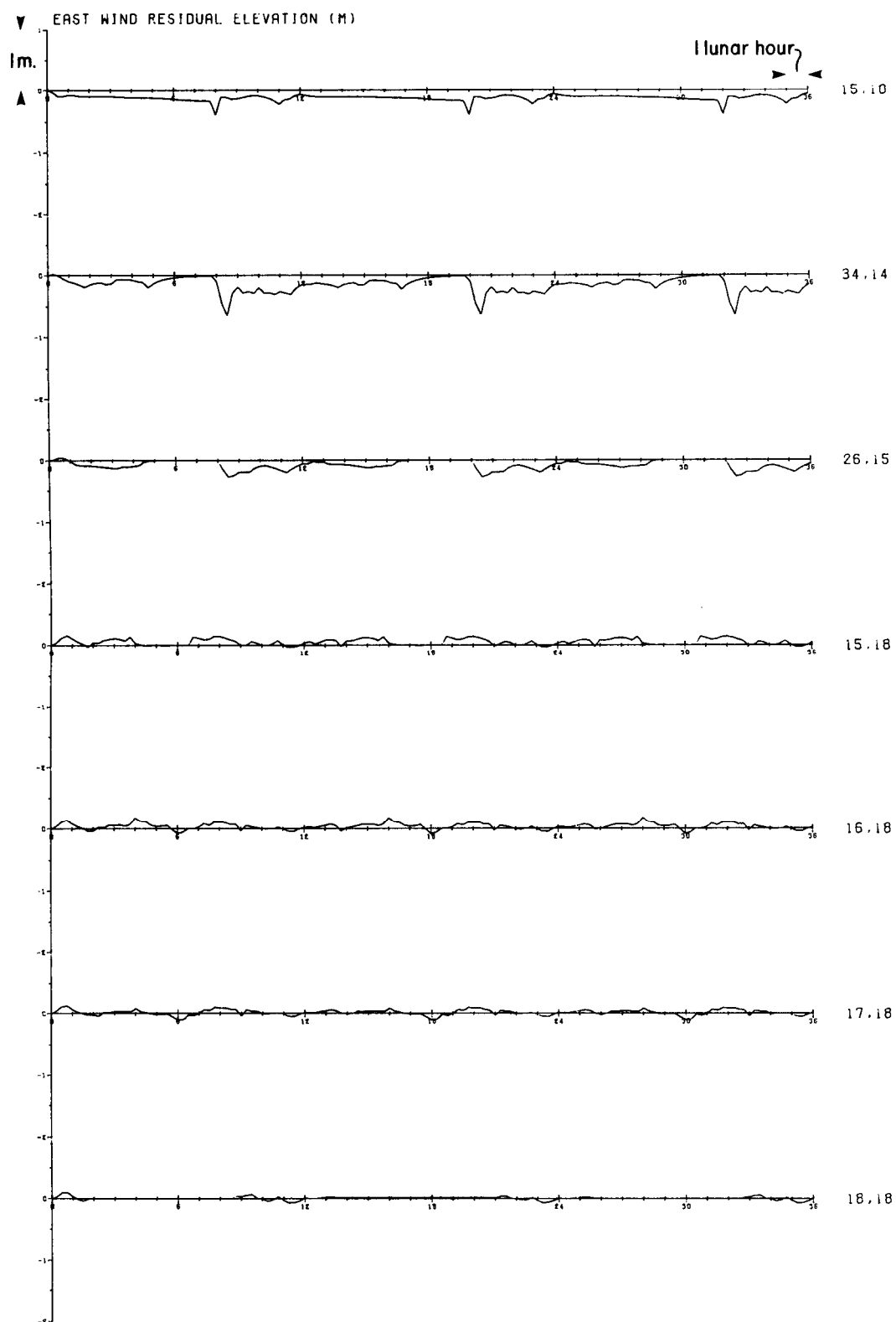


Figure 26: Variation with time of surge residual elevation produced by an easterly wind stress at grid points identified in Fig. 25; sampling is every 1/4 lunar hour over 3 tidal cycles.

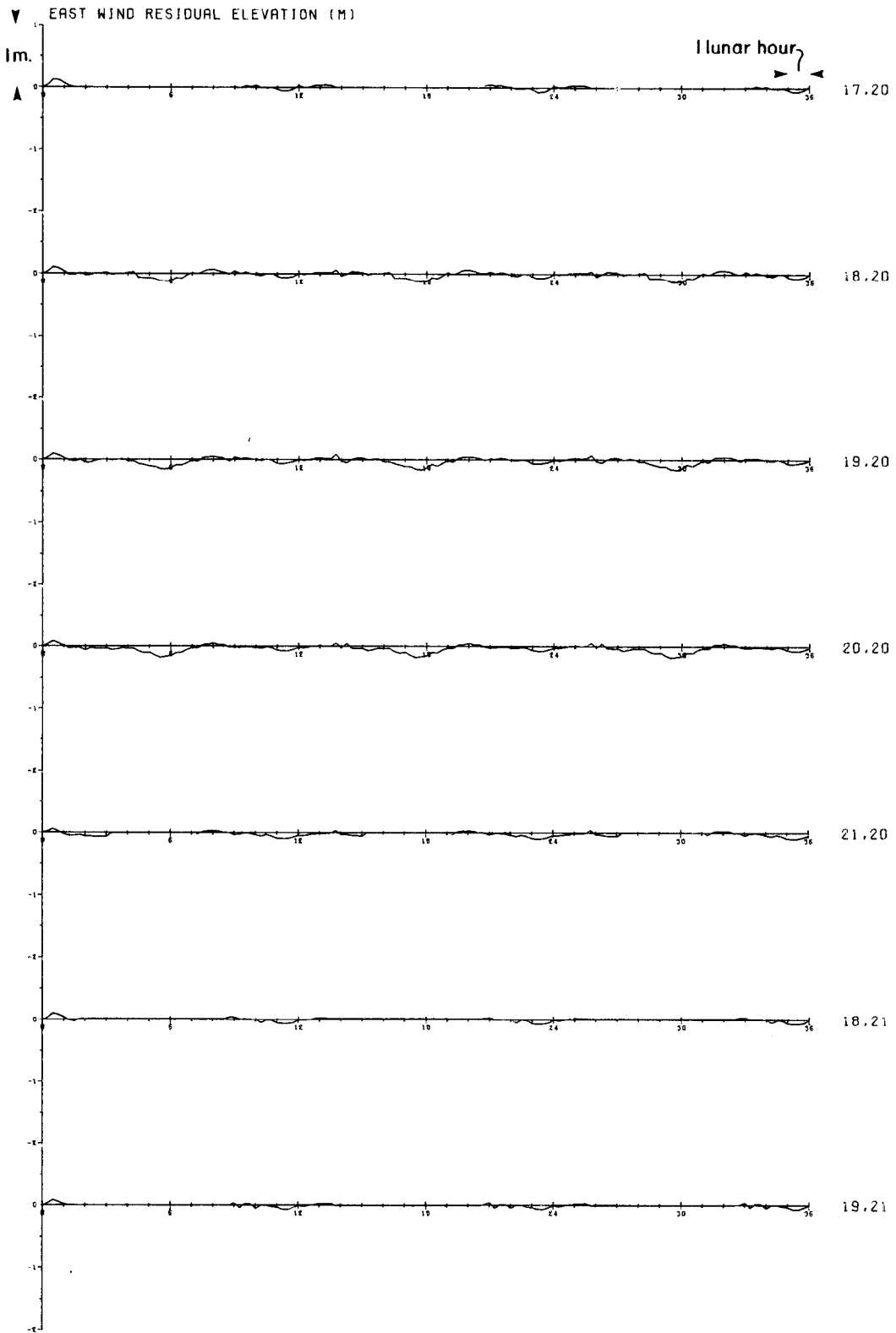


Figure 26: (CONT)



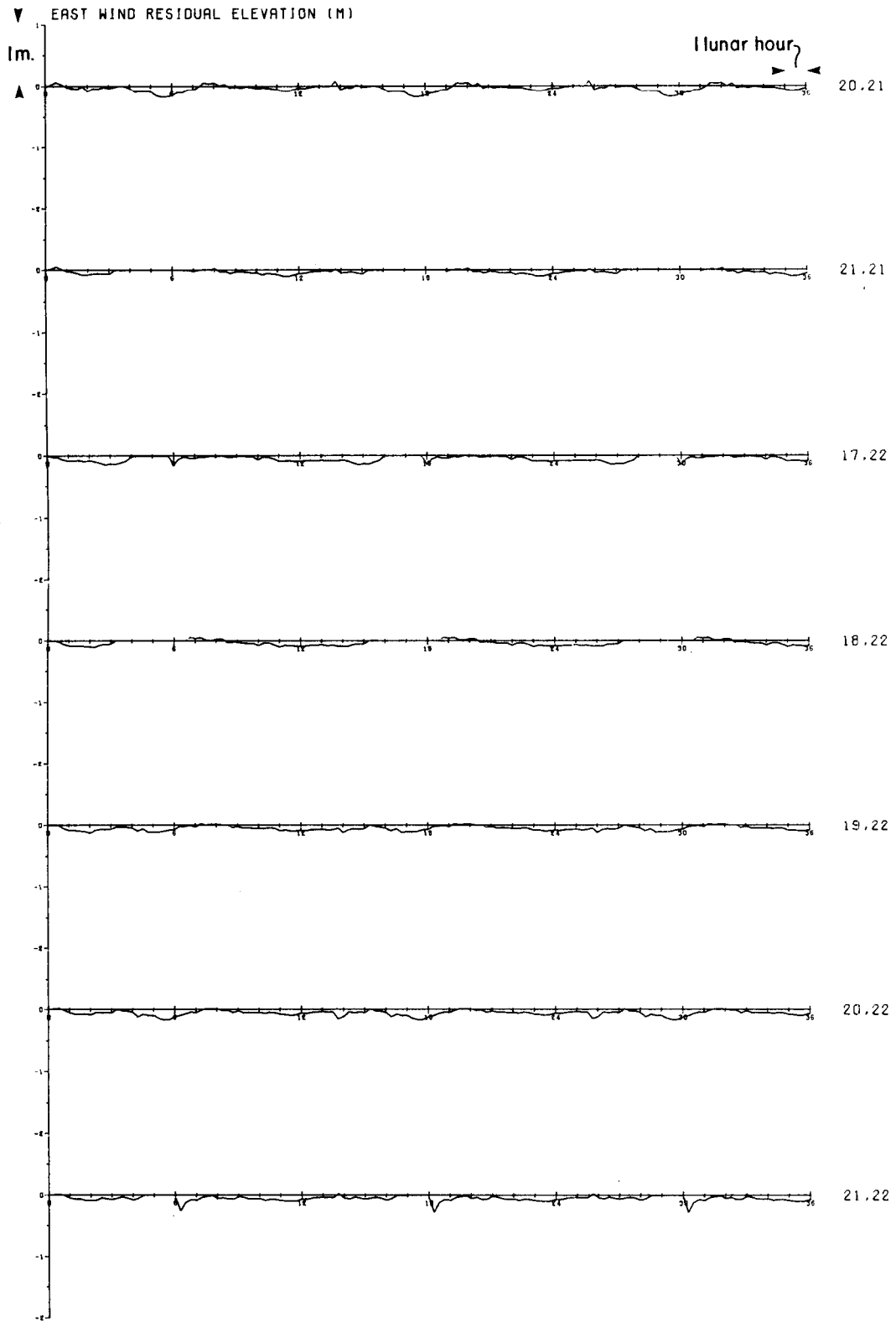


Figure 26: (CONT)



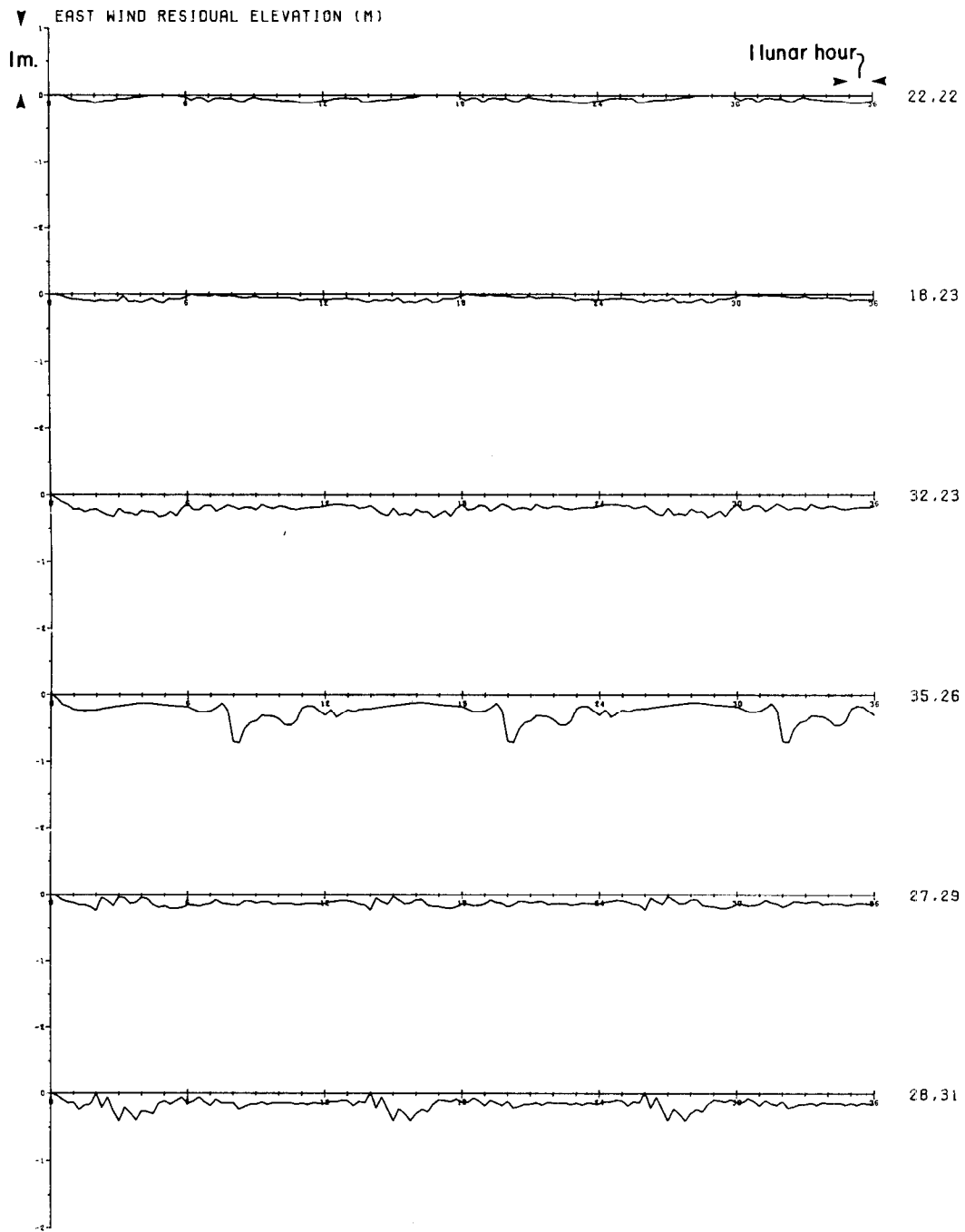


Figure 26: (CONT)

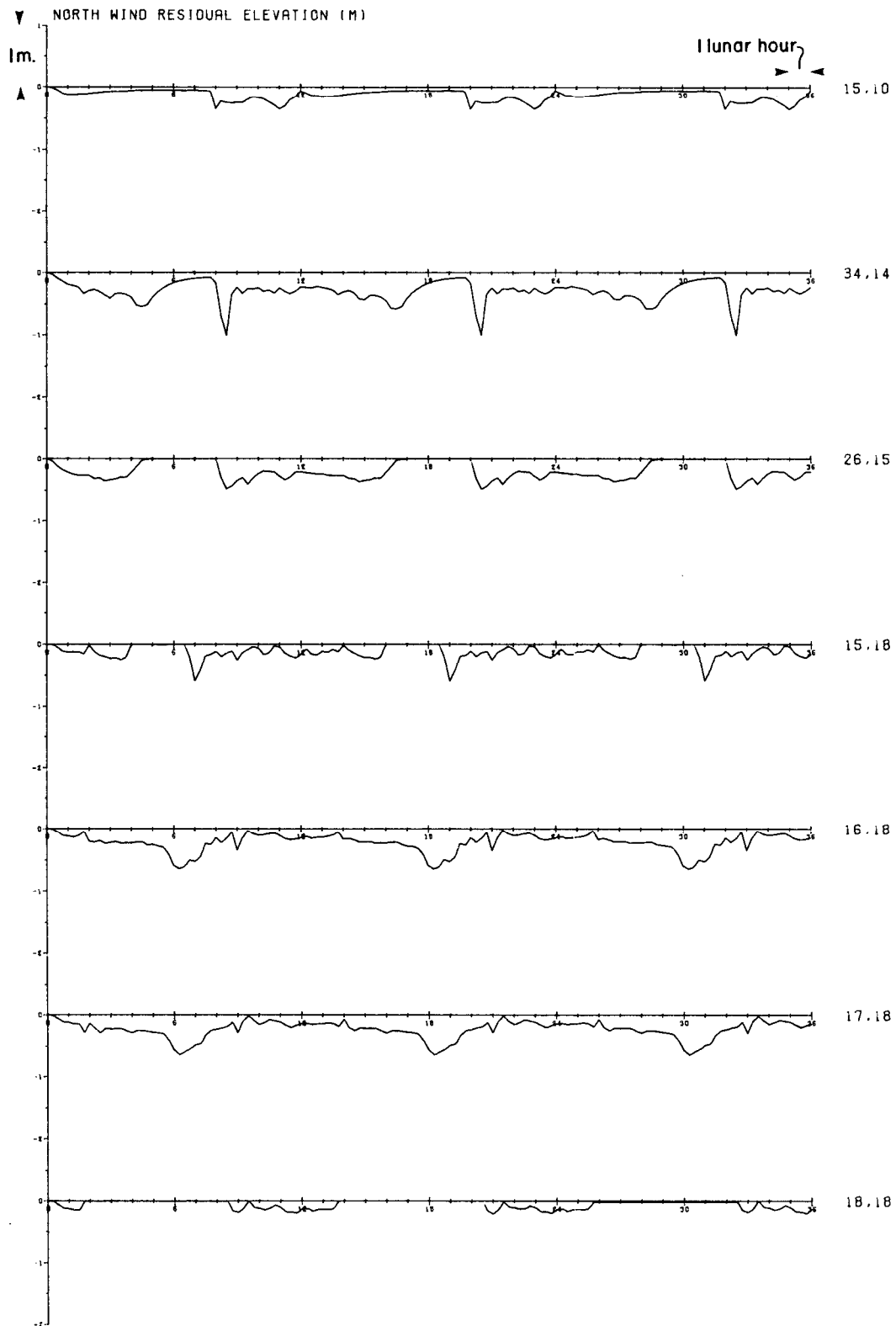


Figure 27: Variation with time of surge residual elevation produced by a northerly wind stress at grid points identified in Fig. 25; sampling is every 1/4 lunar hour over 3 tidal cycles.

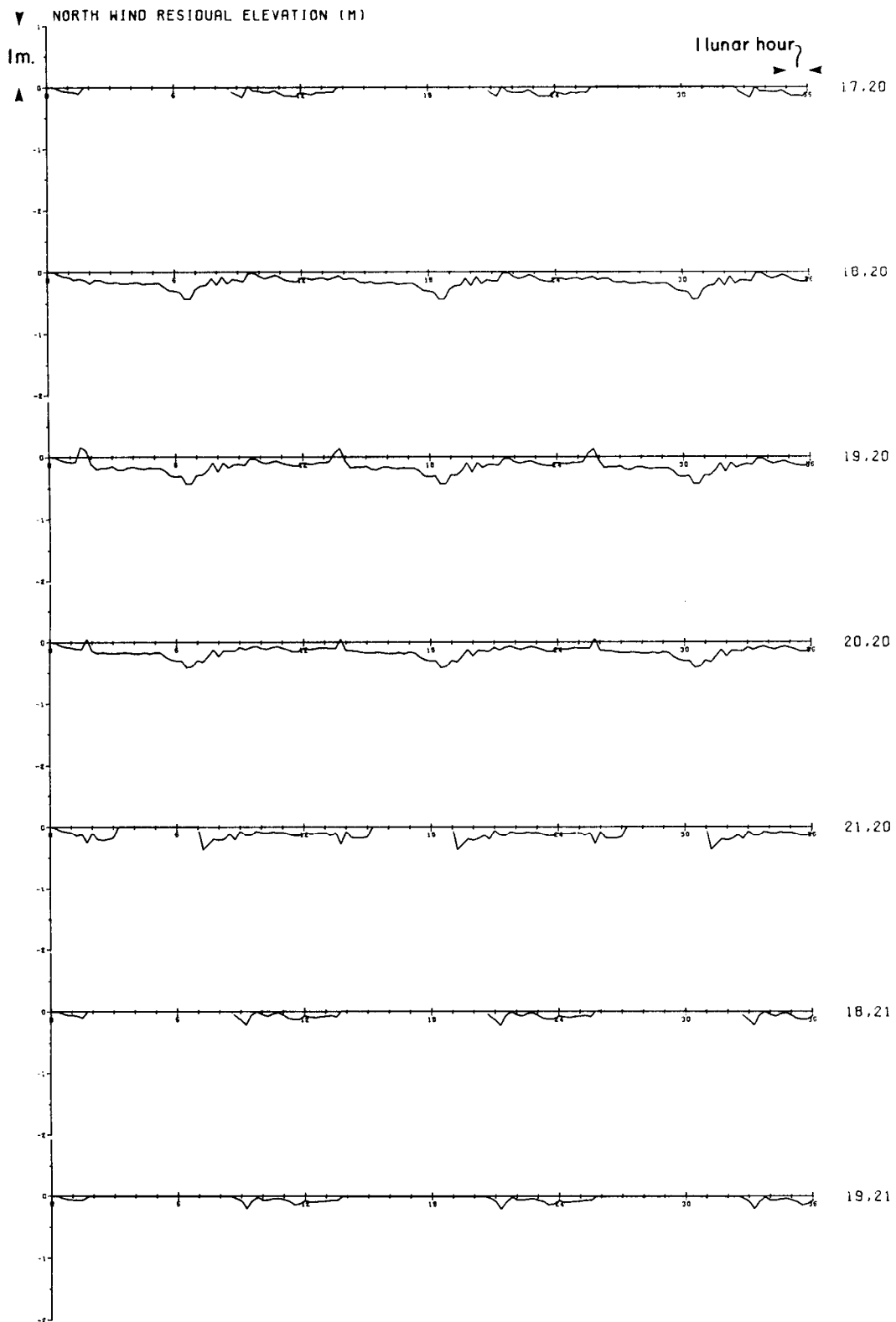


Figure 27: (CONT)

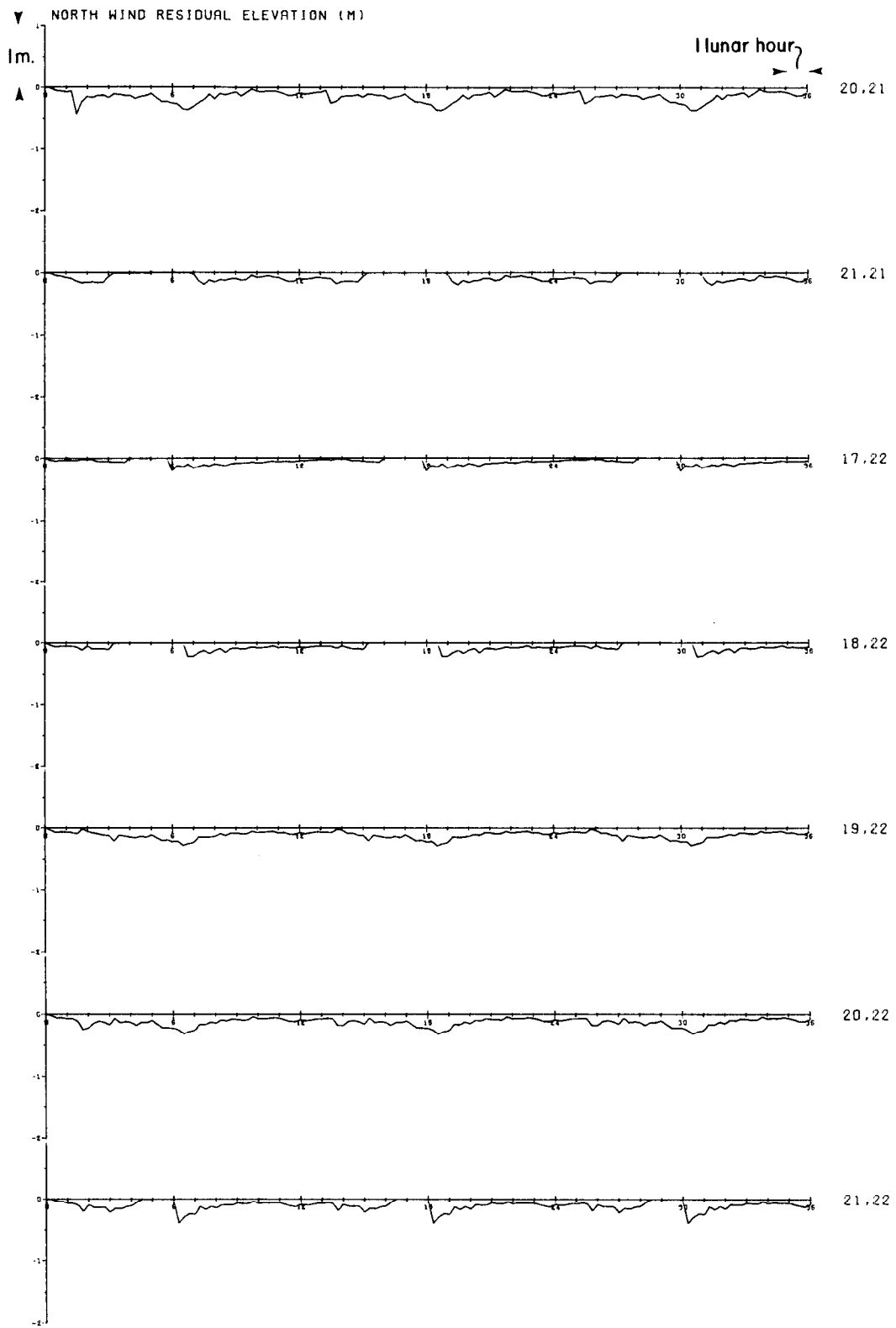


Figure 27: (CONT)

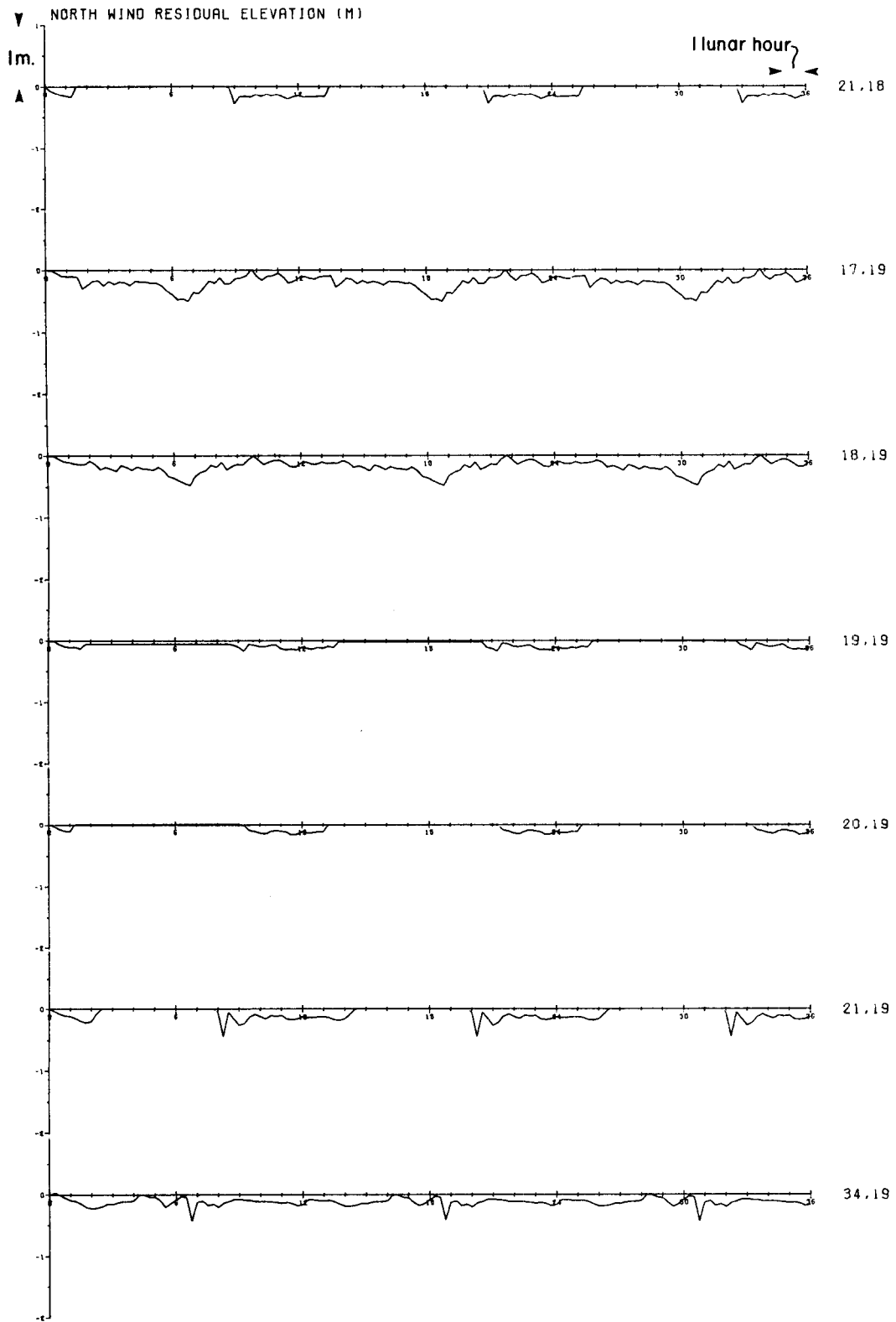


Figure 27: (CONT)





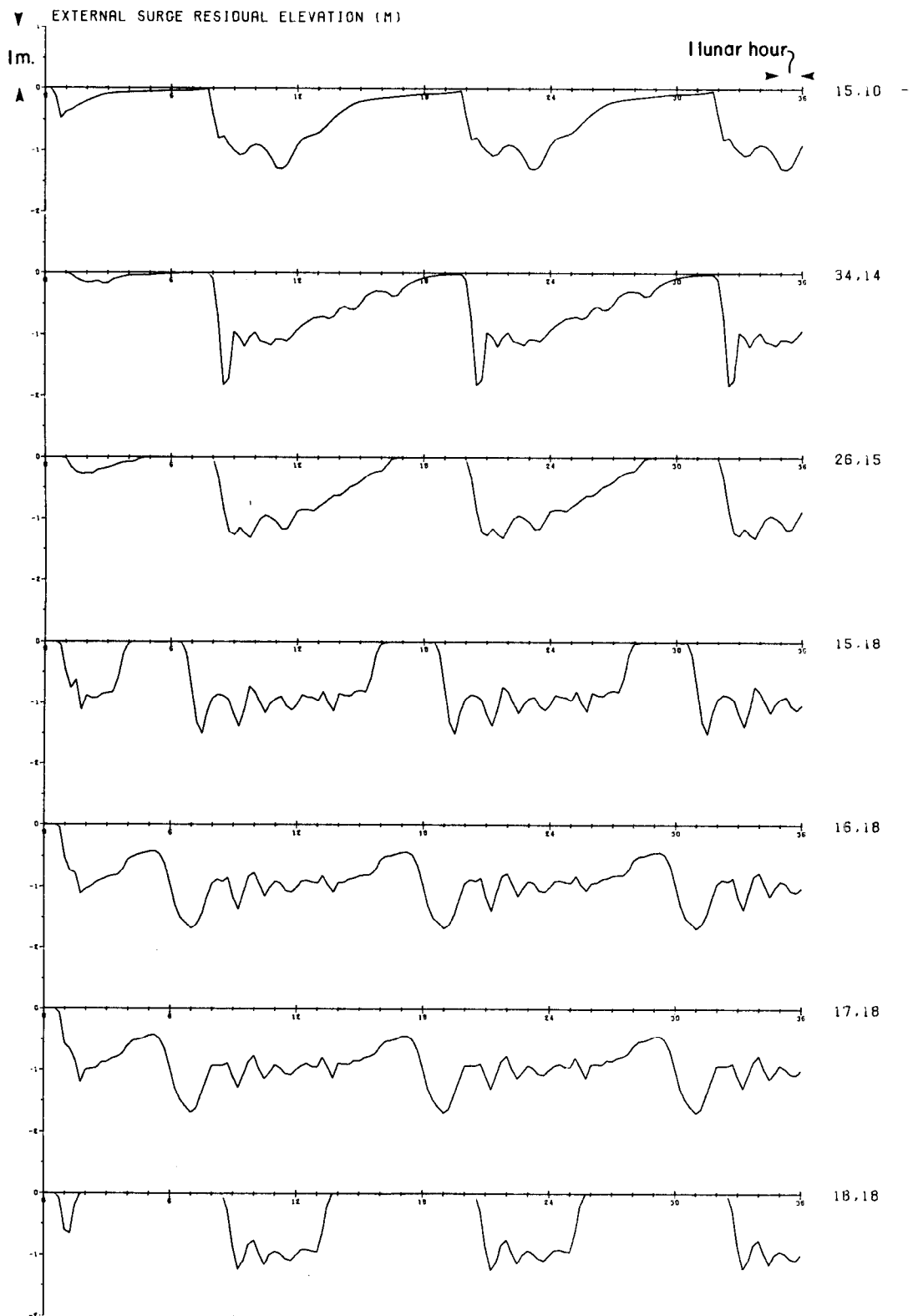


Figure 28: Variation with time of surge residual elevation produced by an external surge of  $-1\text{m}$  imposed at the model openboundary at grid points identified in Fig. 25; sampling is every  $1/4$  lunar hour over 3 tidal cycles.

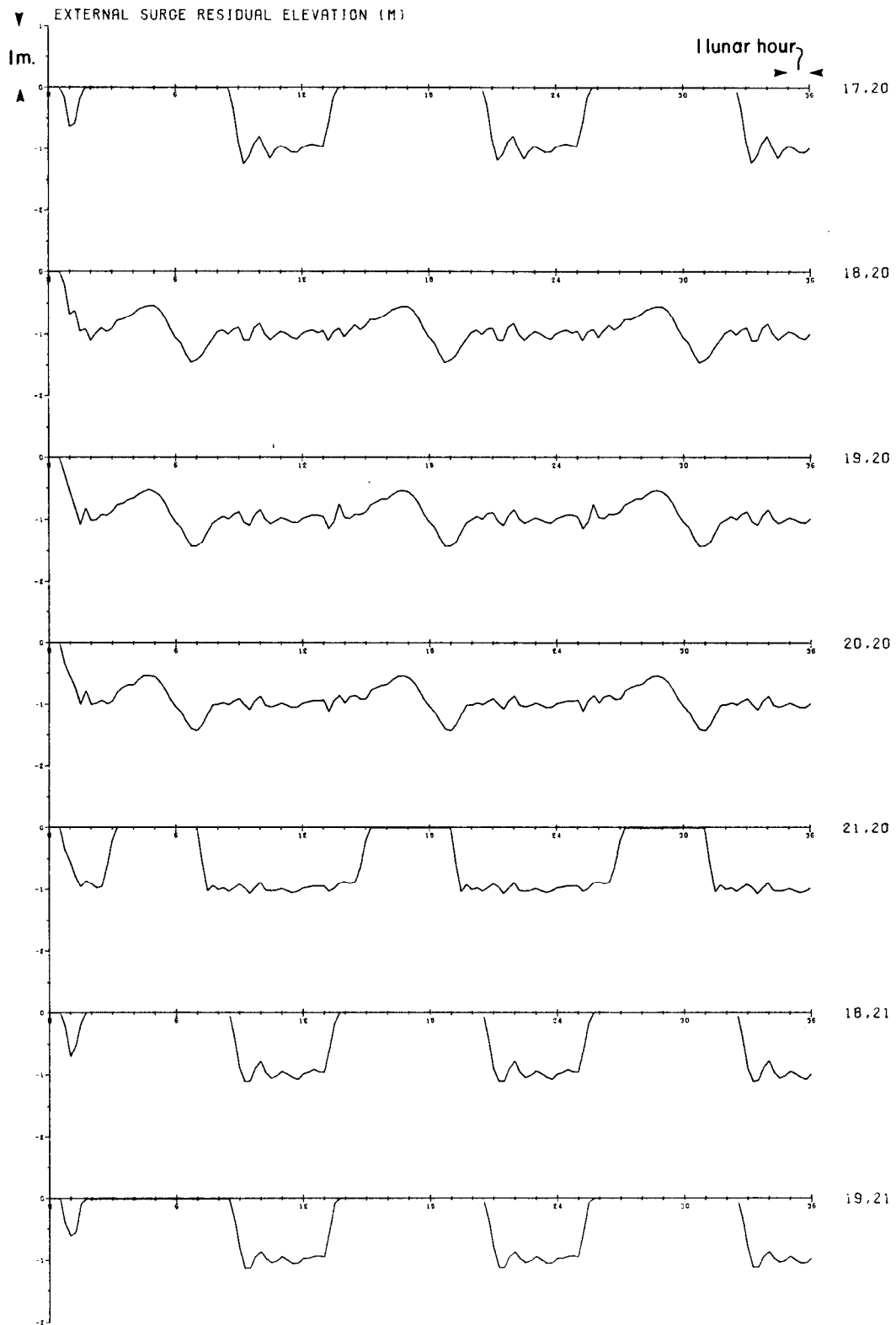


Figure 28: (CONT)

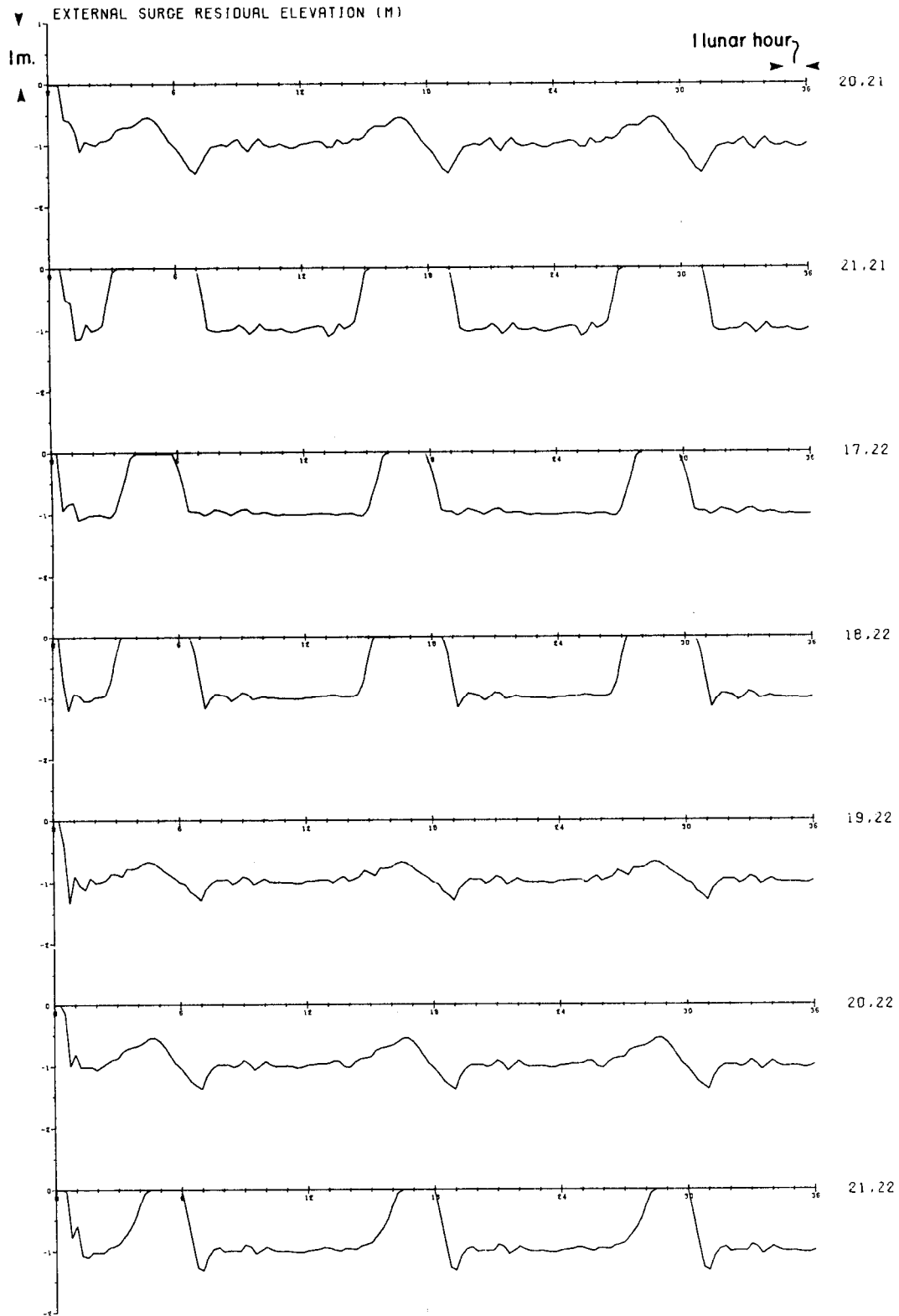


Figure 28: (Cont.)

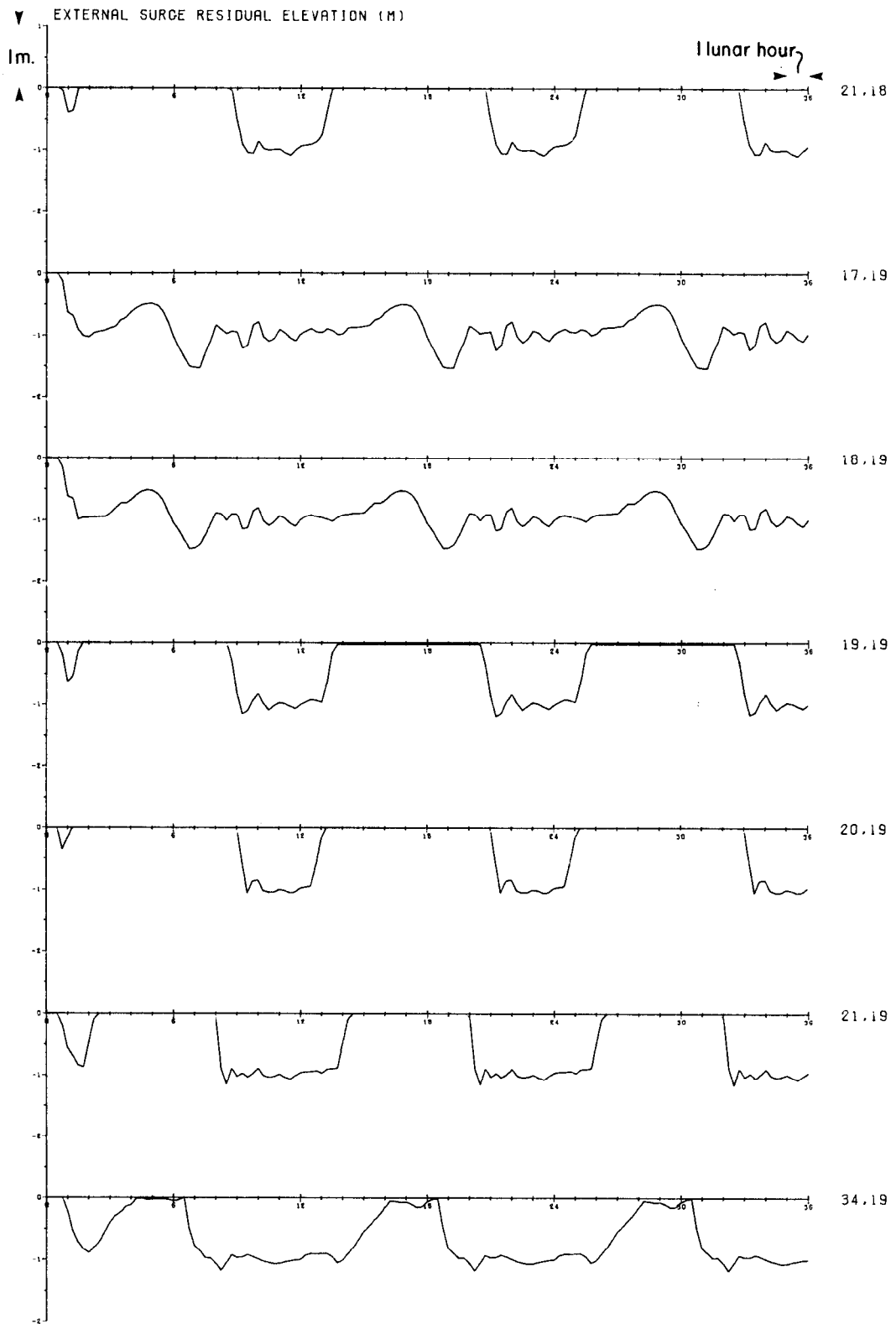


Figure 28: (CONT)

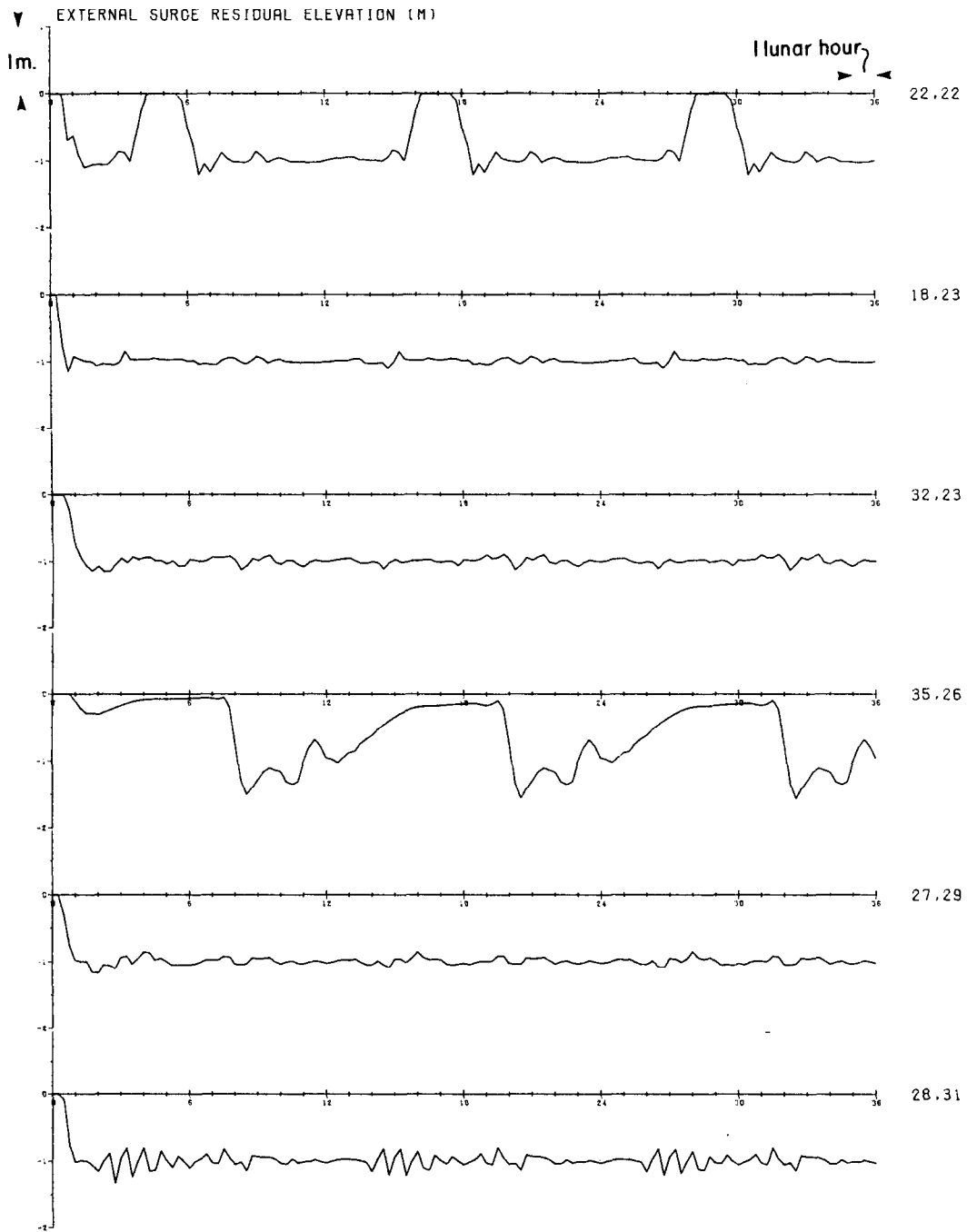


Figure 28: (CONT)

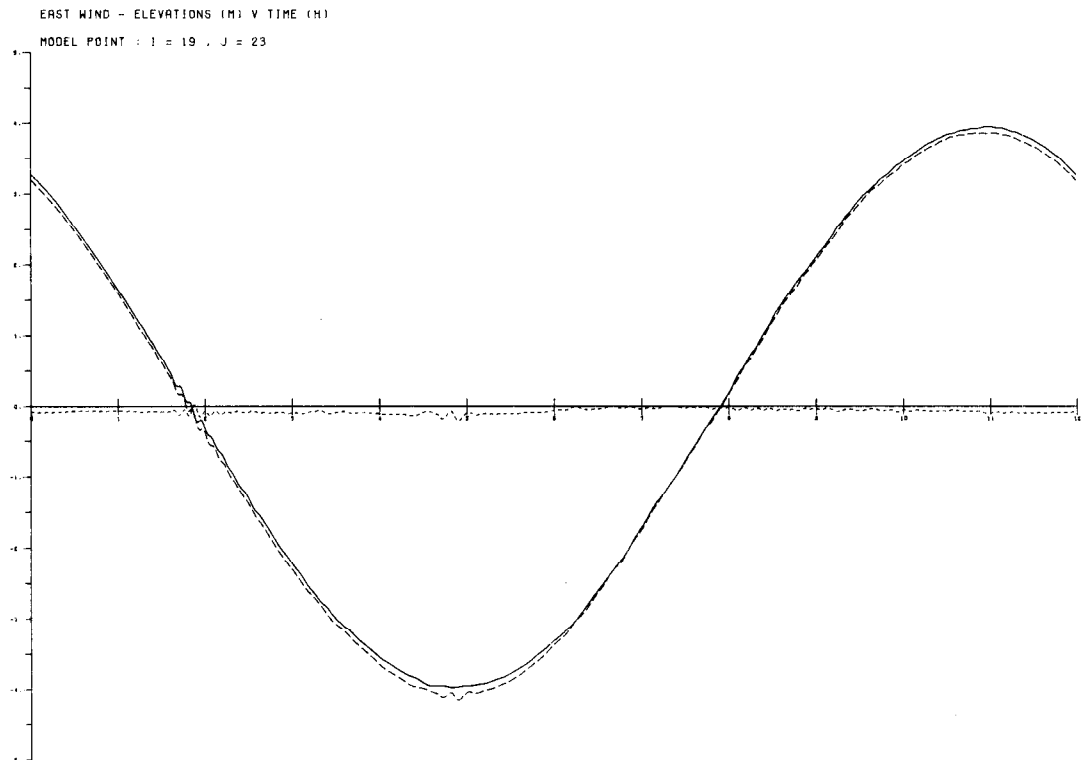
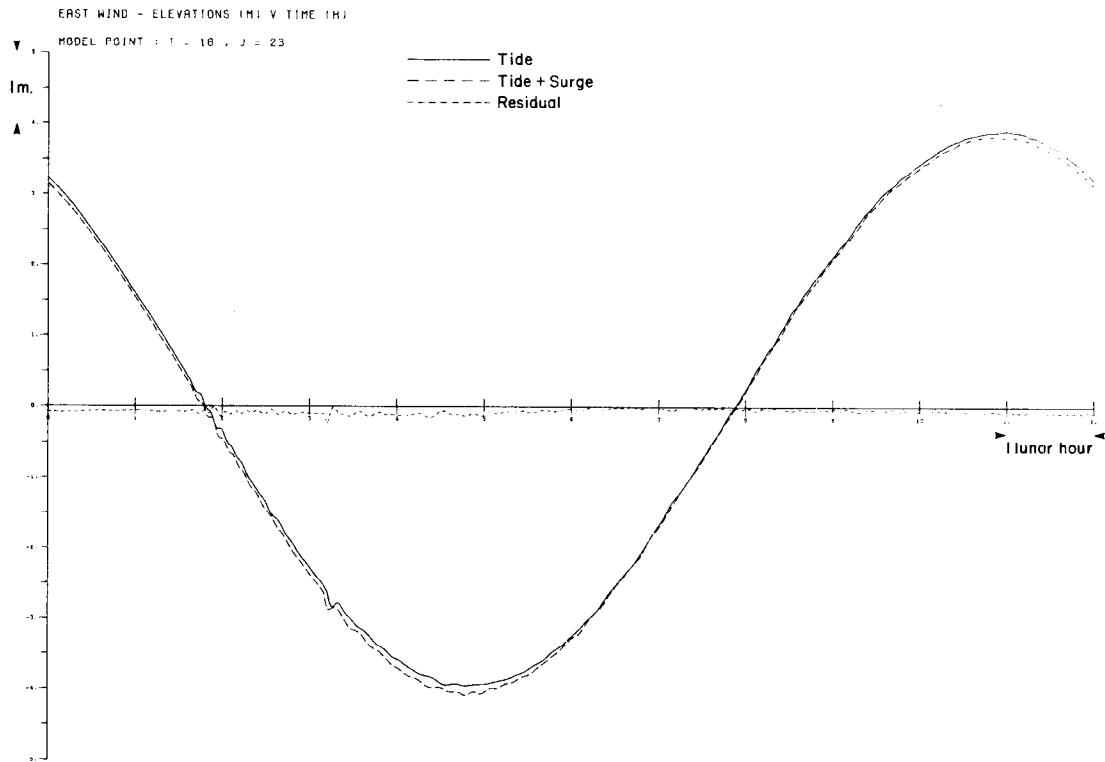


Figure 29: Variation of tide + surge (-----), tide alone (——) and surge residual (.....) produced by an easterly wind stress; sampling at every timestep over 1 tidal cycle.

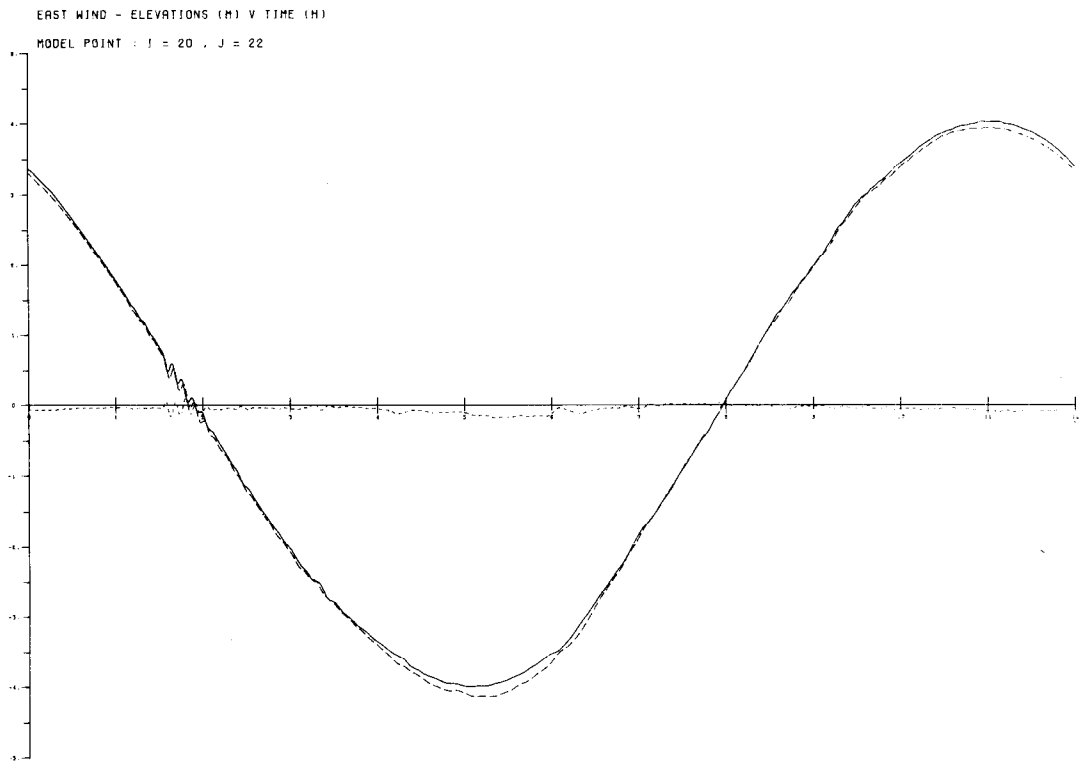
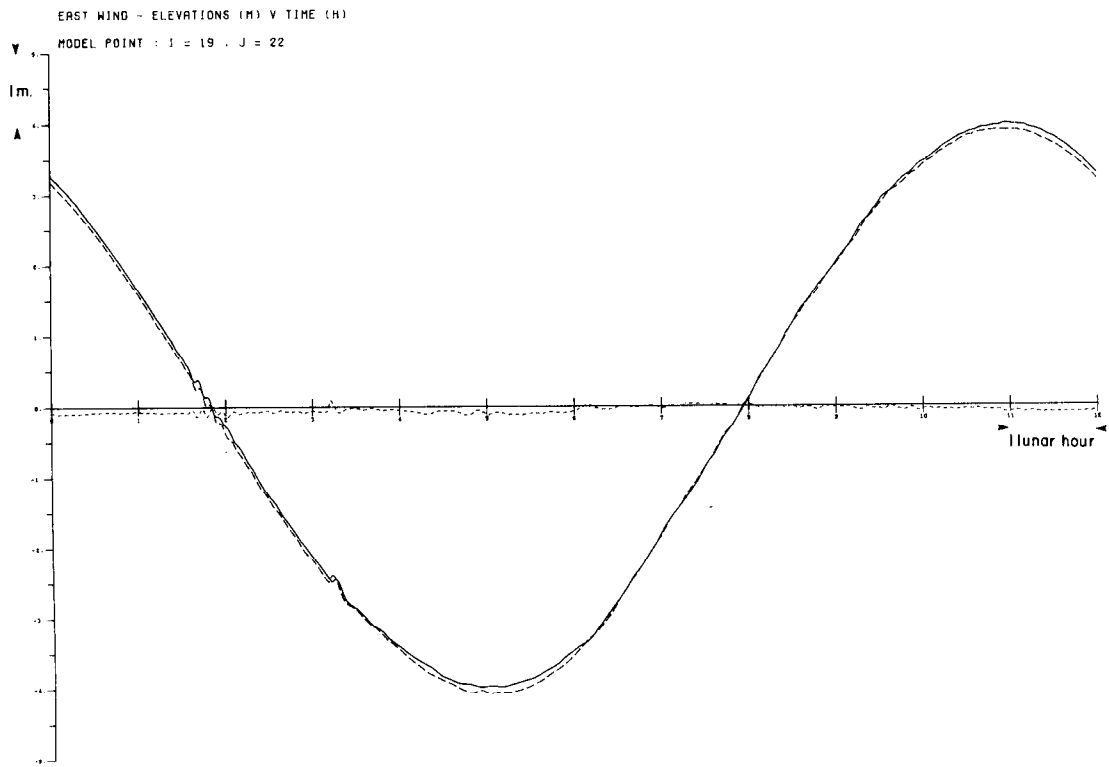


Figure 29: (CONT)

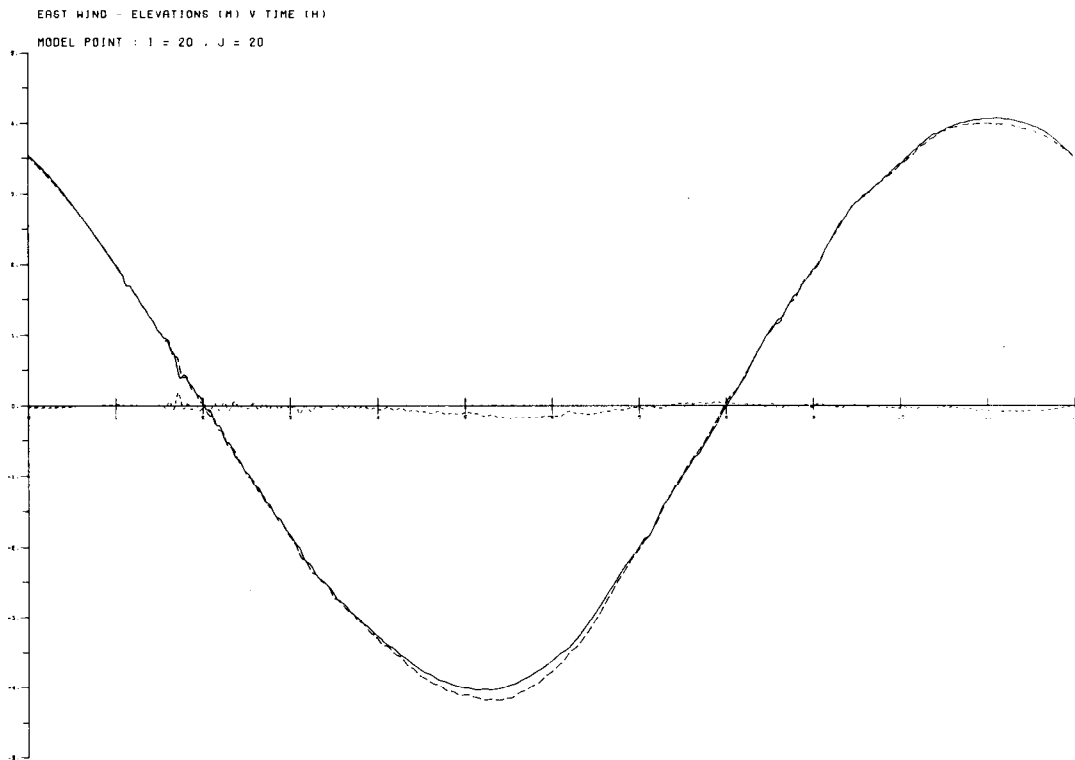
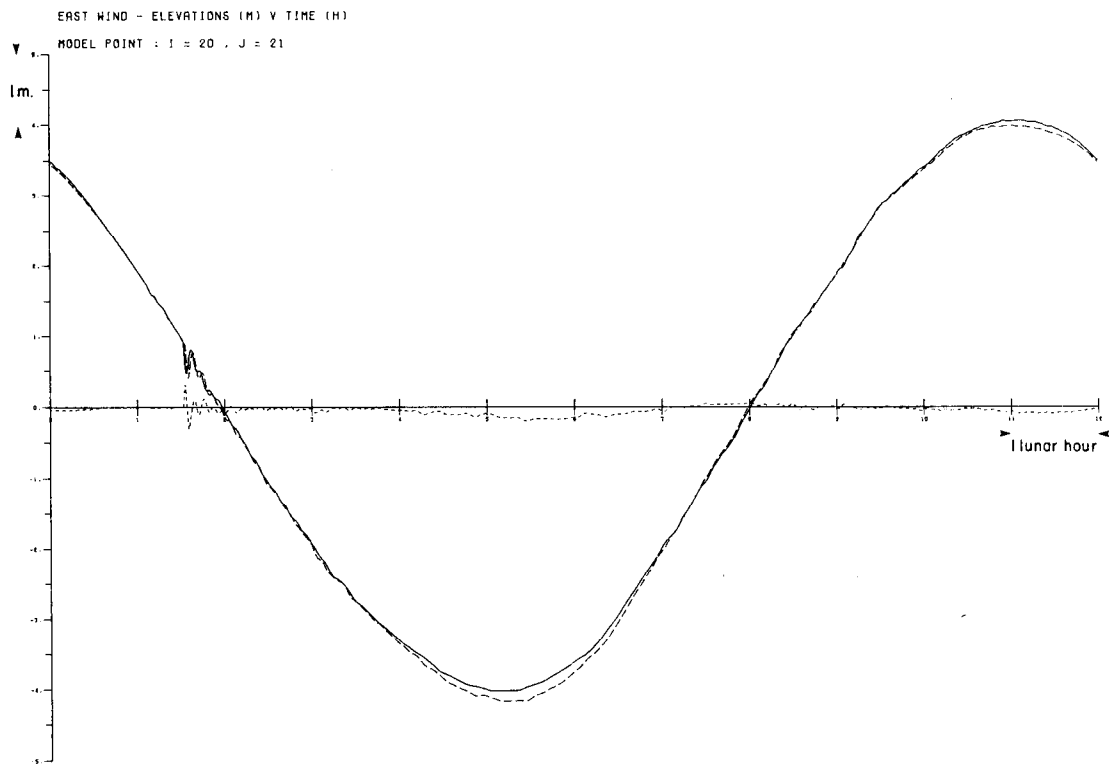


Figure 29: (CONT)



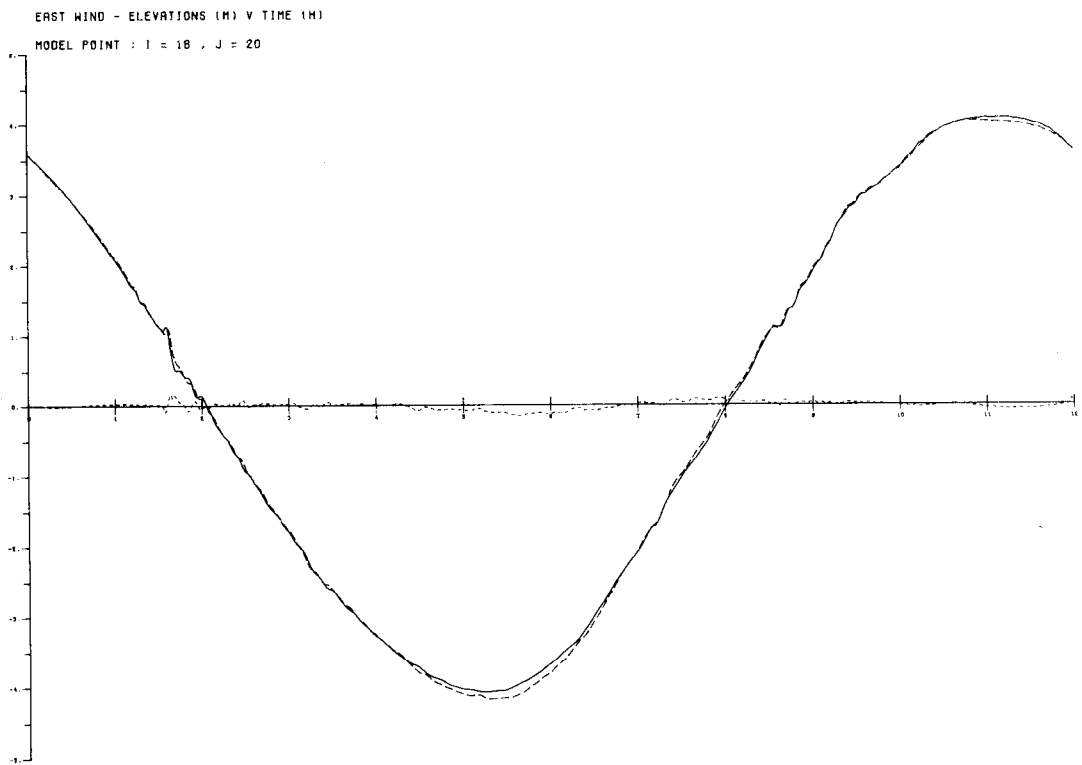
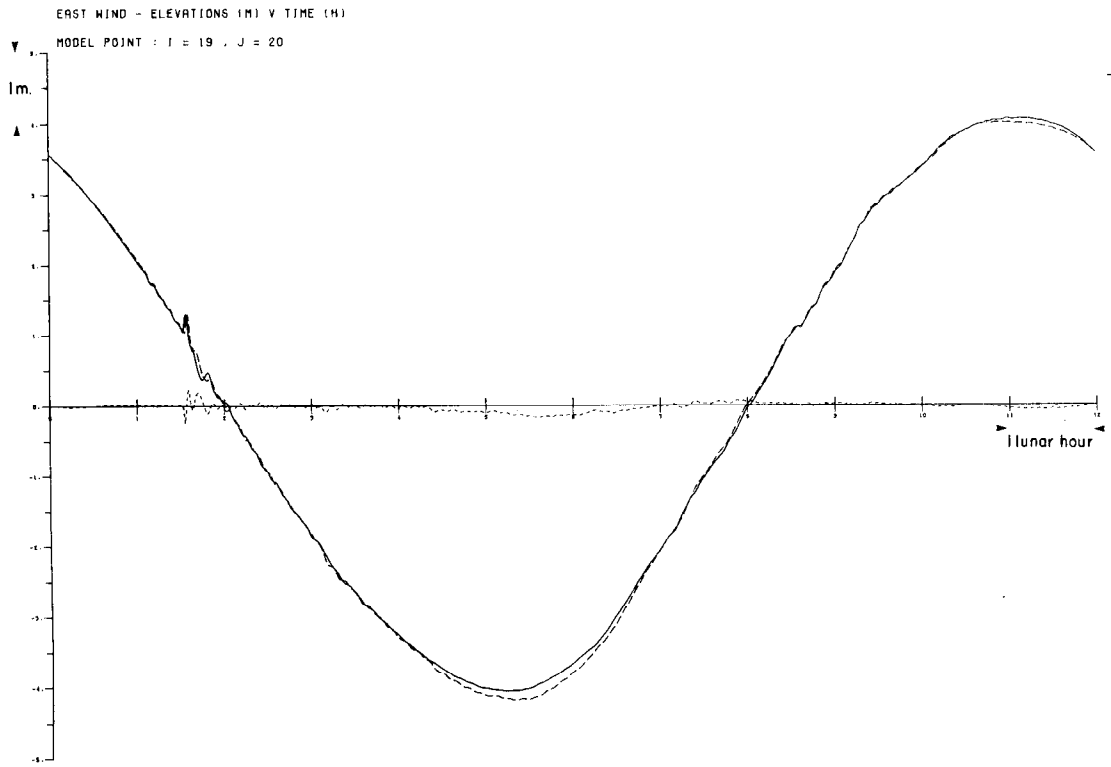


Figure 29: (CONT)

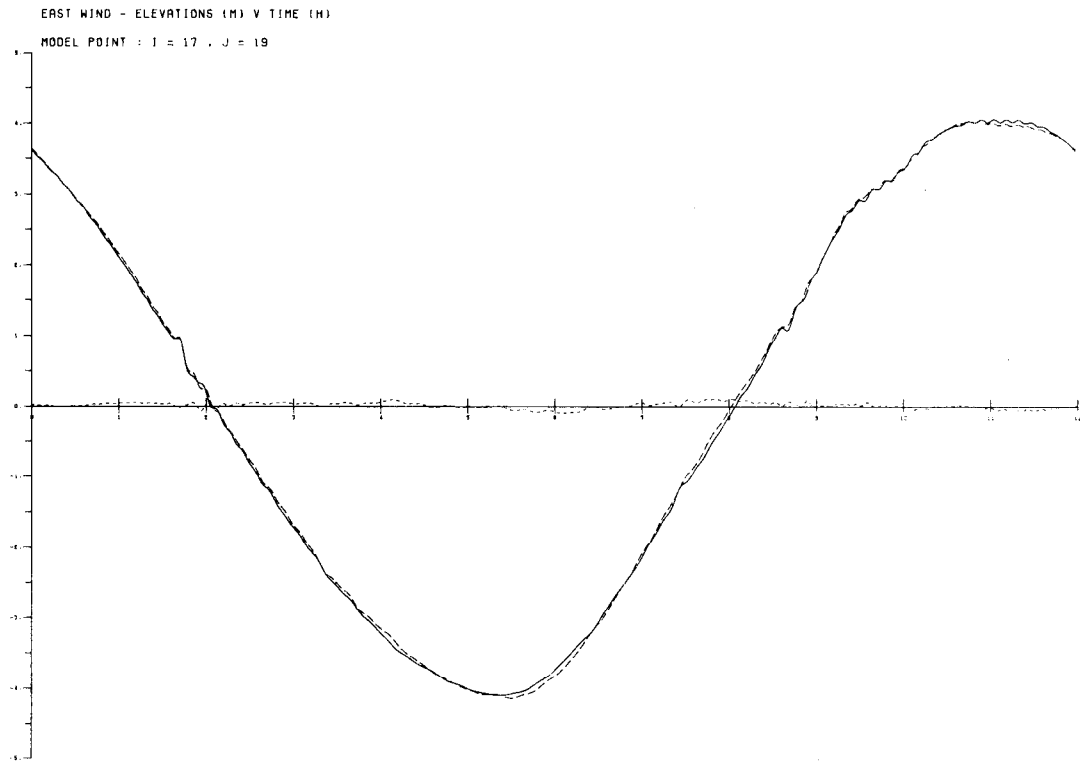
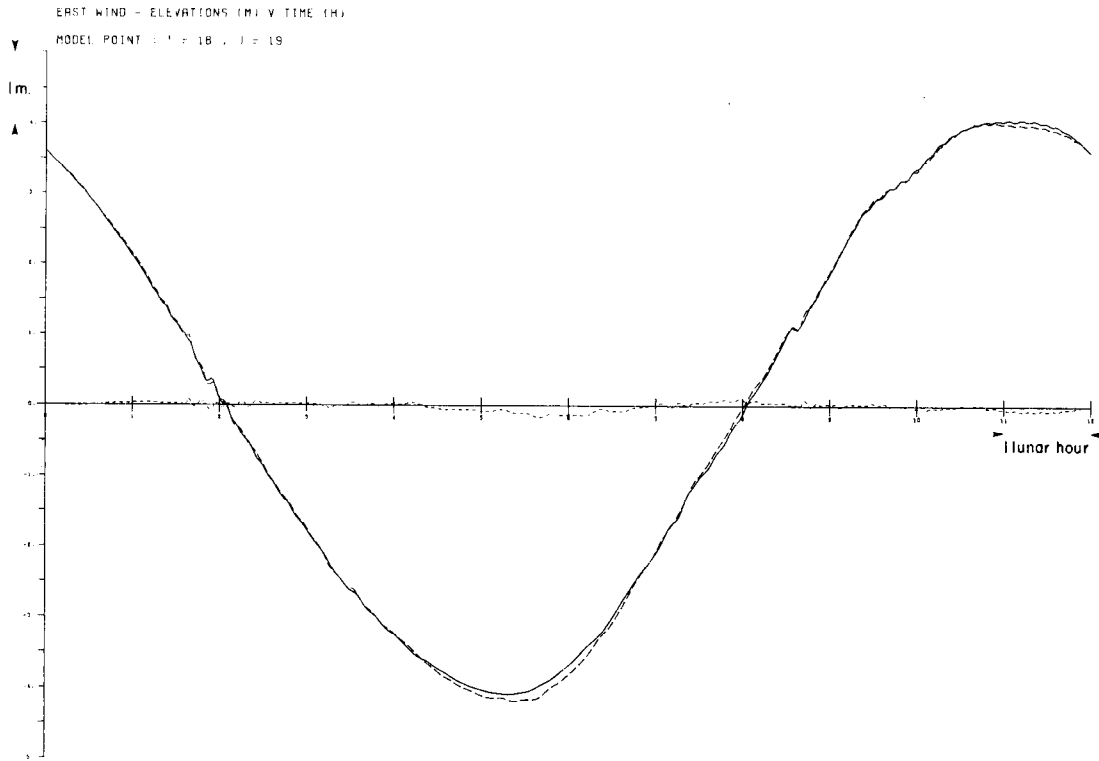


Figure 29: (CONT)

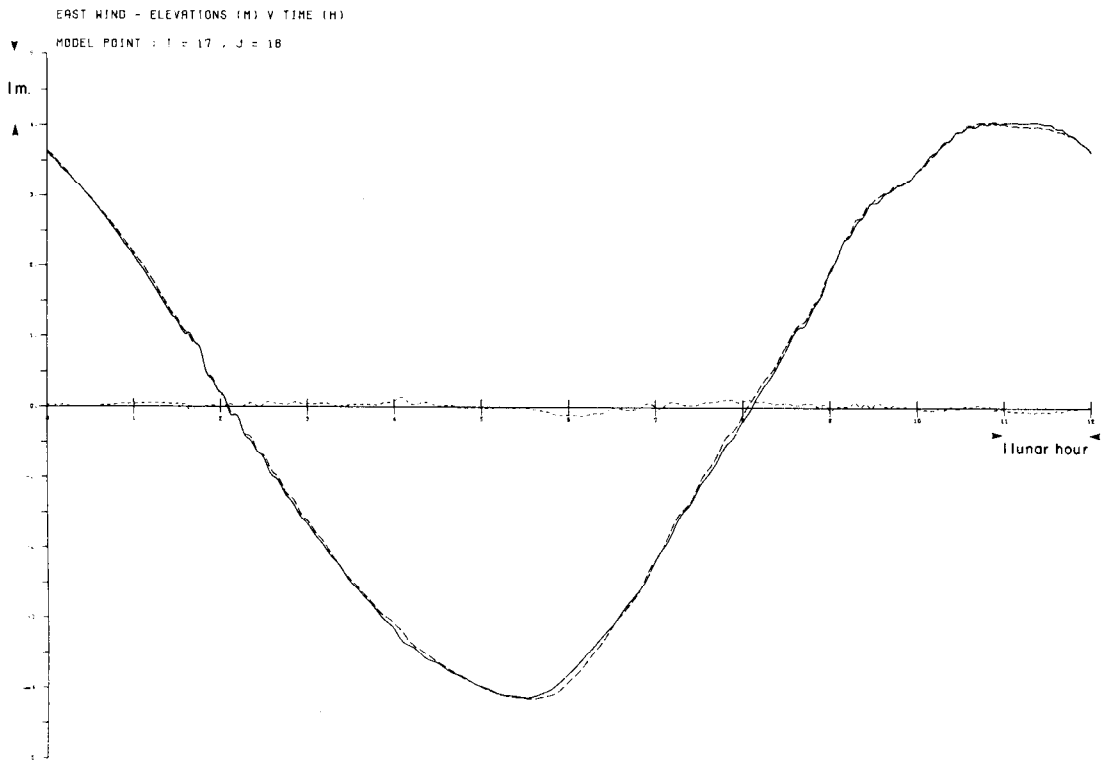


Figure 29: (CONT)

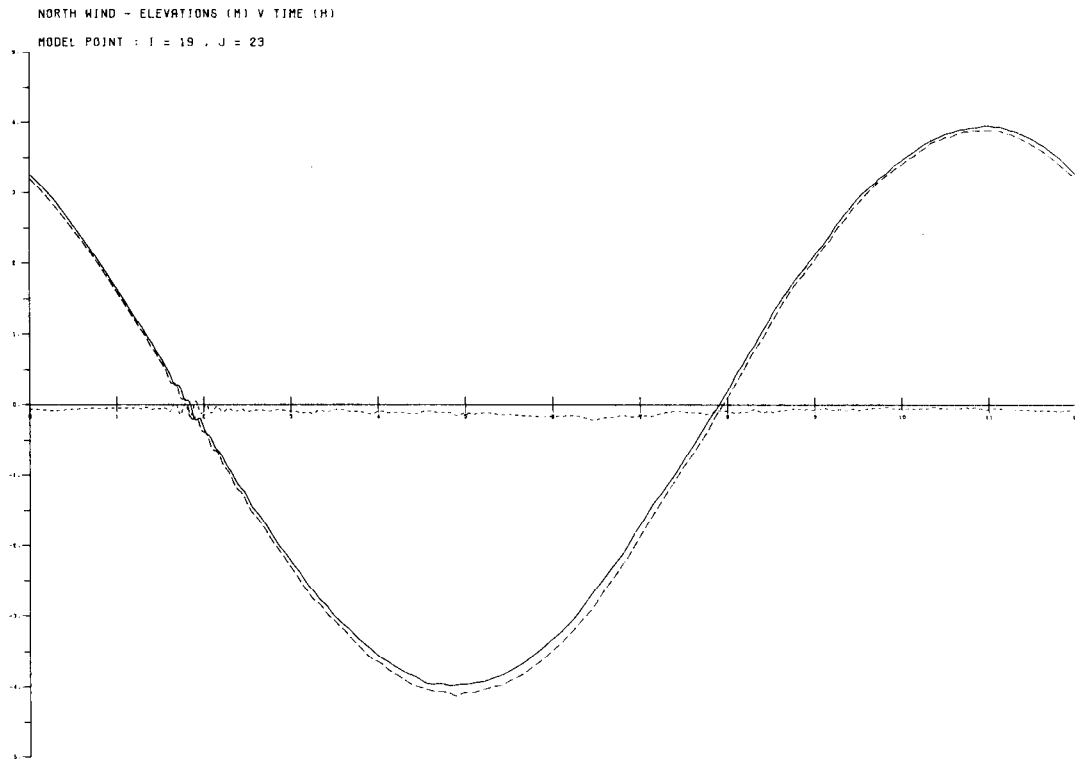
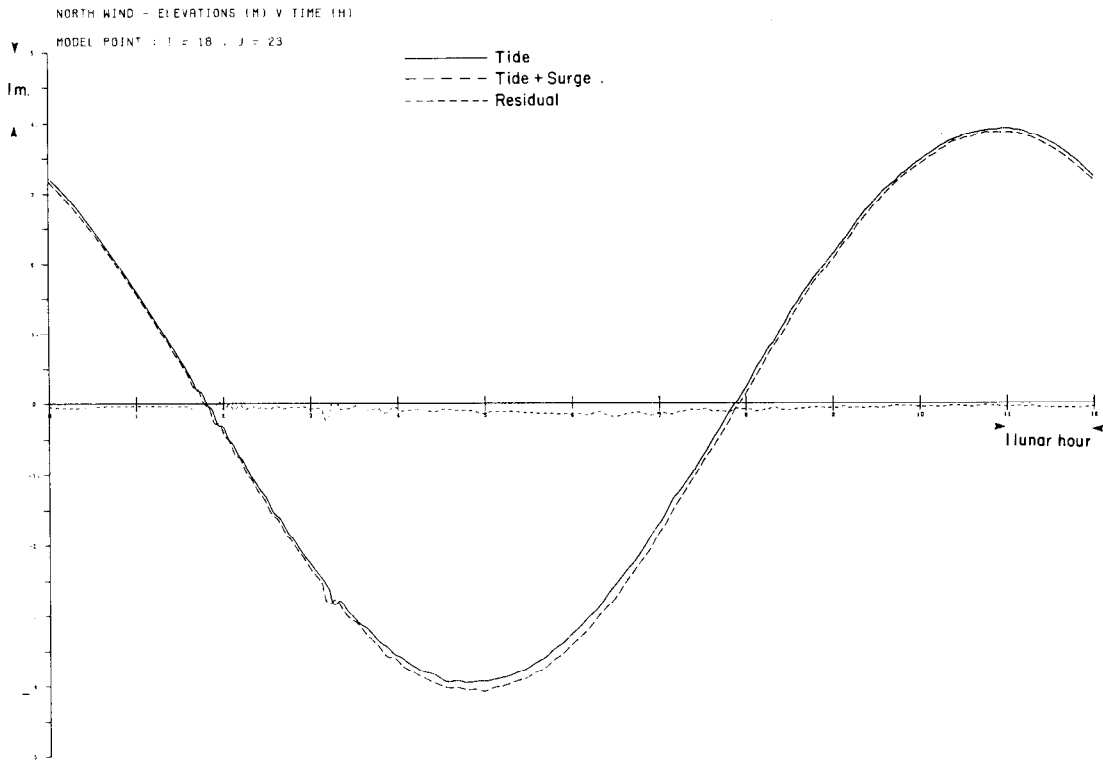


Figure 30: Variation of tide + surge (-----), tide alone (——) and surge residual (.....) produced by a northerly wind stress; sampling at every timestep over 1 tidal cycle.

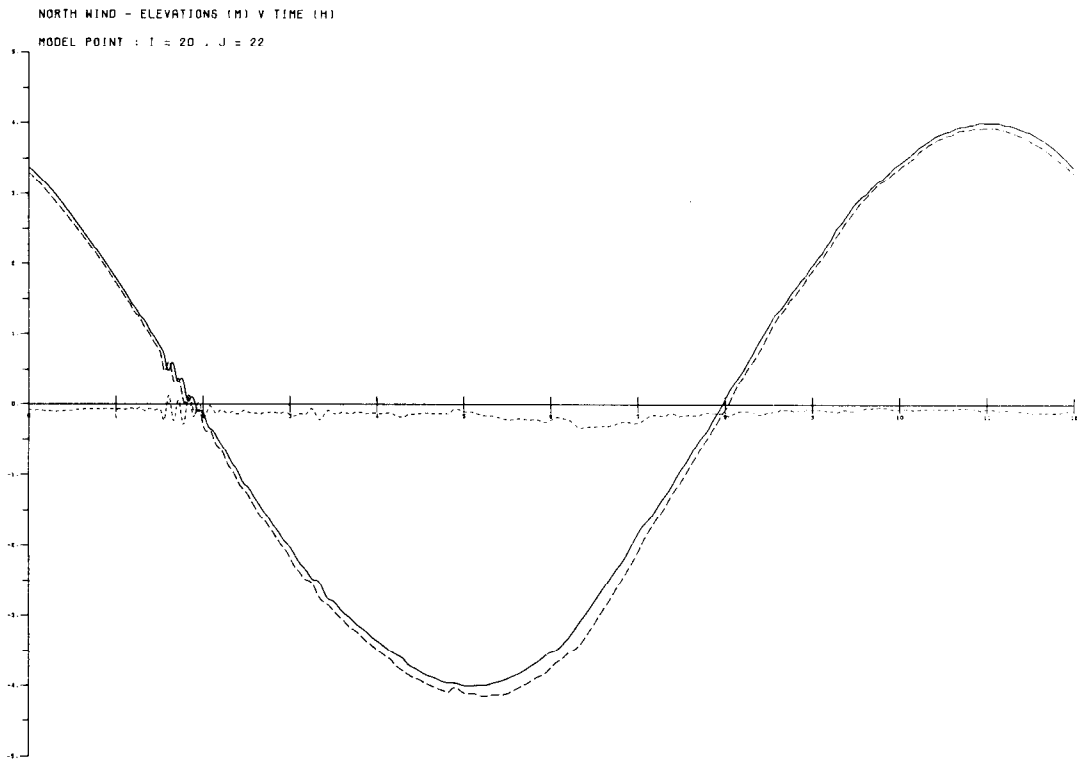
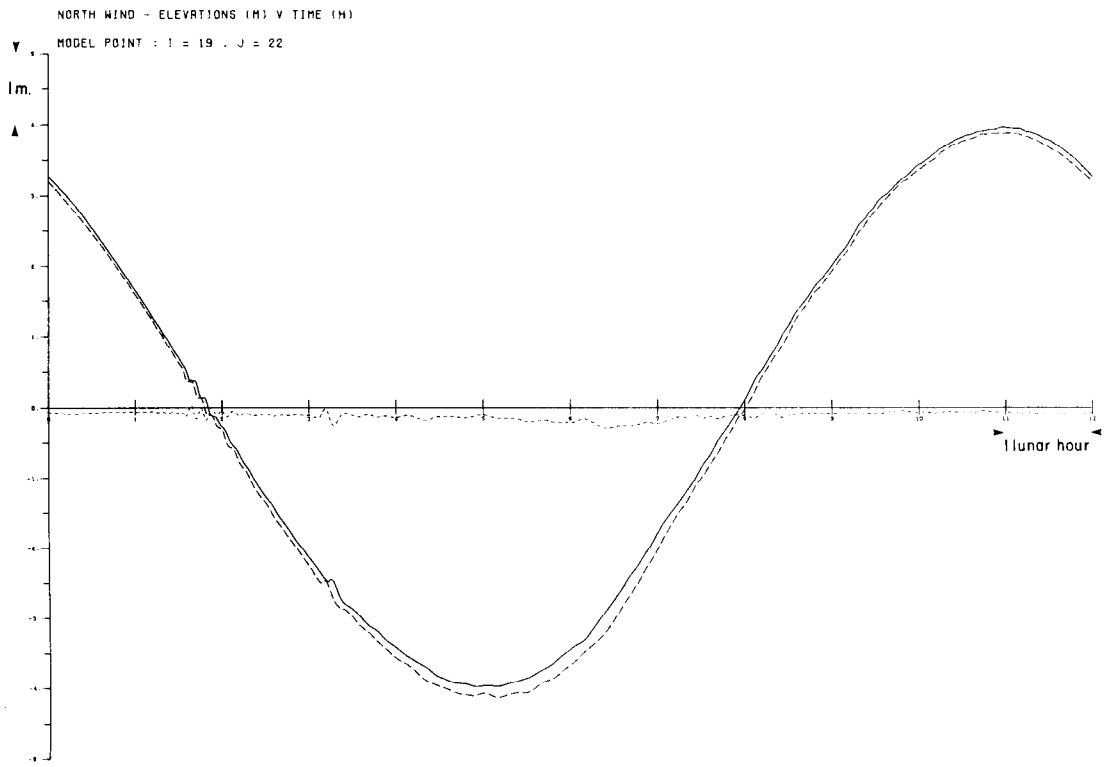


Figure 30: (CONT)

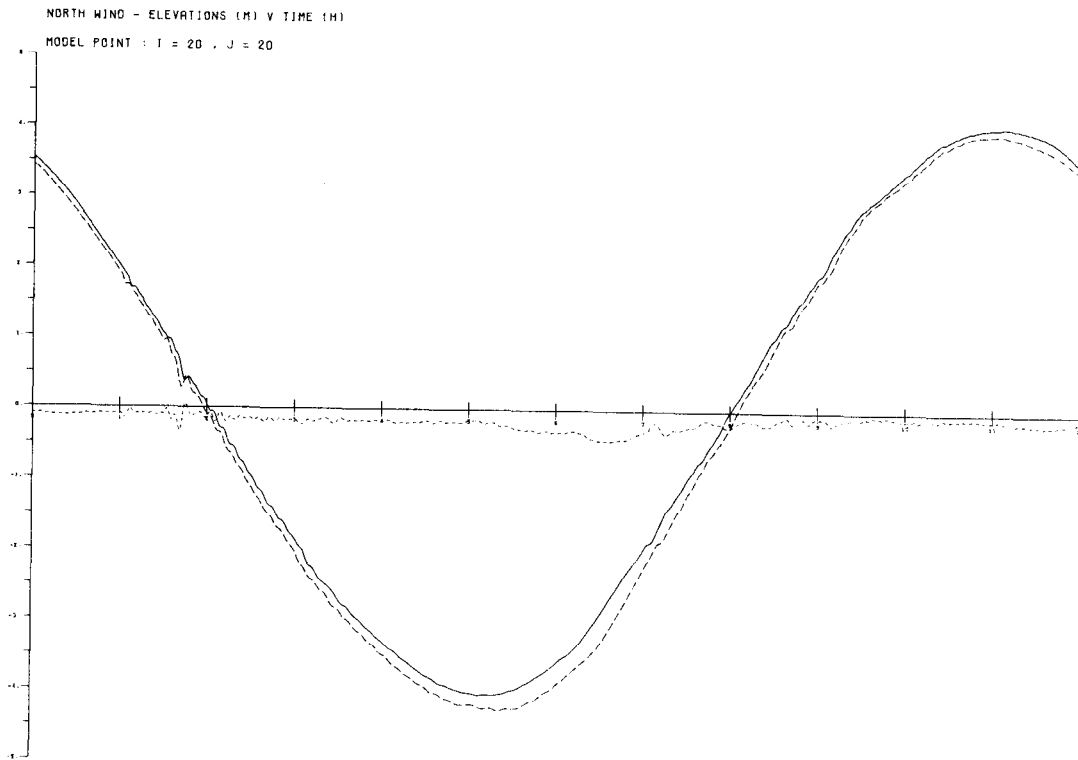
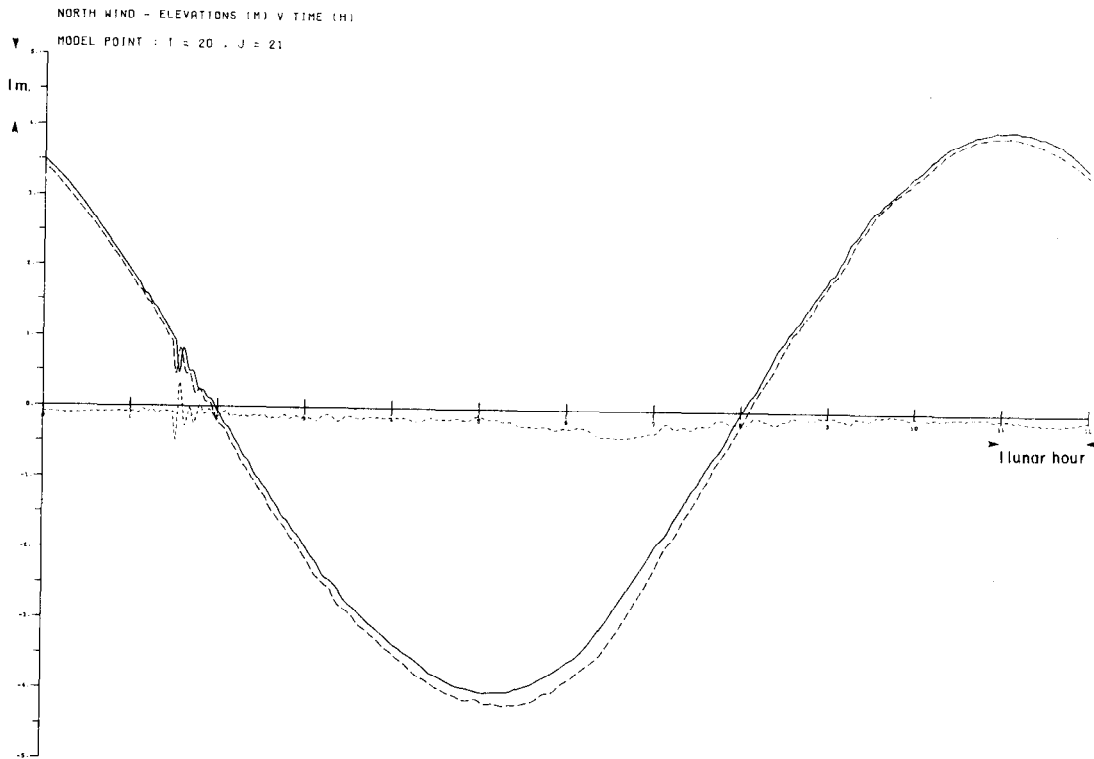


Figure 30: (CONT)

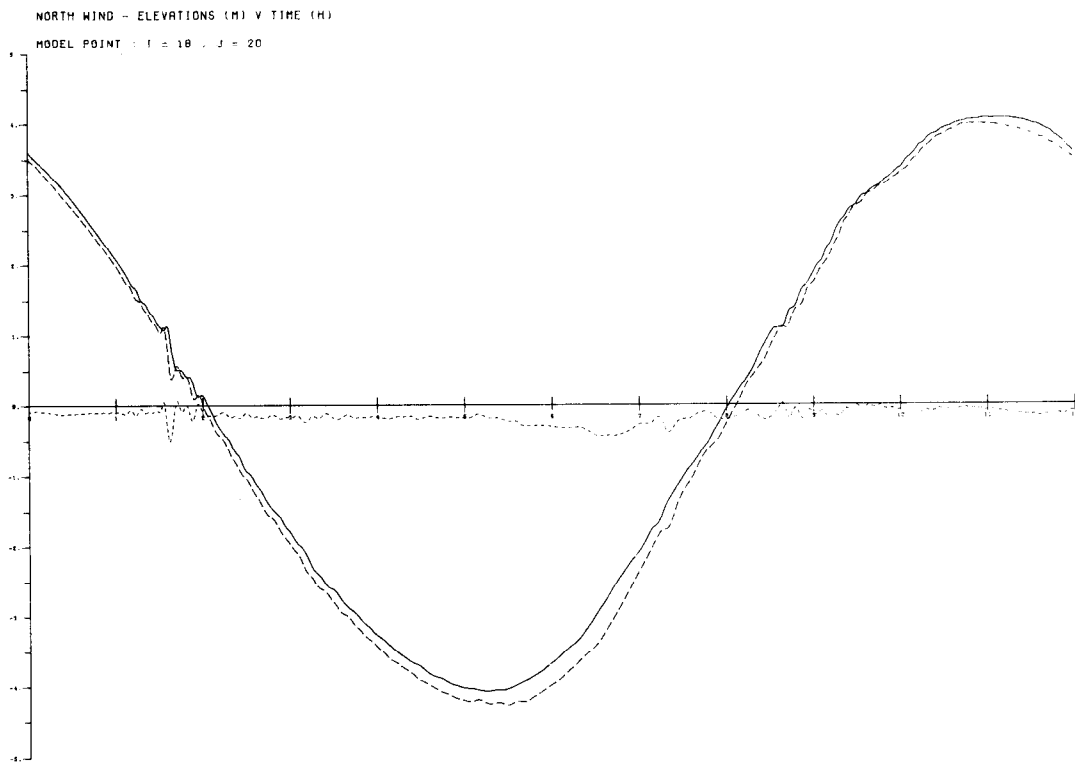
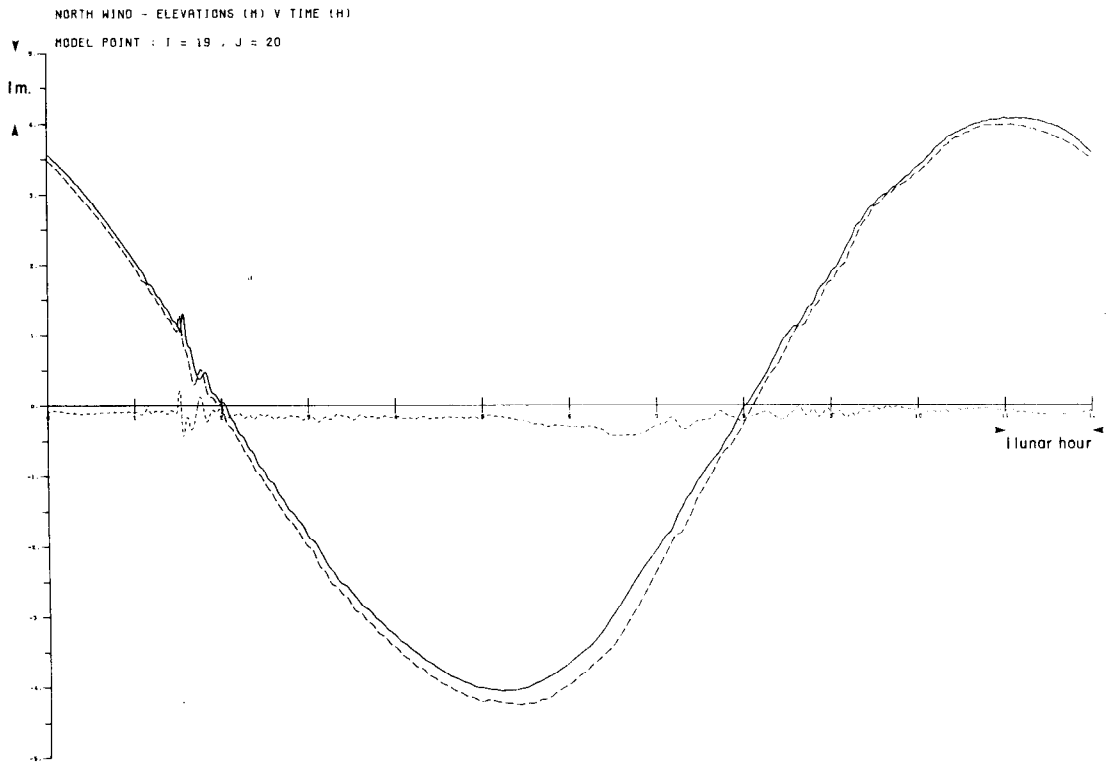


Figure 30: (CONT)

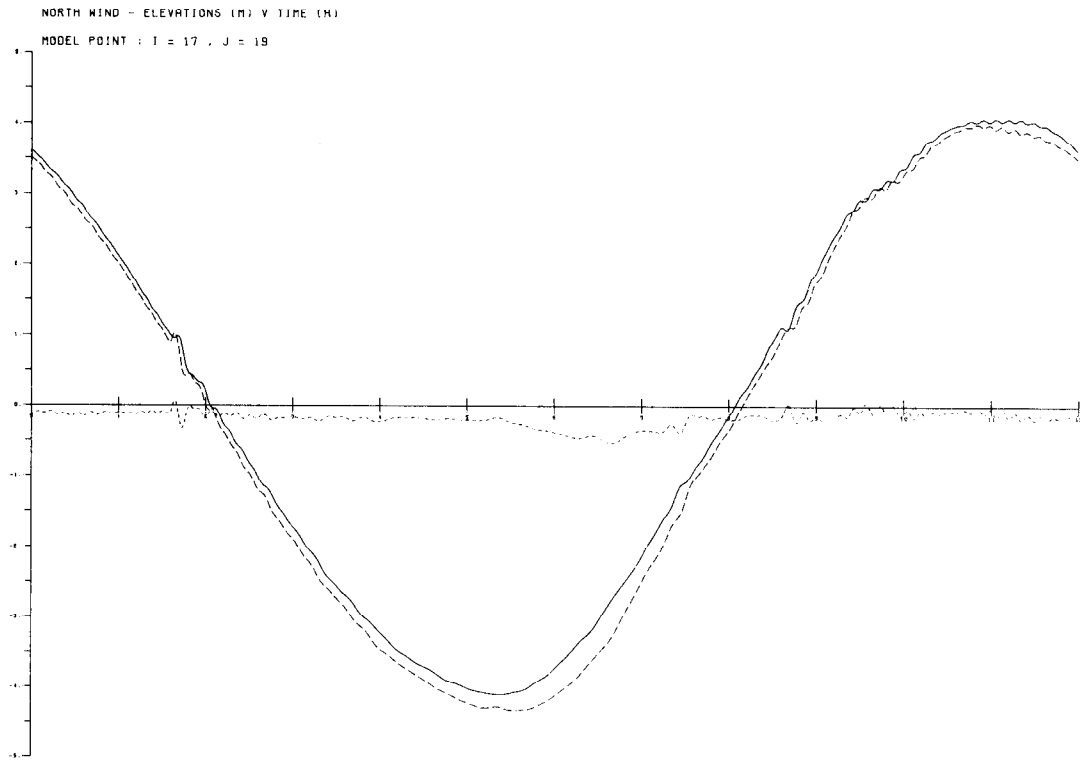
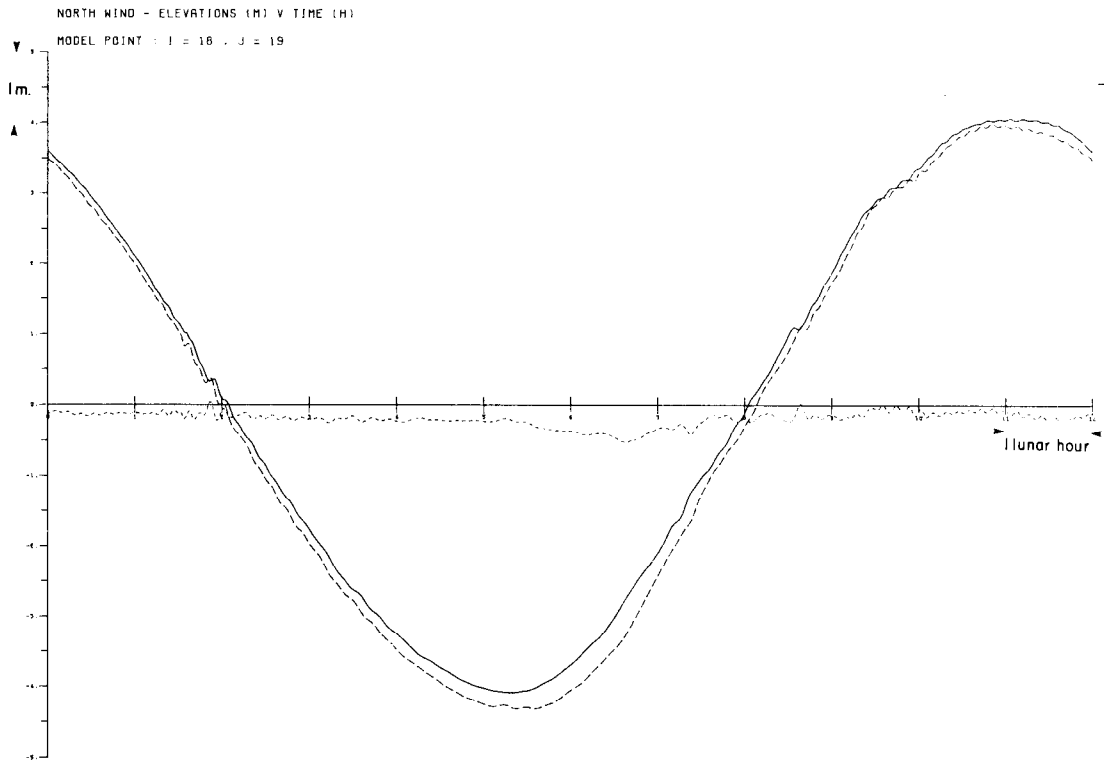


Figure 30: (CONT)



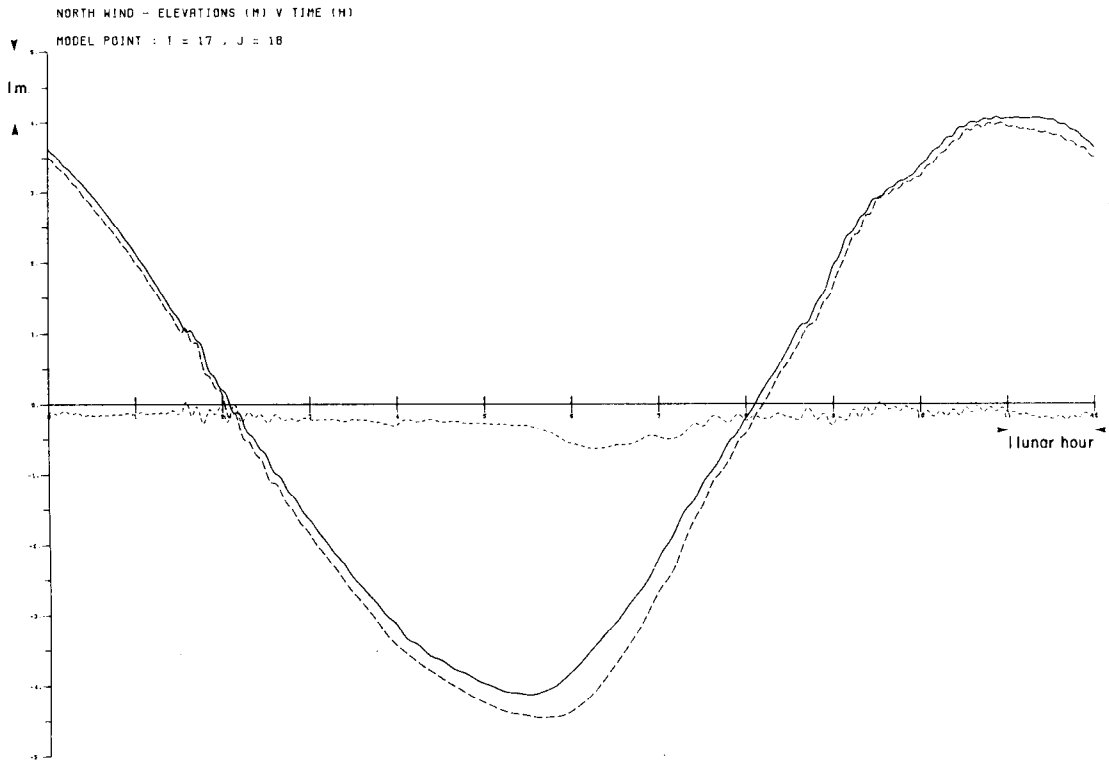


Figure 30: (CONT)

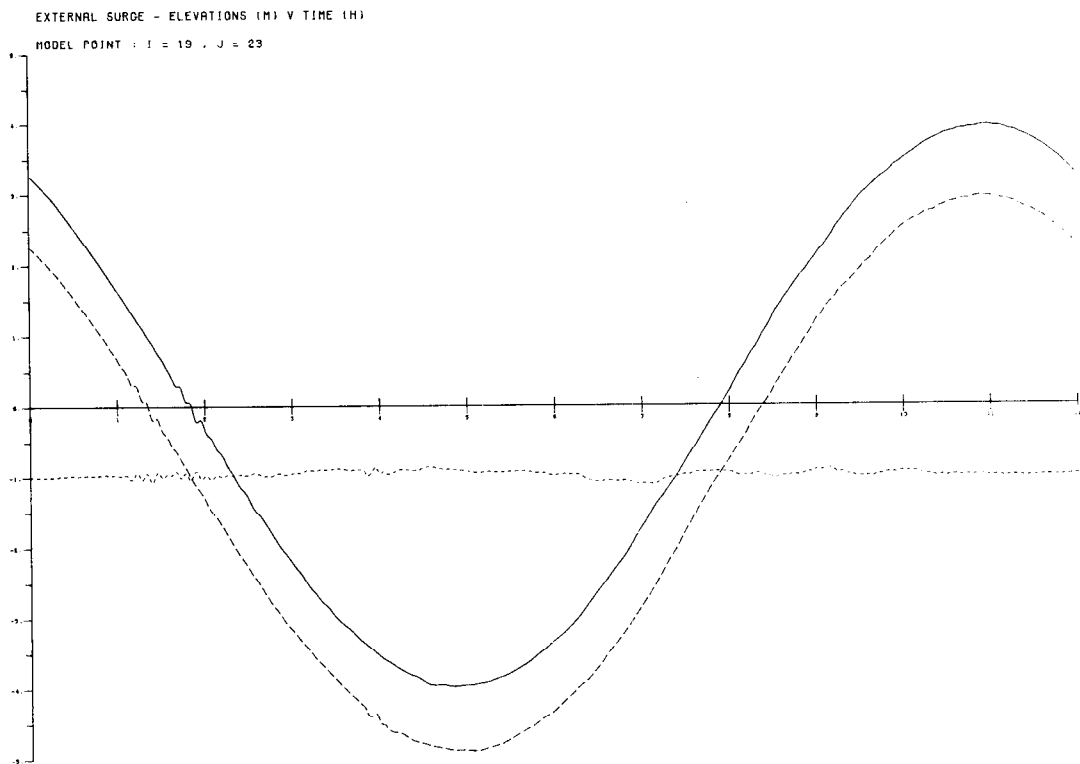
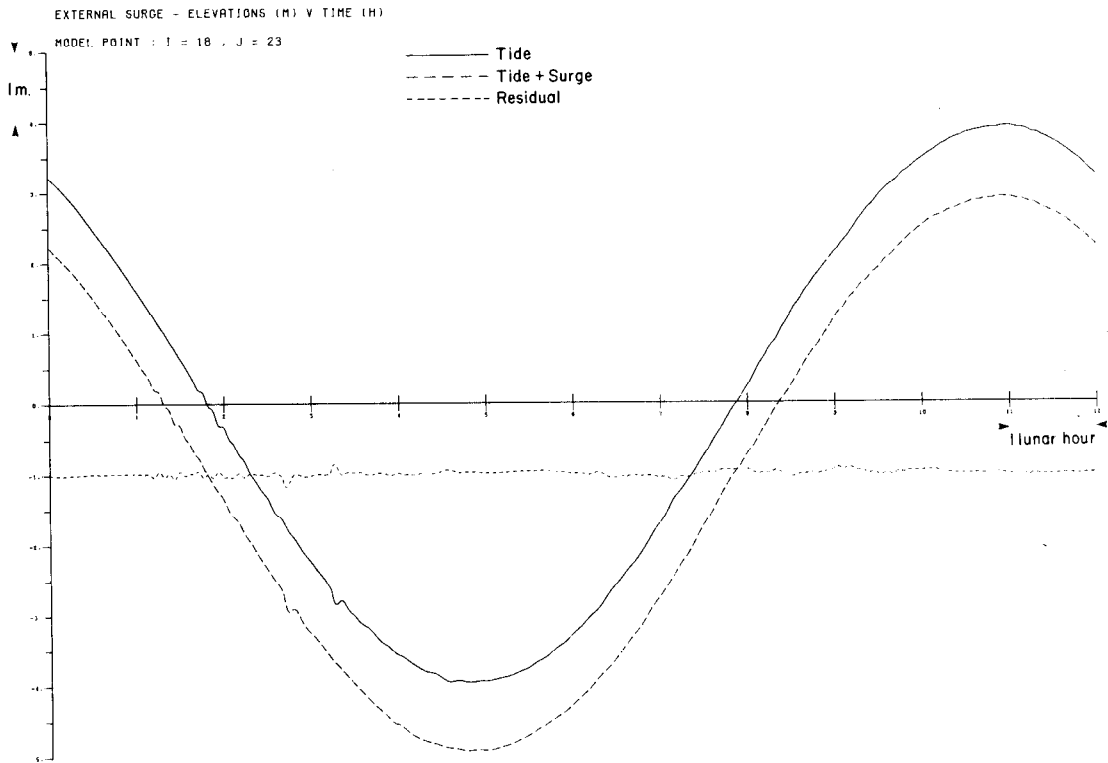


Figure 31: Variation of tide + surge (-----), tide alone (——) and surge residual (.....) produced by a negative external surge; sampling at every timestep over 1 tidal cycle.

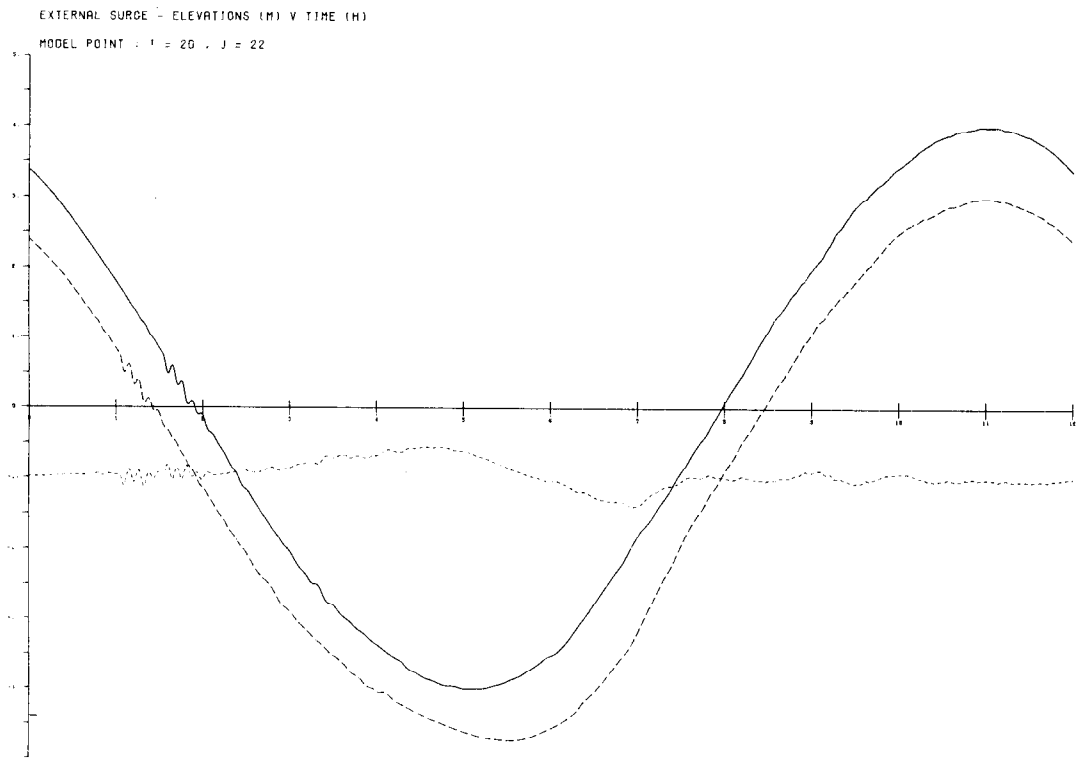
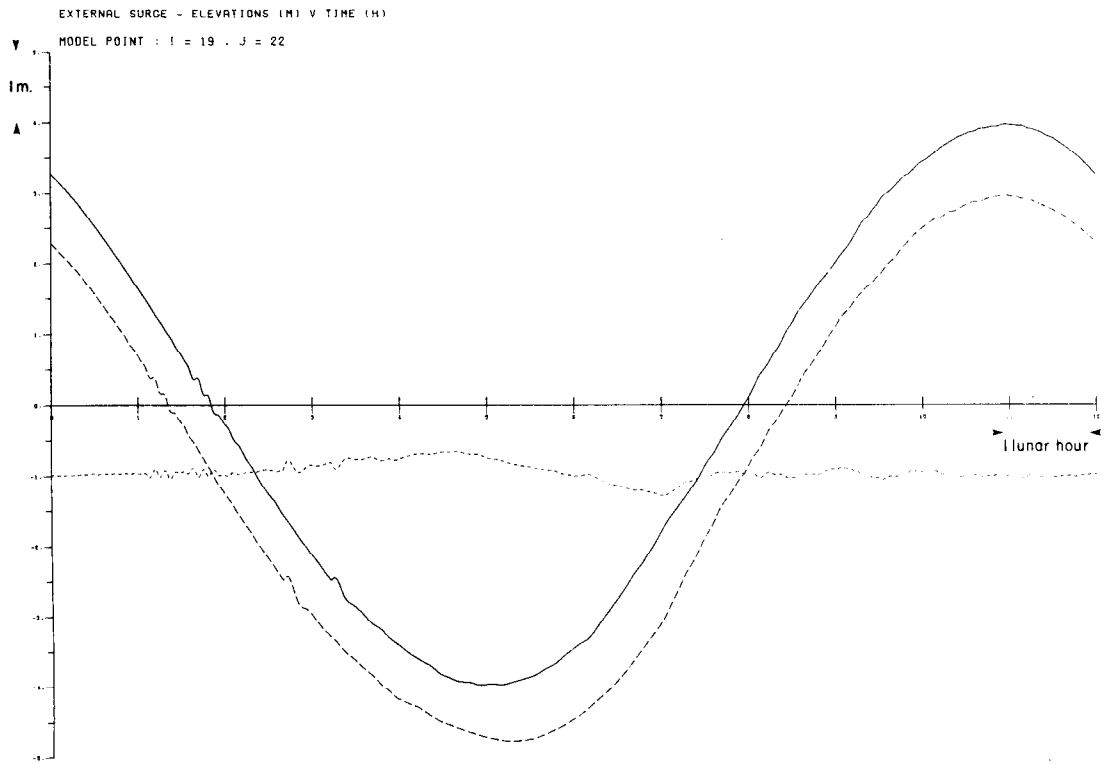


Figure 31: (CONT)

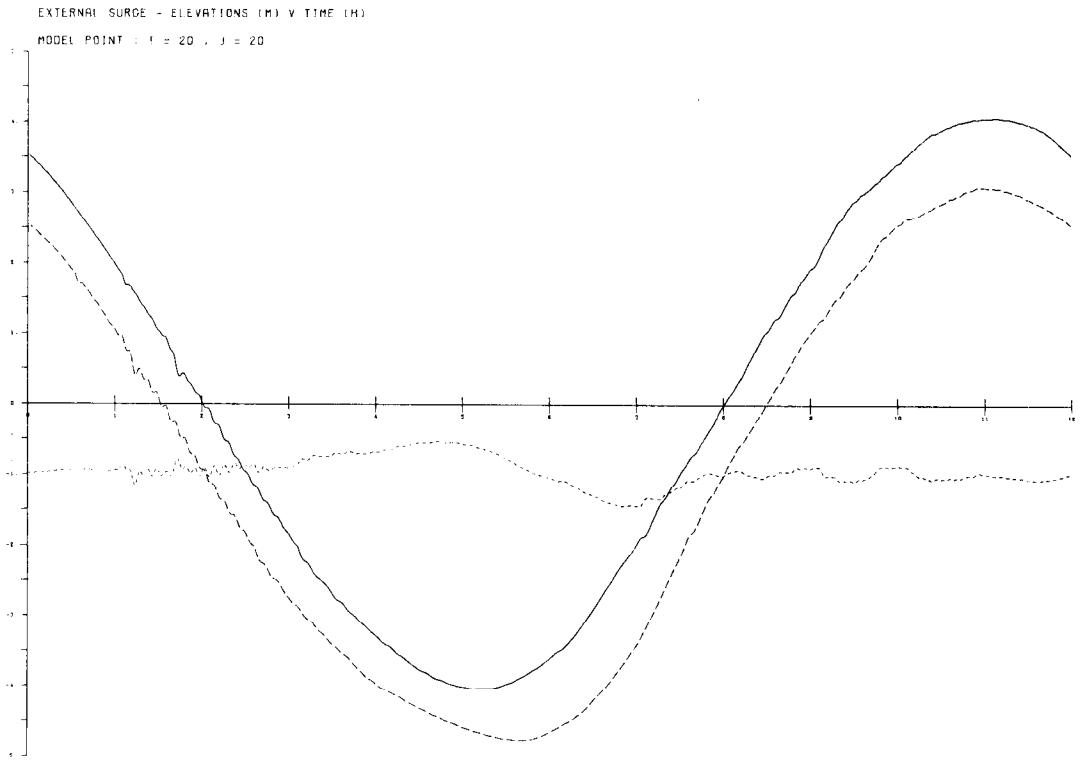
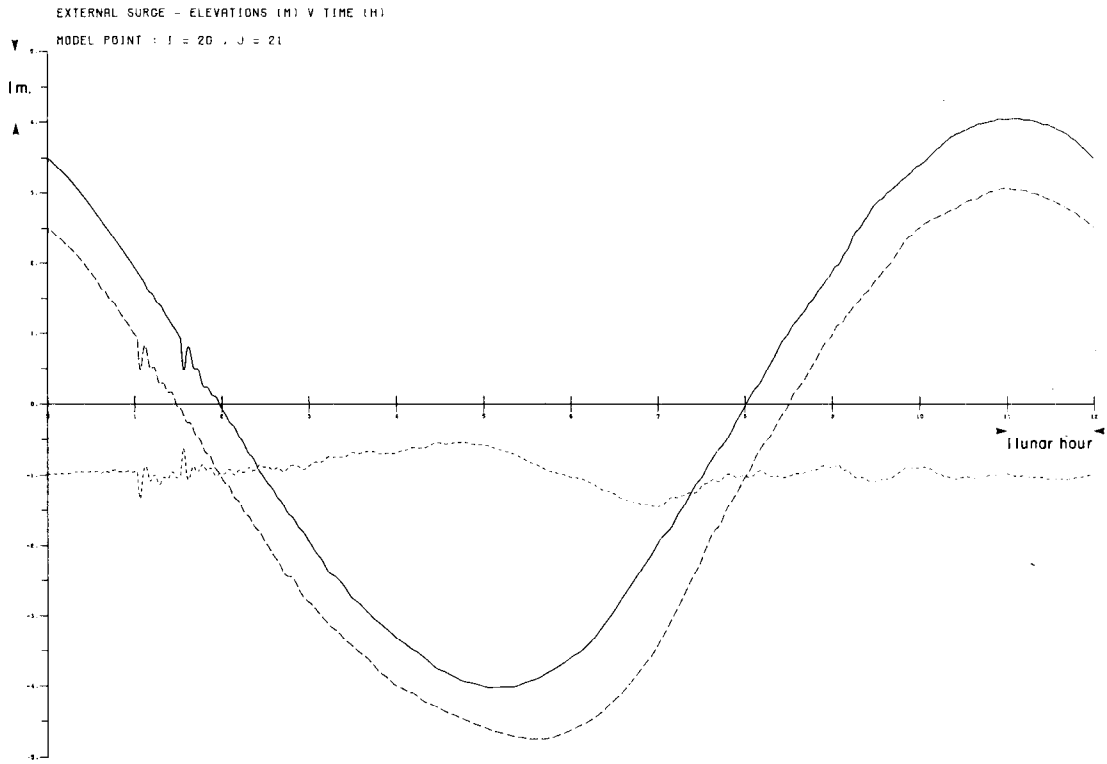


Figure 31: (CONT)

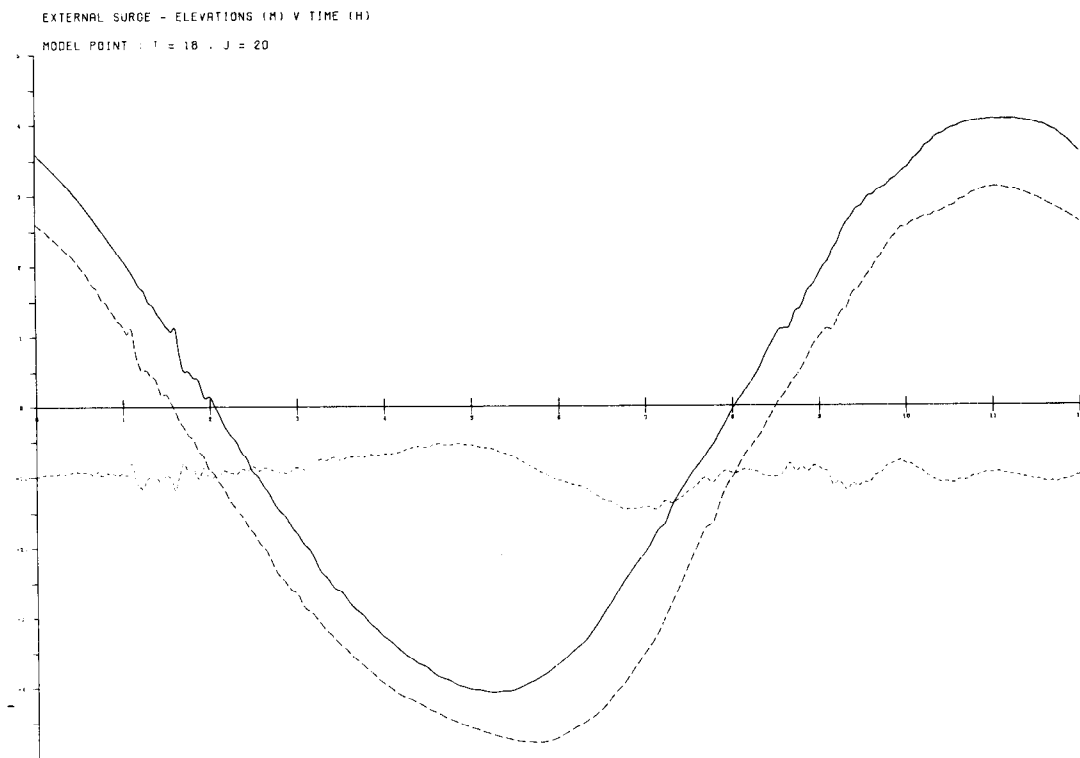
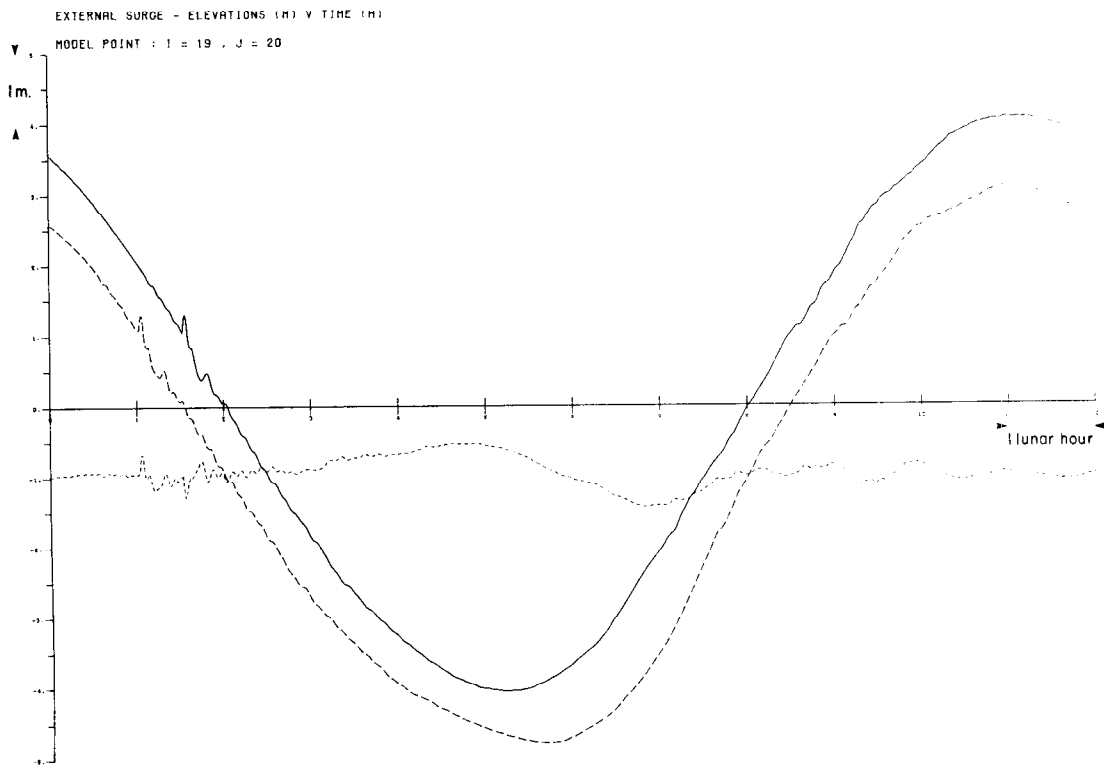


Figure 31: (CONT)

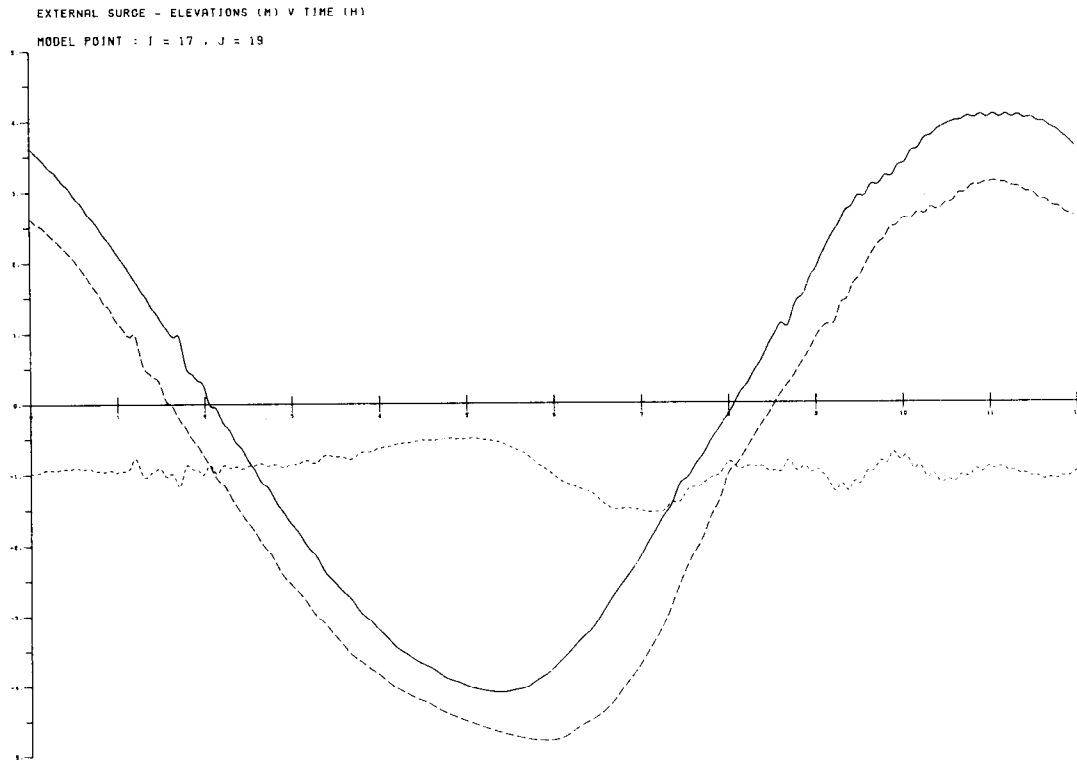
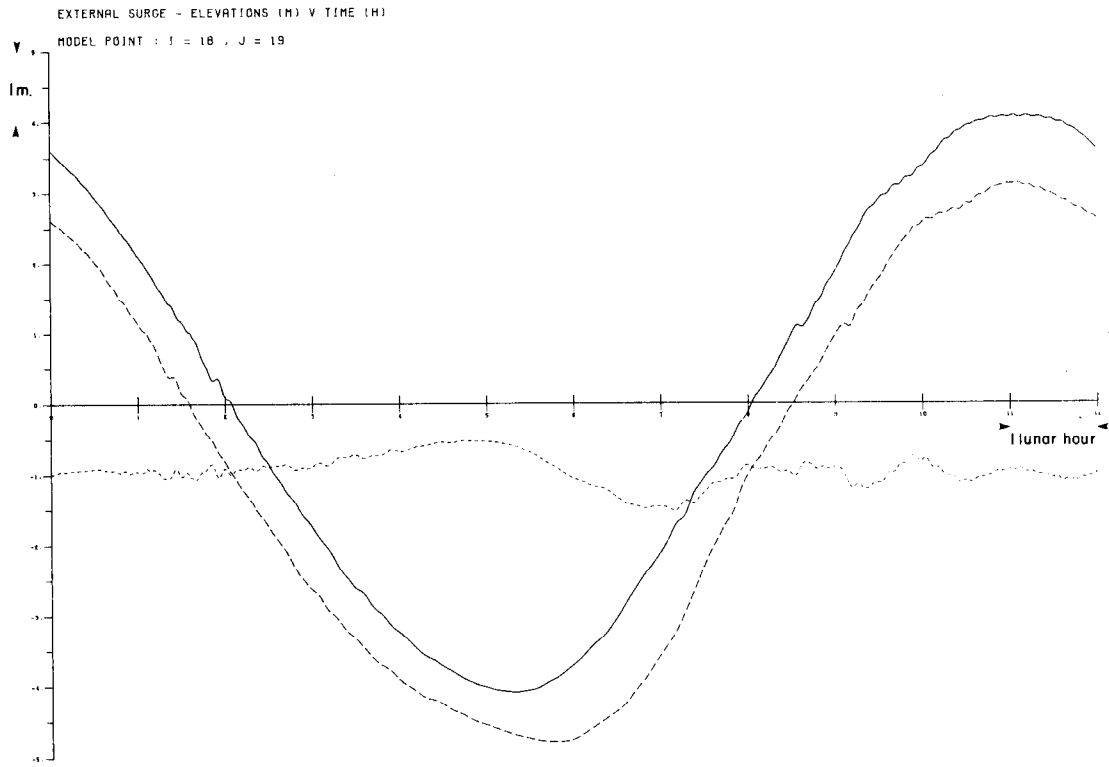


Figure 31: (CONT)

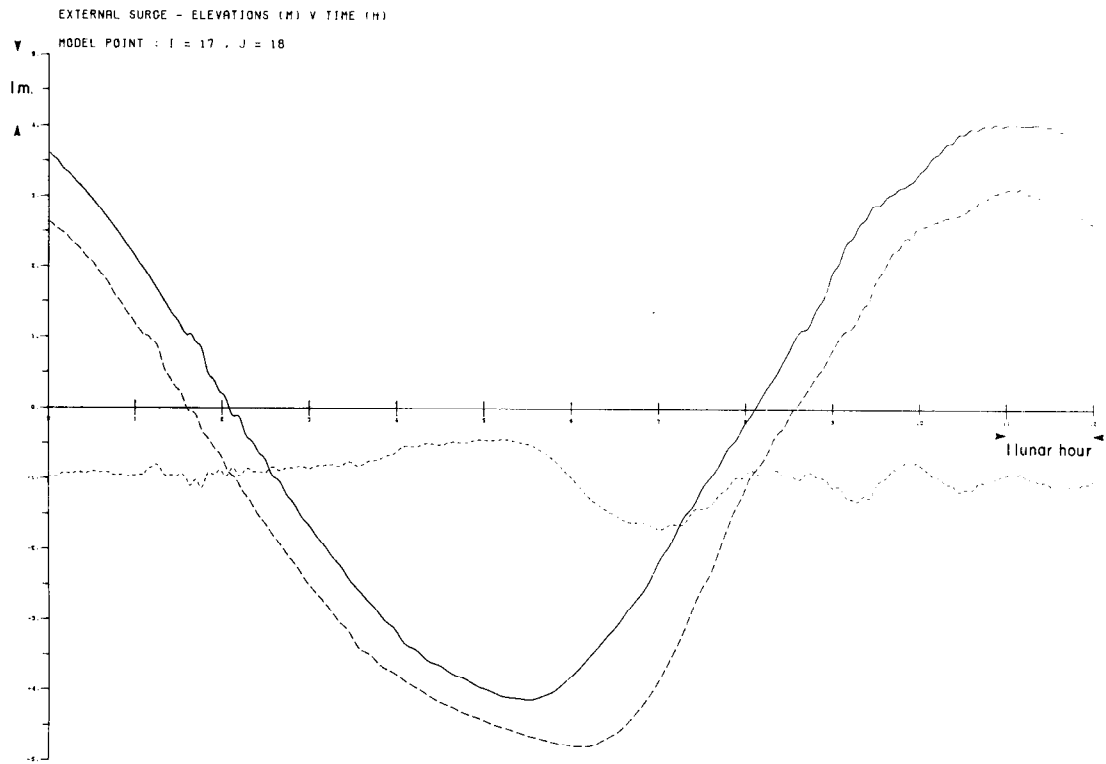


Figure 31: (CONT)

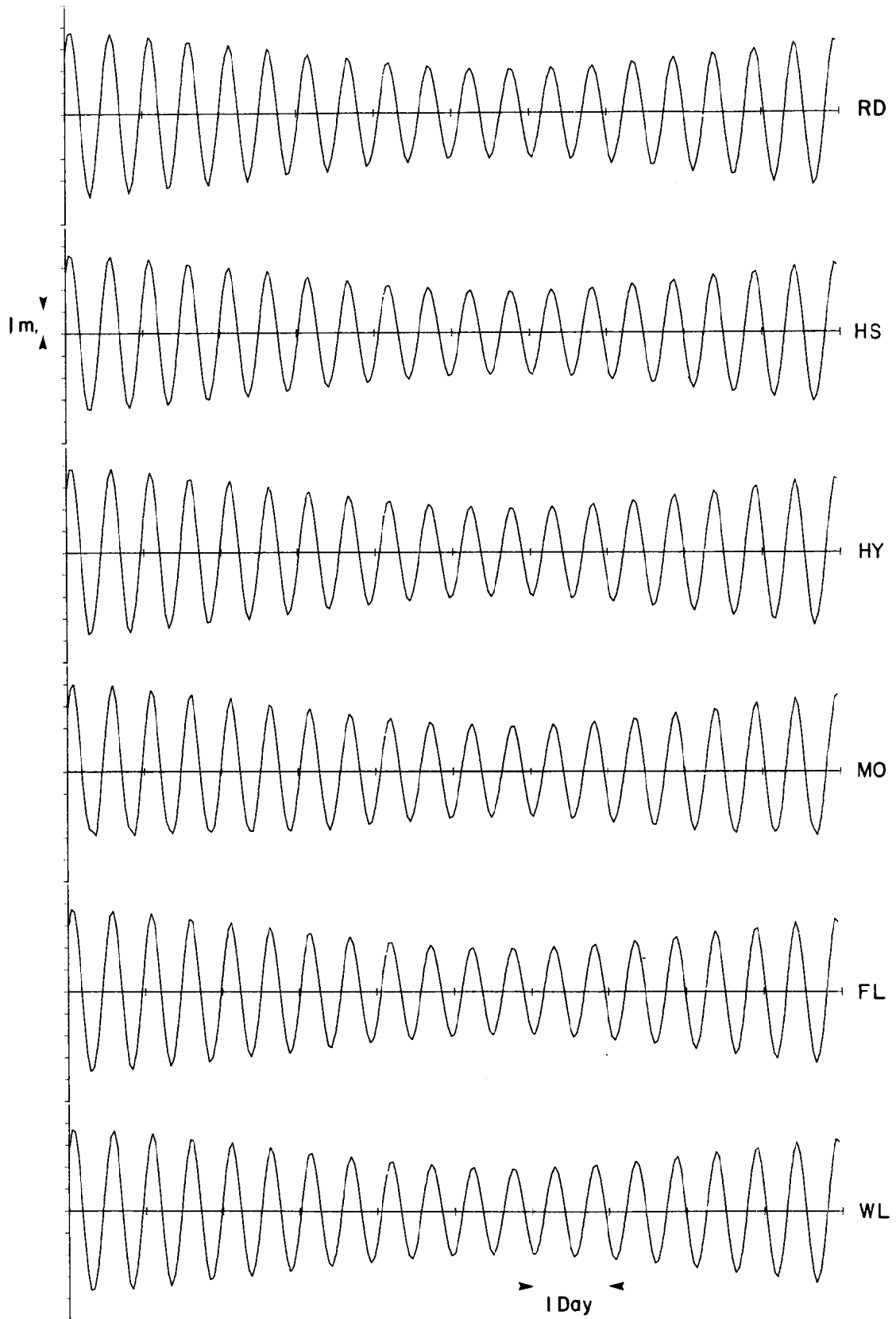


Figure 32: Computed tide at representative locations for the period 29 January to 7 February 1986.



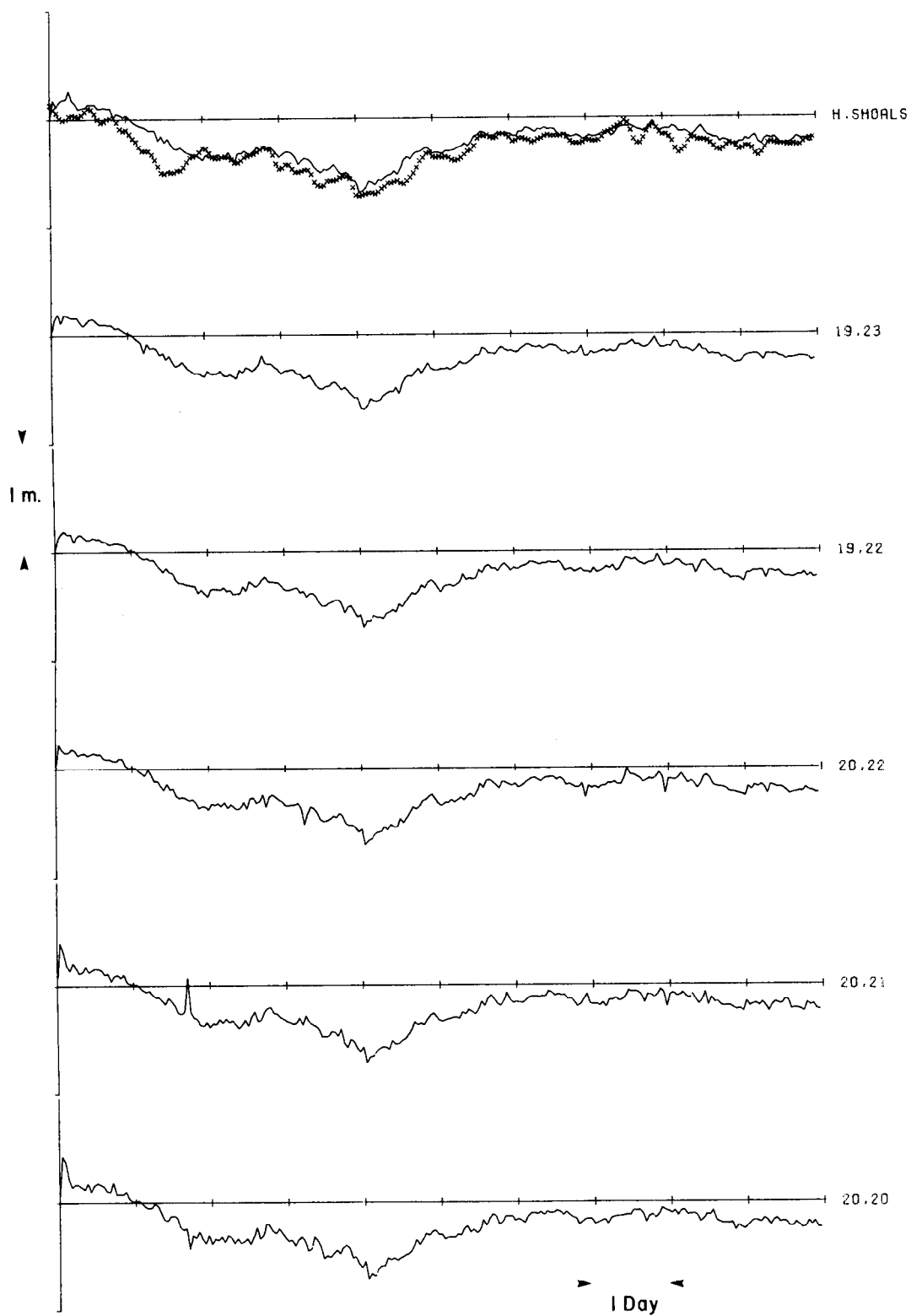


Figure 33: Time series of computed (—) and observed (xxxxx) surge residuals for the period 29 January to 7 February 1986.

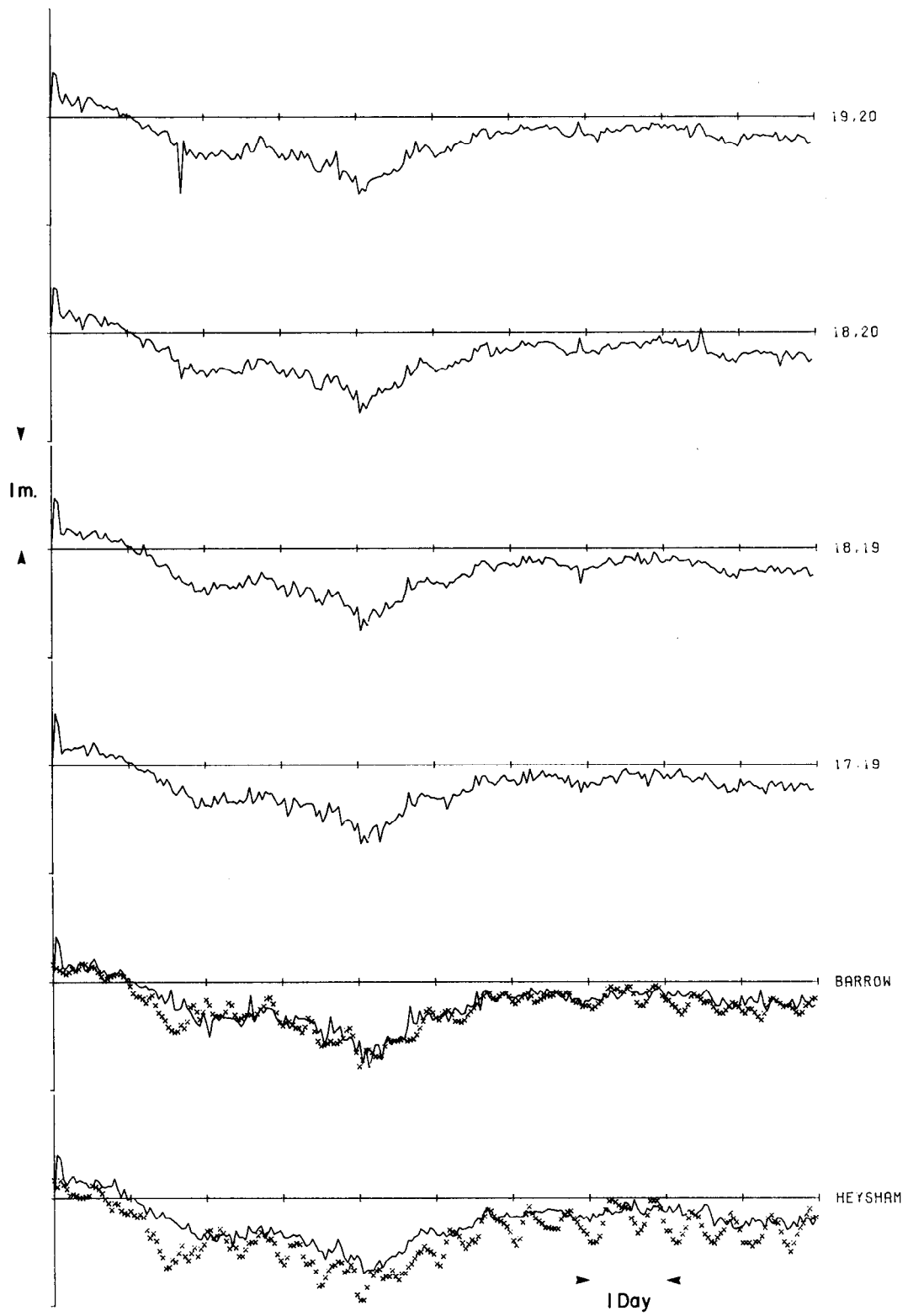


Figure 33: (CONT)

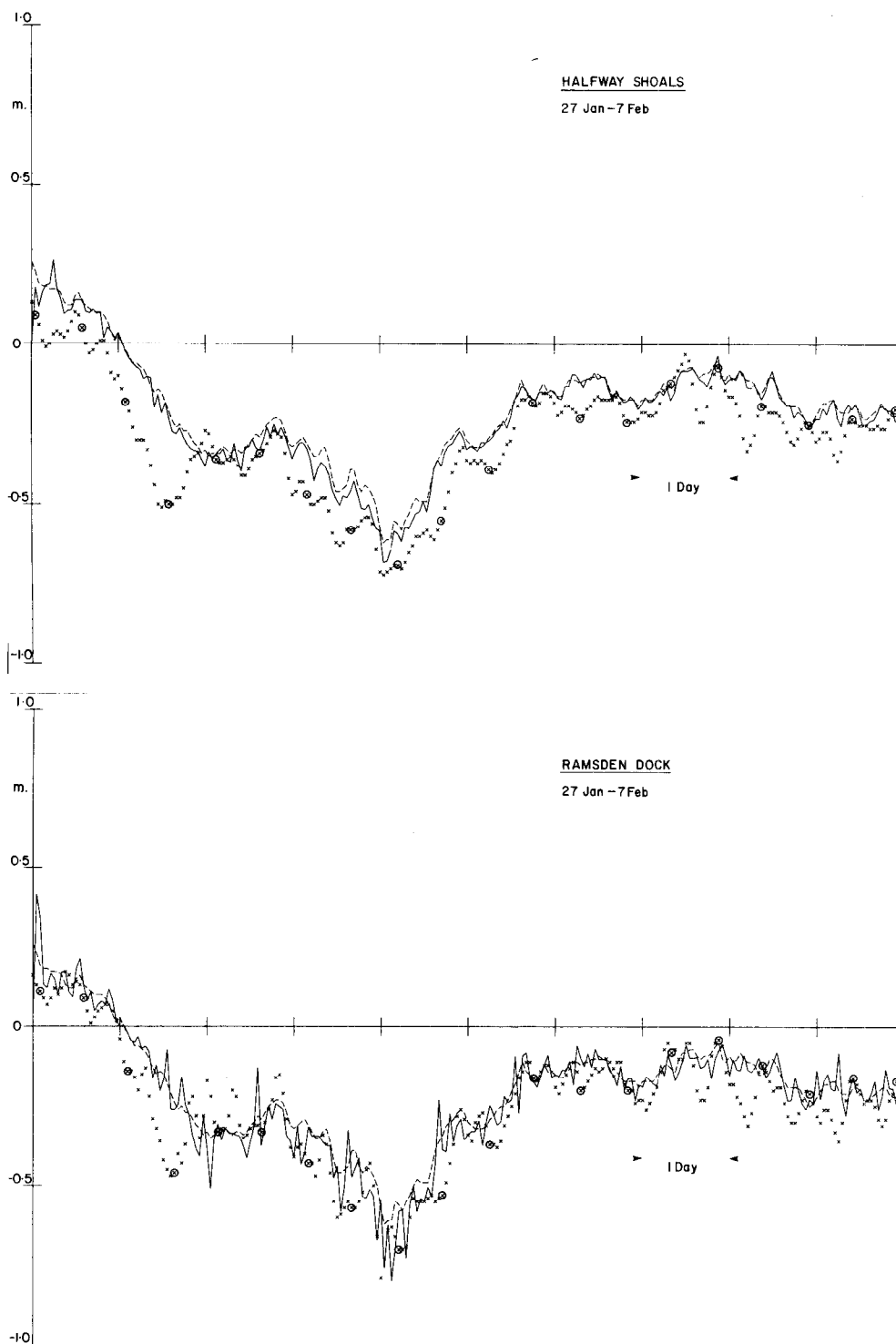


Figure 34: Comparisons of time series of surge residuals for Halfway Shoals and Ramsden Dock:

- a) derived from the present calculation (——);
- b) from observations (xxxxx), with circles indicating approximate times of tidal high water;
- c) from the nearest grid point of the operational surge forecast model (-----).